Synthesis and characterization of new linkers for Zr-based MOFs

Erlend Solbakken Aunan

MSc thesis

[60 credits]

Department of Chemistry

UNIVERSITY OF OSLO

Spring 2018

2018

Synthesis and characterization of new linkers for Zr-based MOFs

Erlend Solbakken Aunan

http://www.duo.uio.no/

Print: Reprosentralen, Universitetet i Oslo

Preface

I would like to begin this section by properly thanking Professor Mats Tilset, and to show him my greatest appreciations for his excellent supervision and advice. He keeps no leashes on his students and allowed me to explore and investigate whatever interests I came across during my MSc project.

Furthermore, I would like to thank Knut Tormodssønn Hylland for being an amazing co-supervisor, and for being the "in-lab guru" teaching me all the tips and tricks that an organic chemist should learn.

Mentioning the Tilset group members is also an absolute necessity. I would especially like to thank Marte Sofie Martinsen Holmsen for her overall great advice (and her infamous puns) and Franziska Ihlefeldt for her overall positive attitude as well as for her opinions on fonts, table borders and otherwise *very* important things. Also, Cristiano Glessi deserves a mention for his always friendly conversations, and Vladimir Levchenko for being a superb office mate.

I also want to thank Sigurd Øien-Ødegaard and Gurpreet Kaur for helping me during the MOF-synthetic part of this work. Your combined knowledge has been inspiring and very helpful! I very much appreciate Gurpreet for assisting me with TGA and SEM in this work. An extra thanks to Sigurd for providing me with the fancy figures of various MOF structures.

I would like to thank Professor Frode Rise and Dirk Petersen for single-handedly managing the NMR lab. The two of you do an amazing job which is very much appreciated. Also, thanks to Osamu Sekiguchi for recording all my mass spectra.

Last, but absolutely not least, I would like to thank Molly for being a super awesome girl-friend. You're always supportive, positive and just an amazing person to be with!

Table of contents

I Abbreviations

Ac	acetyl
AcOH	acetic acid
Ar	aryl
aq.	aqueous
br	broad (NMR)
BA	benzoic acid
Bn	benzyl
COSY	correlation spectroscopy (NMR)
Cy	cyclohexyl
d	day(s)
d	doublet (NMR)
δ	chemical shift (NMR)
DMA	*N*,*N*-dimethylacetamide
DMF	*N*,*N*-dimethylformamide
EI	electron ionization (MS)
equiv.	equivalent(s)
ESI	electrospray ionization (MS)
Et	ethyl
EtOAc	ethyl acetate
EtOH	ethanol
h	hour(s)
HRMS	high resolution mass spectrometry
HSQC	heteronuclear single quantum coherence (NMR)
m	multiplet (NMR)
m	meta
Me	methyl
MeCN	acetonitrile
MeOH	methanol
MOF	metal-organic framework
M_p	melting point
MS	mass spectrometry
m/z	mass to charge ratio (MS)
NMR	nuclear magnetic resonance
NOESY	nuclear overhauser effect spectroscopy (NMR)
o	ortho
p	para
Ph	phenyl
ppm	parts per million (NMR)
q	quartet (NMR)
r.t.	room temperature
s	singlet (NMR)
SEM	scanning electron microscope
sept	septet (NMR)
t	triplet (NMR)
THF	tetrahydrofuran

II Key compounds

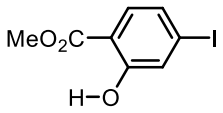

Starting material

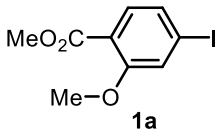

1a

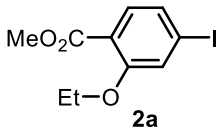

2a

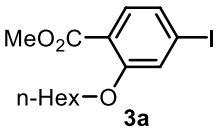

3a

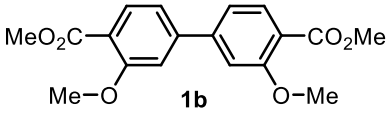

1b

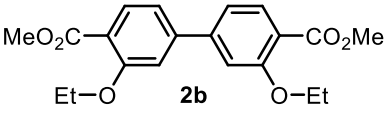

2b

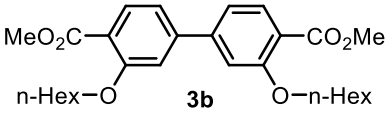

3b

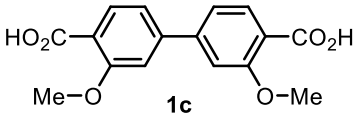

1c

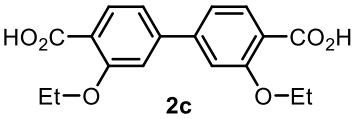

2c

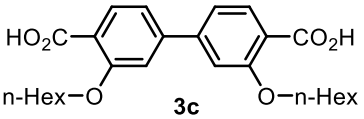

3c

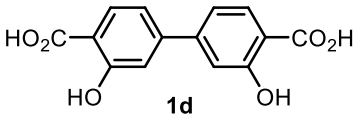

1d

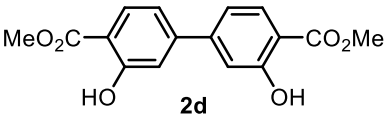

2d

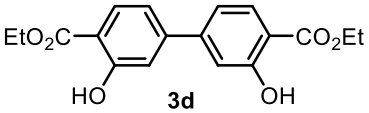

3d

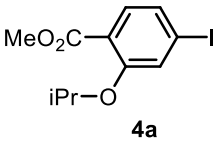

4a

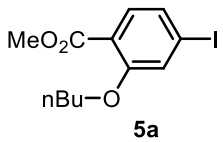

5a

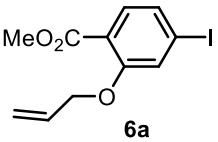

6a

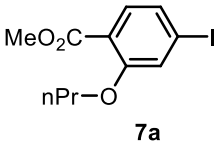

7a

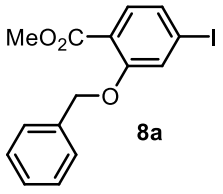

8a

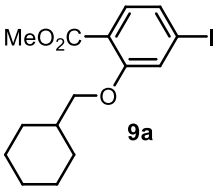

9a

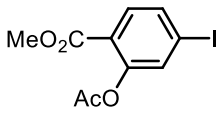

10a

III The aim of the project

The Catalysis group at the University of Oslo has for the previous decade been studying their successful series of metal-organic frameworks (MOFs). These MOFs, being a class of coordination polymers, consist of octahedral, hexametallic zirconium oxo clusters which serve as cornerstones that are bound together with organic dicarboxylic acids, which are commonly referred to as *linker*s. The series, consisting of the so-called UiO-66, UiO-67 and UiO-68 MOFs, has received a lot of attention due to the MOFs unprecedented resistance to thermal, chemical and physical decomposition. [1] A major part in the recent studies has been the development of new, functionalized linkers for these MOFs, meaning linkers that have other functional groups in addition to the two carboxylic acids which can be used for specific chemical applications, such as catalysis or gas adsorption.

The aim of this MSc project is the synthesis of new, functionalized linkers for UiO-67 type MOFs. The project therefore has two goals, where the primary goal is to synthesize and characterize the new, functionalized UiO-67 linkers. More specifically is the interest of this primary goal synthesizing 3,3'-dialkoxy-substituted linkers (**Figure 1**) due to their potential in the tunability of important chemical properties, such as hydrophobicity and steric hindrance. The secondary goal of the project is to put these linkers into a UiO-67 metal-organic framework.

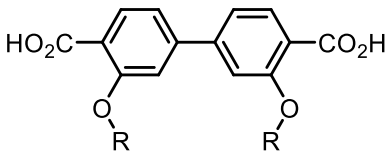

Figure 1: 3,3-dialkoxy-1,1'-biphenyl-4,4'-dicarboxylic acid

Theoretical background

1 Introduction to metal-organic frameworks

Metal-organic frameworks (MOFs) are being classed as coordination polymers, which are defined by the IUPAC as following:

Coordination polymer: A coordination compound continuously extending in 1, 2 or 3 dimensions through coordination bonds.[2]

Furthermore, a metal-organic framework is defined as a "*coordination polymer with an open framework containing potential voids*". It is therefore by these definitions clear that MOFs are a class of porous materials. In addition, it is common (but not required) that a MOF exhibit a high degree of crystallinity. As a result of this there have been several developed MOFs with enormous internal surface areas, some with reported surface areas greater than 6000 m^2g^{-1}.[3] It is obvious that materials that possess such properties have a lot of potential in industrial applications.

The MOF structure is built using cationic metal clusters or metal ions as cornerstones and organic ligands (often dicarboxylic acids) bridging the cornerstones together. (**Scheme 1**) The ligands, commonly referred to as organic linkers, can be functionalized in order to fine tune the MOF's properties, such as pore size, the active site for a catalyst or chemical stability. The resulting metal-organic framework has shown great potential as *i.e.* a catalyst support, gas adsorber, gas separator or as a drug delivery system.[4, 5]

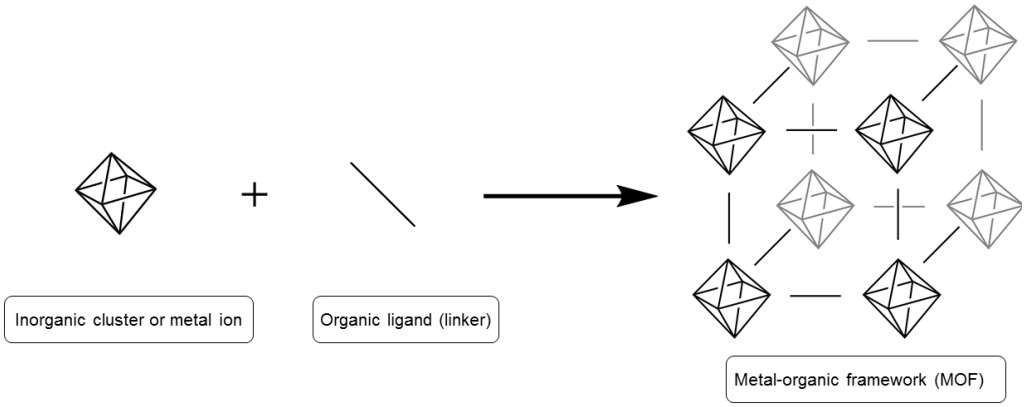

Scheme 1 A general schematic representation of the construction of a metal-organic framework

1.1 Brief history of metal-organic frameworks

The concept of metal-organic frameworks is not a new concept. Historically there are a few reported structures that would fit the definition of a MOF, one from all the way back in 1959.[6] But the term "metal-organic framework" was first coined by Yaghi *et al.* in 1995 with the reported structure of a copper 4,4'-bipyridine metal-organic framework[7]. These early MOFs were not particularly stable and often collapsed after removing the guest solvent molecules. The first breakthrough was arguably not before 1999 when Yaghi *et al.* reported the now famous MOF-5, shown in **Figure 4**. It quickly became famous in the material science community because it allowed for the complete removal of solvent molecules from the pores. MOF-5 also had a reported surface area of *ca.* 3000 m^2g^{-1}. This was a ground-breaking record, beating the current zeolite-based record holder with more than three times the surface area.[8] The discovery of MOF-5 resulted in an enormous boom of scientific research to try and discover new potential metal-organic frameworks, and to further study their properties. This boom is very obvious when is looking at the statistics over the reported structures of metal-organic frameworks to the Cambridge Structural Database. (**Figure 2**)

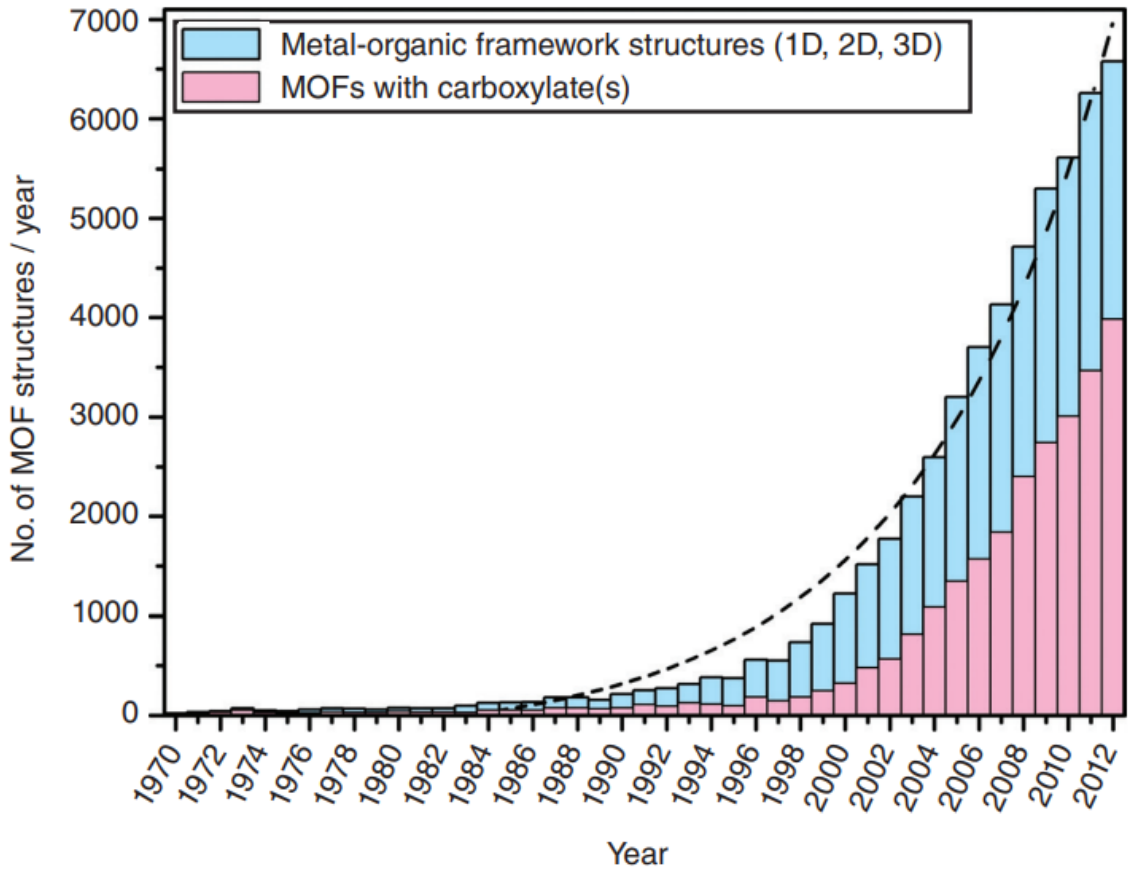

Figure 2 Chart over reported MOF structures to the Cambridge Structural Database between 1970 and 2012[9]

MOF-5 is a zinc-based metal-organic framework with terephthalic acid as the organic linker. The publication of MOF-5 laid the ground for the now popular concept of *reticular chemistry* (reticular meaning "net"). The idea of reticular chemistry is to keep the same scaffold (number of possible connections) while increasing the size of the linker, making the framework bigger (**Figure 3**). MOF-5 is also known as IRMOF-1, where IR stands for *isoreticular*.

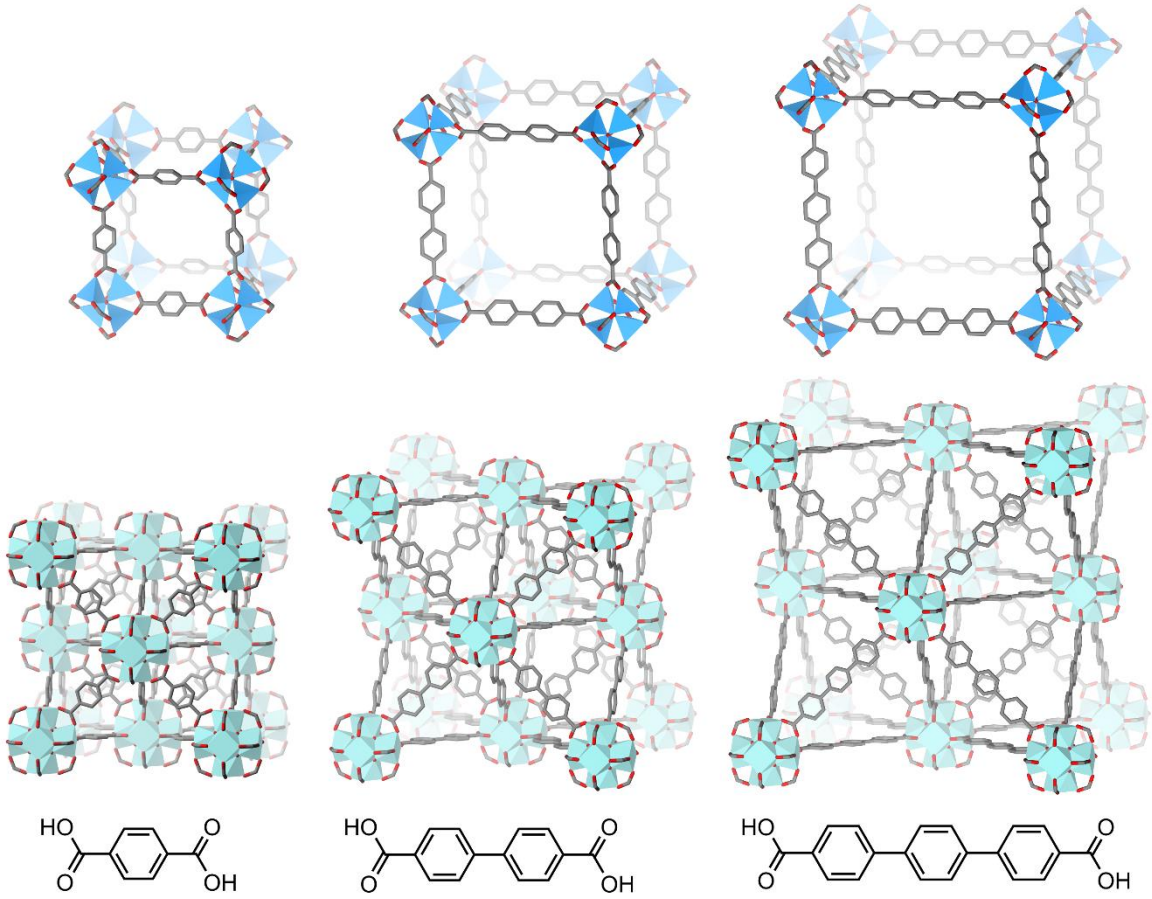

Figure 3 Concept of reticular chemistry. Top row consists of IRMOF-1 (MOF-5), IRMOF-9 and IRMOF-16, second row: UiO-66, UiO-67 and UiO-68. Hydrogen atoms are omitted for clarity. The bottom row is displaying the dicarboxllic acids used as linkers for the respective MOFs.

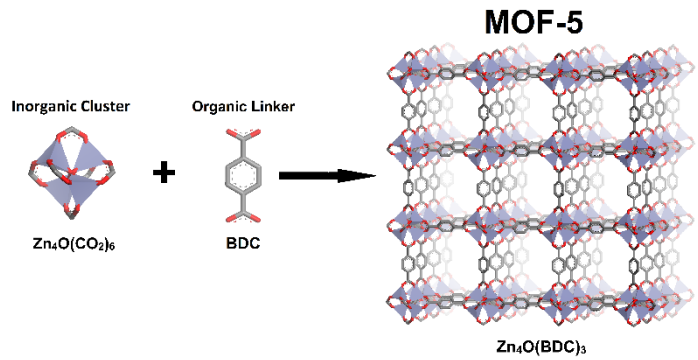

Figure 4: Structure of MOF-5 as reported by Yaghi in 1999. Hydrogen atoms have been omitted for clarity.

1.2 UiO-series

The Catalysis group at the University of Oslo has shown a great interest in the research of metal-organic frameworks. A breakthrough in the research appeared in 2008 when the UiO MOF series (UiO: Universitetet i Oslo) was reported by Lillerud *et al.*[1] A figure showing the series is given below in **Figure 5**.

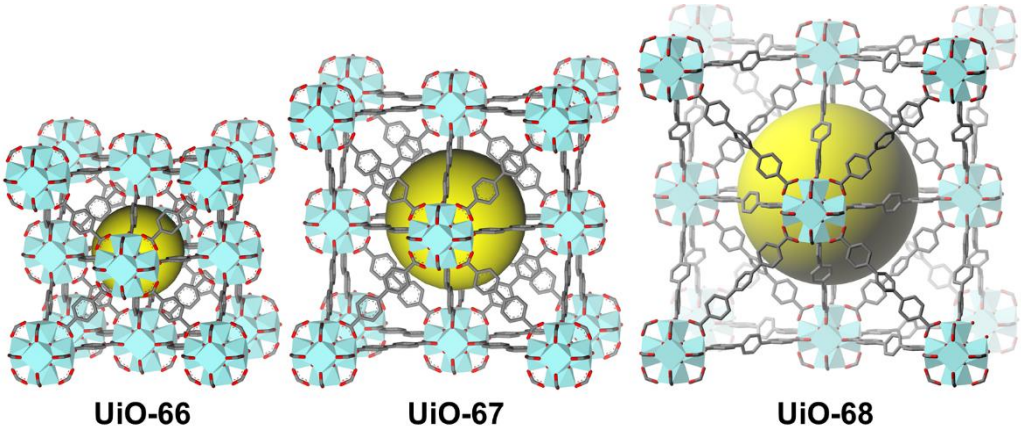

Figure 5 The UiO-series of metal-organic frameworks, containing UiO-66, UiO-67 and UiO-68. The yellow ball indicates the octahedral pore structures of the structure. Hydrogen atoms are omitted for clarity.

1.2.1 UiO-66

As previously mentioned was the UiO-66 MOF reported for the first time in 2008 and showed an incredible chemical, physical and thermal stability. Because of this stability it has a great potential in industrial usage, and scientific groups all over the world are actively studying the system. The UiO-66 is, as shown in **Figure 6**, a zirconium(IV)-based MOF in contrast to Yaghi's zinc-based MOF-5. The organic linker, terephtalic acid, is the same in both MOF-systems.

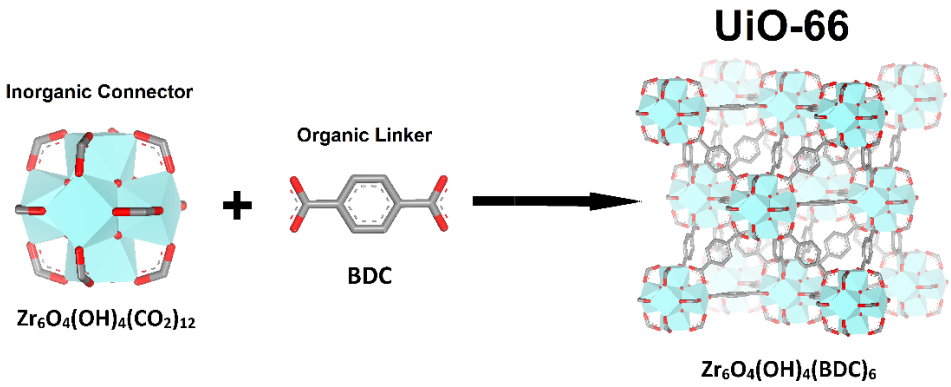

Figure 6 Structure of the UiO-66. Hydrogen atoms are omitted for clarity

The UiO-66 has an octahedral structure, with each zirconium cluster being surrounded by twelve coordinated terephtalic acids giving the stoichiometric composition of $Zr_6O_4(OH)(BDC)_6$, where "BDC" is referring to the terephtalic acid (benzene dicarboxylic acid). The MOF has a face centered cubic (fcc) structure, with a pore structure comprising of both octahedral and tetrahedral pores in a 1:2 ratio. UiO-67 has a theoretical BET surface area of 1241 m^2g^{-1}, which is on the modest side for metal-organic frameworks. The modest surface area is due to the highly interconnected structure, which is also contributing to the stability of the MOF.

1.2.2 UiO-67

UiO-67 is the MOF-structure that will be primarily discussed in this project. It is isoreticular to the UiO-66 with the linkers changed to biphenyl-4,4'-dicarboxylic acid instead of terephtalic acid. The extra phenyl ring increases the size of pores and therefore the surface area, giving UiO-67 a theoretical surface area of 3000 m^2g^{-1}.[1] Some examples of some previously synthesized functionalized linkers for UiO-67 type MOFs are shown in **Figure 7**.

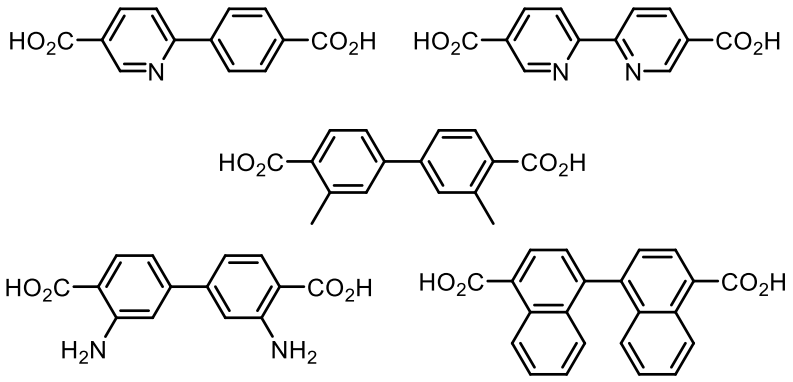

Figure 7 Examples of linkers for UiO-67 type MOFs: Top row: phenylpyridinedicarboxcylic acid[10], bipyridinedicarboxcylic acid[11]. Middle row: 3,3'-dimethylbiphenyldicarboxcylic acid[12]. Bottom row: 3,3'-diaminobiphenyldicarboxcylic acid[12], binaphthalenedicarboxcylic acid.[13]

1.2.3 UiO-68

The UiO-68 metal-organic framework is the largest in the series, but the least studied. Its linkers are based on the terphenyl-4,4"-dicarboxylic acid-scaffold following the same isoreticular expansion as with UiO-67 where another phenyl-group is added. As the third phenyl is added, the theoretical surface area increases to 4170 m^2g^{-1}. An important note about the UiO-series is that the stability of the MOF is not compromised due to the increased linker length.

The three MOFs in the series all show similar patterns of decomposition at similar temperatures ($T_{decomp.}$ > 500 °C), with benzene as the major decomposition product showing that the weakest link is the C-C-bonds on either sides of the benzene ring, and not the coordination between the linker and the clusters.[1]

1.3 Requirements for linkers

The linkers for metal-organic frameworks have some requirements being associated with them in order to function both as structural elements, and as a functionalized part of the MOF. Firstly, the linker must be able to coordinate to two or more metal clusters at the same time. This is usually through functional groups containing oxygen or nitrogen atoms, such as carboxylic acids or nitrogen-containing heterocycles (such as bipyridine). Secondly, the linker must exhibit some chemical resistance to the conditions for the synthesis of the MOF itself. For instance, the synthesis of UiO-type MOFs proceeds at high temperatures (120 - 140 °C) in a highly acidic medium, rendering it difficult to have functional groups such as esters or amides present. Thirdly, to obtain crystalline MOFs the linkers should be rigid in order to reduce the amount of conformations or disorder in the structure. This is usually being solved by using aromatic systems, such as phenyl- or pyridyl-based scaffolds for the linkers. The aromaticity increases both the stability of the system, but also the rigidity due to them being planar because of the sp^2-hybridization. The argument of price is also a valid requirement for the linker. If the linker is to be produced industrially, a low cost of the starting materials or synthetic reagents is an important consideration.

1.4 3,3'-dialkoxy functionalized UiO-67 linkers

As previously mentioned is the primary aim of this project the functionalization of UiO-67 linkers, more specifically synthesizing 3,3'-dialkoxy functionalized linkers as shown in **Figure 1**. The motivation behind the synthesis of these kind of molecules is their potential as selective "tuners" in the field of gas separation or gas purification. By adjusting the length of the alkyl chain, the available pore size should decrease, allowing for greater selectivity of gas molecules entering the pores based on their size. Another aspect is the increase in hydrophobicity due to the longer alkyl chains, which could aid the selectivity of lipophilic gasses such as hydrocarbons due to their increased solubility. It is important to note that testing of the final products in regards of these fields is not considered an aim of this thesis and won't be conducted.

Results and discussion

2 Synthesis and characterization of UiO-67 linkers

2.1 Synthetic strategy

Synthetic pathways for UiO-67 linkers have been thoroughly developed at the University of Oslo.[12, 14] In most cases is the biphenyl skeleton not commercially available, with the exception of the standard biphenyl-4,4'-dicarboxylic acid (**Figure 8**) and its methyl ester derivative.

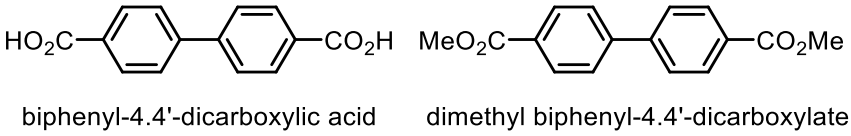

biphenyl-4.4'-dicarboxylic acid dimethyl biphenyl-4.4'-dicarboxylate

Figure 8: The standard linker for UiO-67: Biphenyl-4,4'-dicarboxylic acid and its methyl ester derivate. Commercially available from Sigma Aldrich at 120 NOK/g and 40 NOK/g, respectively.[a]

In order to obtain more functionalized UiO-67 type linkers is a clever use of various cross coupling reactions a necessity, and the most common one is the palladium catalyzed Suzuki-Miyuara cross coupling reaction or variations of it. Good candidates for starting material are therefore functionalized 4-halobenzoic acids or benzoates. The halogen is the reactive specie in the cross-coupling reaction and could be introduced synthetically. However, due to the vast availability of halogenated phenyl derivatives this is usually not necessary. Other good starting material candidates are the various functionalized 4-halotoluenes or 4-halobenzonitriles. The two last candidates give the possibility of introducing the carboxylic acid through oxidation or hydrolysis, respectively. For this project the readily available methyl 4-iodosalicylate was chosen as a starting material for synthesizing 3,3'-dialkoxy substituted UiO-67 linkers. From this compound was a synthetic pathway designed. (**Scheme 2**)

[a] Prices calculated from 25 g and 50 g, respectively from www.sigmaaldrich.com, 02.04-2018

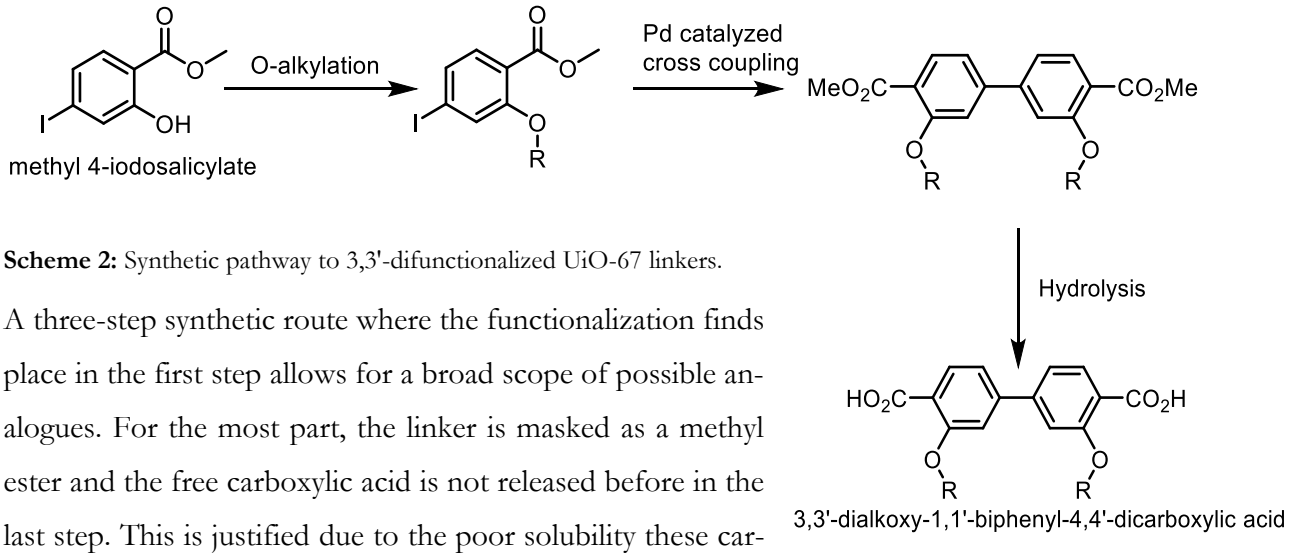

Scheme 2: Synthetic pathway to 3,3'-difunctionalized UiO-67 linkers.

A three-step synthetic route where the functionalization finds place in the first step allows for a broad scope of possible analogues. For the most part, the linker is masked as a methyl ester and the free carboxylic acid is not released before in the last step. This is justified due to the poor solubility these carboxylic acids often express in most common laboratory solvents.

2.1.1 Methyl 4-iodosalicylate

Methyl 4-iodosalicylate was selected as starting material partially due to its relative cheapness. It is listed for approximately 50 NOK/g at Sigma Aldrich.[b] Other groups have published procedures using different starting materials for similar, or in one case identical target molecule (compound **1c**).[15] In this case, Wang *et al.* report the use of 4-aminosalicylic acid as the starting material to synthesize linker **1c**. (**Scheme 2**) Although 4-aminosalicalic acid is cheaper (approximately 20 NOK/g)[b] is the synthetic scheme of Wang *et al.* one step longer due to halogenation by the Sandmeyer reaction. It is worth noting that they combine the O-alkylation step with an esterification step, to yield methyl **1a** directly. For their homo coupling reaction they chose the copper-based Ullmann coupling reaction instead of a palladium catalyzed Suzuki-Miyuara reaction.

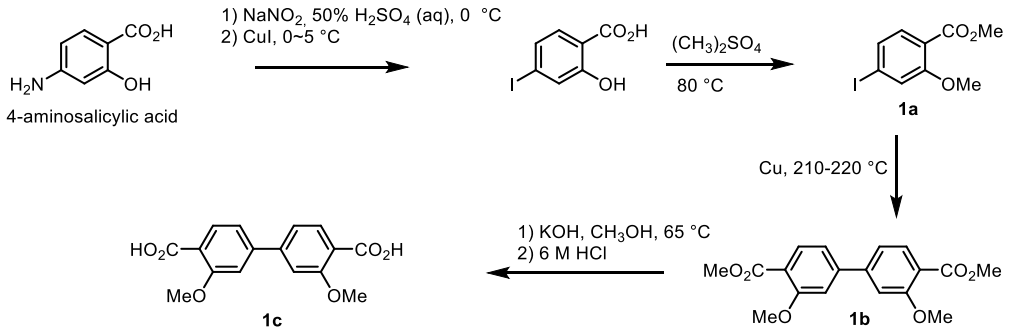

Scheme 3 Synthetic route to **1c** by Wang *et al.* [15]

[b] Price calculated from 25 g at www.sigmaaldrich.com, 15/01/2018

2.2 Alkylation of methyl 4-iodosalicylate

2.2.1 Motivation

As shown in **Scheme 2** is the first step of the synthetic pathway an alkylation of the phenolic position of the salicylate starting material. A justification of having this as the first step is being able to produce and screen through many different alkyl-substituted analogues. For this reason, alkylation by Williamson's ether synthesis by the use of alkyl halides was selected as the synthetic method. As a comparison to Wang's synthetic pathway discussed in **Section 2.1.1**, would analogization not be as easy due to the use of dimethyl sulfate as a methylating agent to simultaneously methylate the carboxylic acid and the phenolic position. This is problematic due to several reasons: Firstly, analogization would require other dialkyl sulfates, which is difficult to obtain with the exception of diethyl sulfate. Secondly, the usage of these dialkyl sulfates would also yield the corresponding alkyl salicylate ester, which could become problematic in terms of solubility, reactivity, or other chemical or physical properties. And thirdly, it is worth noting that dialkyl sulfates (especially dimethyl sulfate [16]) express a far greater toxicity than alkyl halides.

When the description for this MSc project was written was **2a** selected to be the first target molecule. The reasoning was that the ethyl substituent could express a middle ground in stericity and hydrophobicity and therefore a good starting point for the project.

A previously published procedure for the alkylation reaction was found in an article by Duckie *et al.* from 2013, who have been working with the same starting material.[17] Their procedure is shown in **Scheme 4**.

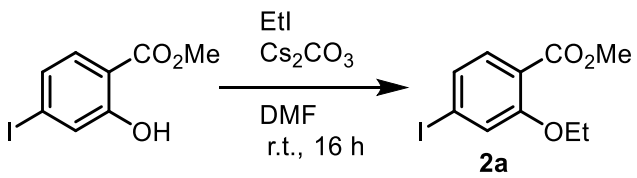

Scheme 4: Reaction procedure for the alkylation of methyl 4-iodosalicylate[17]

As the scheme shows, their procedure calls for the use of Cs_2CO_3 as a base, and N,N-dimethylformamide (DMF) as a solvent. Cesium carbonate is a common choice for a base in these kinds of reactions, especially when using DMF due to the increased solubility.

However, it is more expensive than other, more conventional bases such as sodium or potassium carbonate. Sigma Aldrich lists Cs_2CO_3 for approximately 5 NOK/g, while K_2CO3 is listed for 1.5 NOK/g.[c]

After some early attempts of this reaction it was clear that residual DMF was prone to be problematic, even after several washings and dryings of the products. In order to prevent this problem an attempt was made to change the solvent system from DMF to something that is easier to remove in the workup. For this, acetonitrile was chosen due to its similar solvating properties and higher vapor pressure. In the same experiment an attempt to use the cheaper potassium carbonate was additionally done. To overcome the solubility problem was the reaction in this case also heated to reflux conditions. The overall optimized reaction conditions are given in **Scheme 5**.

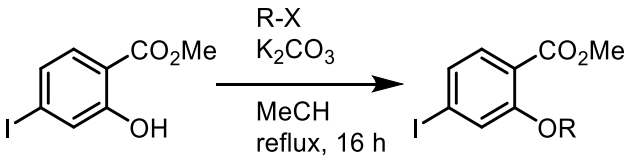

R: Me, Et, nPr, iPr, nBu, nHex, MeCy, Bn, allyl

Scheme 5: Optimized reaction conditions for the alkylation of methyl 4-iodosalicylate.

[c] Prices calculated from 500 g at https://www.sigmaaldrich.com/, 09.01-2018

2.2.2 Synthesis of methyl 2-methoxy-4-iodobenzoate (1a)

1a was synthesized using methyl iodide as the alkylating reagent. The reaction yielded a clear viscous oil as a product, which in several replications contained residual amounts of solvent (such as acetonitrile, ethyl acetate or dichloromethane) that was difficult to remove. To mediate this, diethyl ether was used during the work up instead of ethyl acetate, making it easier to remove the solvent residuals. Despite the change of solvent is the presence of residual acetonitrile still observed. No further attempts of removing this was made, due to it having no implications on the proceeding reaction. The ^{1}H NMR spectrum is shown in **Figure 9**.

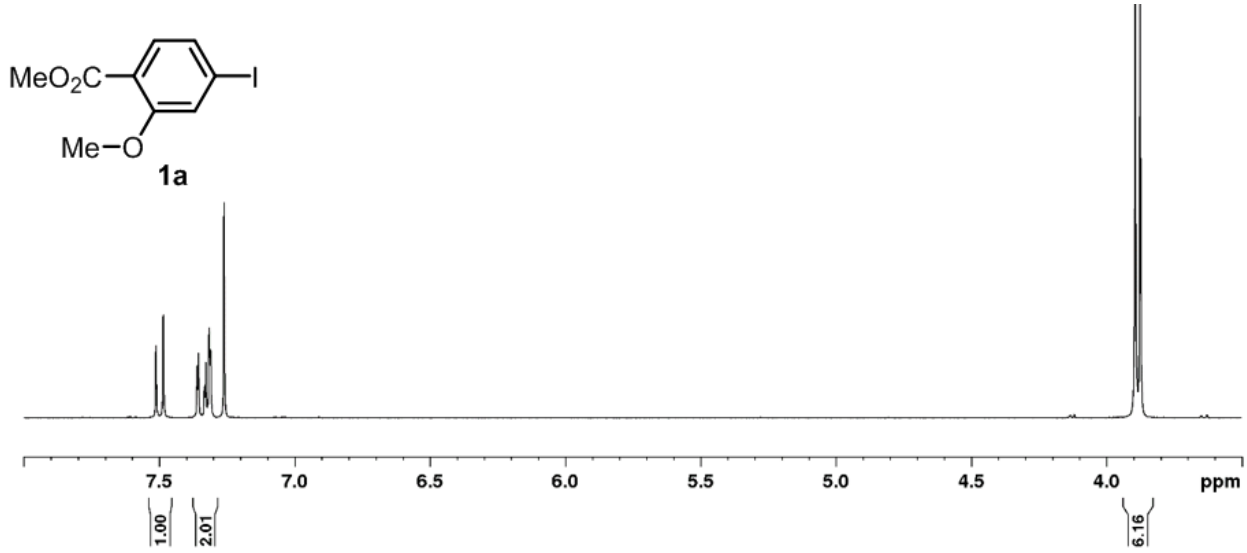

Figure 9 ^{1}H NMR spectrum of **1a**. (300 MHz, $CDCl_3$)

2.2.3 Synthesis of methyl 2-ethoxy-4-iodobenzoate (2a)

The synthesis of **2a** was, as mentioned in **Section 2.2.1**, the first synthesis in this project, which laid the ground for the other alkylated analogues by the means of reaction optimization. This synthesis has been repeated a handful of times in order to obtain the best conditions for the reaction. After the first couple of replications of the reaction, the improved reaction conditions resulted in a yield range of between 85 – 96 % from the theoretical yield. Later replications have improved the yield range to be consistently above 95 %. The reaction has also been scaled up to 10 g (36 mmol), yielding 98 % of the theoretical yield.

It is also worth noting that in the beginning of the optimization the isolated product was in all cases a slight yellow oil, while the original procedure reports it as a brown oil. After several

replications product **2a** is now isolated as a white or slight yellow solid, with a melting point between 43 – 44 °C. The ^{1}H NMR spectrum of **2a** is given below in **Figure 10**.

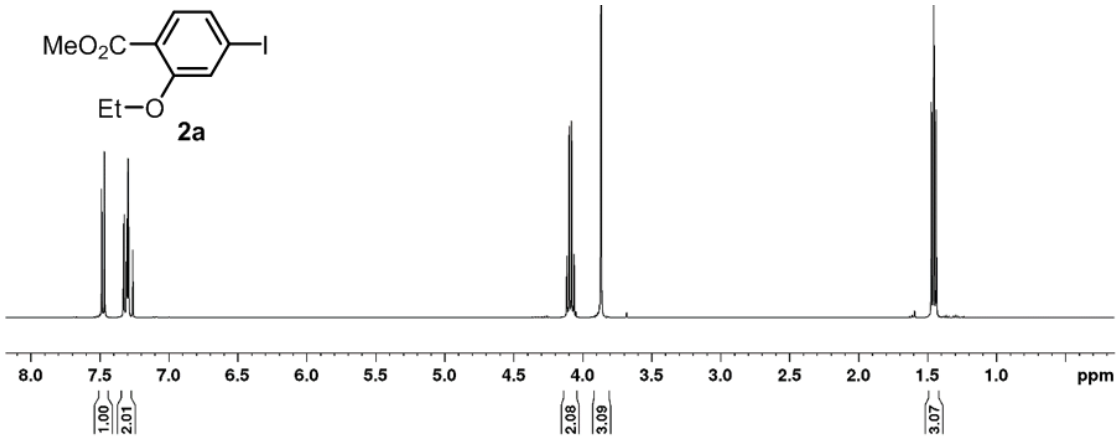

Figure 10: ^{1}H NMR spectrum of **2a**. (400 MHz, $CDCl_3$)

2.2.4 Synthesis of methyl 2-(n-hexyloxy)-4-iodobenzoate (3a)

n-Hexyl was selected to be the largest linear alkyl chain for this project, **3a** was synthesized using 1-bromohexane. The product was for the first replication isolated in 87 % yield, then in >95 % yield after repeated attempts at a 5 g scale. In all repetitions was a trace amount of 1-bromohexane present in the final product, as displayed in the NMR spectrum (**Figure 11**). Due to no apparent complications with this minor impurity in further reactions, was no further purification was performed.

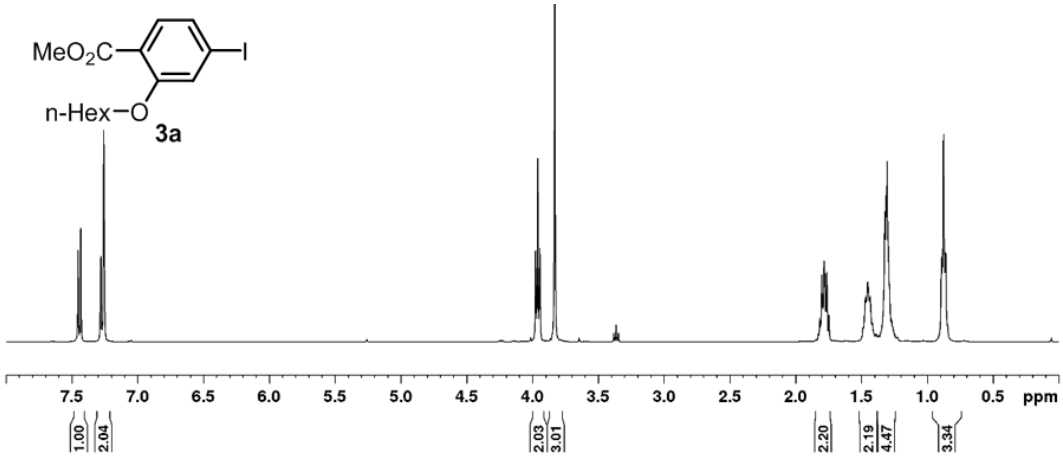

Figure 11: ^{1}H NMR spectrum of **3a**. Note the residual 1-bromohexane peak at 3.4 ppm.

2.2.5 Synthesis of methyl 2-isopropoxy-4-iodobenzoate (4a)

4a was synthesized in the same manner as previous analogues, using isopropyl iodide as the alkylating reagent. Compound **4a** was isolated in 92 % yield, as a yellow oil with small amounts of starting material present. It was later purified by washing the product with an aqueous base, yielding pure **4a**. (**Figure 12**)

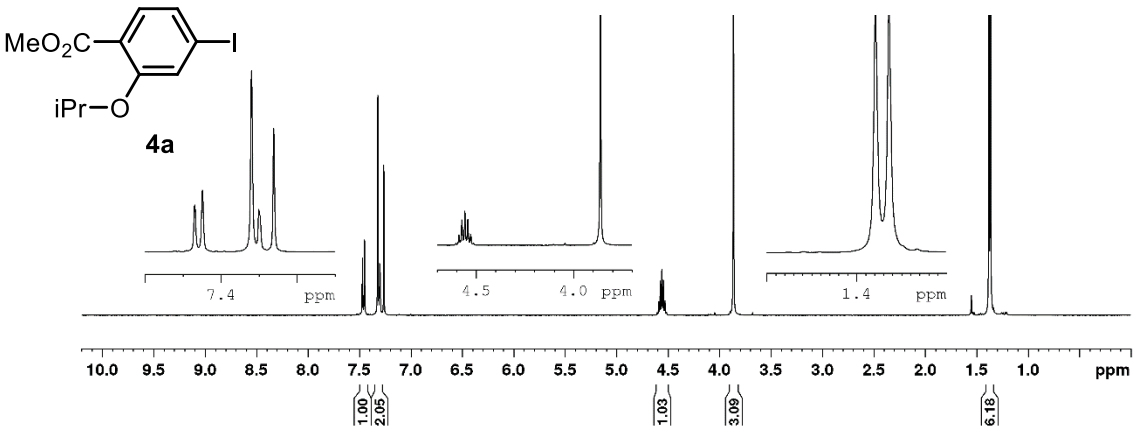

Figure 12 ^{1}H NMR spectrum of **4a**. (400 MHz, $CDCl_3$)

2.2.6 Synthesis of methyl 2-(n-butoxy)-4-iodobenzoate (5a)

n-Butyl ether **5a** was synthesized in similar manners as previous ethers, by reacting methyl 4-iodosalicylate with n-butyl bromide. **5a** was synthesized twice; where the first attempt resulted in a yellow oil with impurities and a relatively low yield (60 %). The second attempt gave a slight yellow oil with some acetonitrile present in 80 % yield. The ^{1}H NMR spectrum is shown below in **Figure 13**

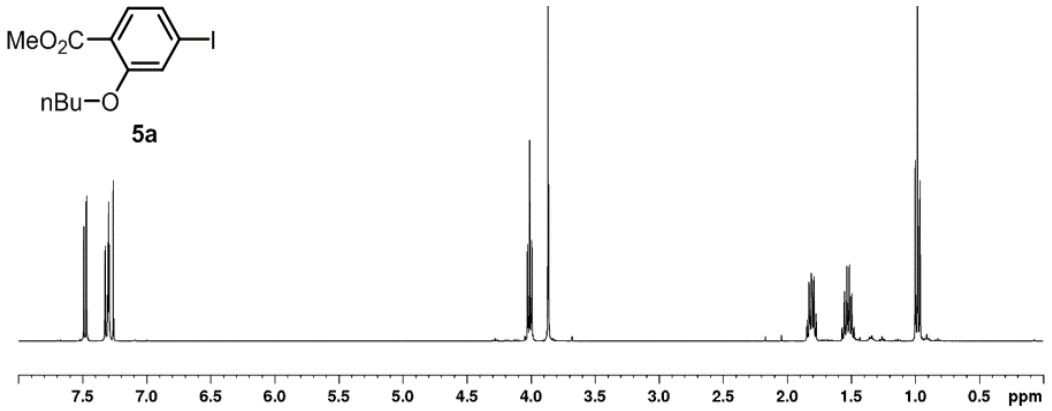

Figure 13: ^{1}H NMR spectrum **5a**. (400 MHz, $CDCl_3$)

2.2.7 Synthesis of methyl 2-allyloxy-4-iodobenzoate (6a)

Allyl ether **6a** was synthesized using allyl bromide (3-bromoprop-1-ene). The reaction yielded a thick, yellow oil that one week later solidified into a brown solid with a wax-like texture. The isolated compound was of decent purity but was recrystallized from a mixture of hexanes and methanol for the sake of interest. The compound melted during the process and resulted in poor growth of crystals.

The synthesis was later on repeated at a ten times larger scale resulting in 5.5 g of **6a**, corresponding to a yield of 96 %. **6a** was pure by ^{1}H NMR. (**Figure 14**)

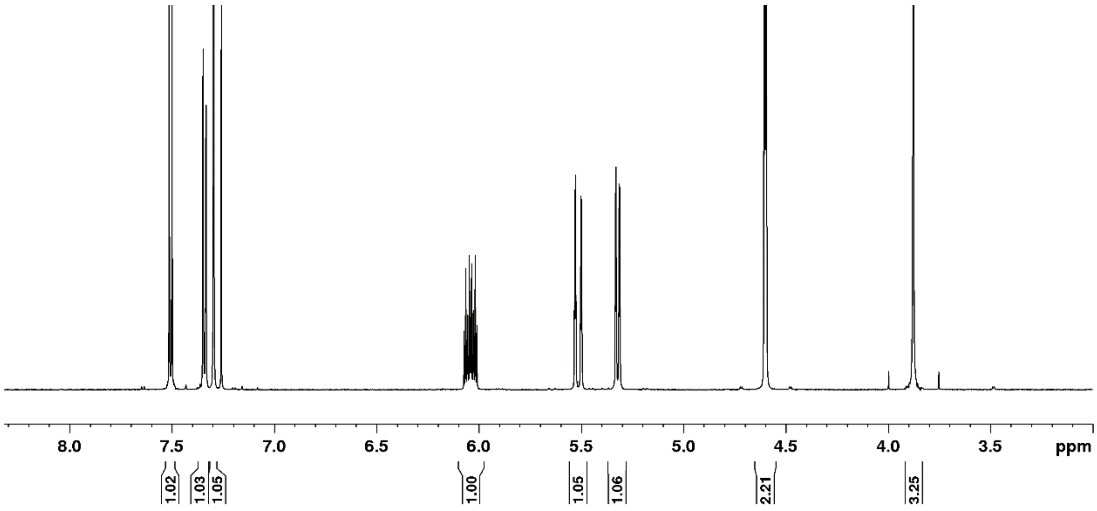

Figure 14: ^{1}H NMR spectrum of **6a**. (600 MHz, $CDCl_3$)

It is worth taking an extra look at the ^{1}H NMR spectrum of **6a**, due to the interesting allylic splitting patterns. There are four interesting peaks, which are shown in more detail in **Figure 15**.

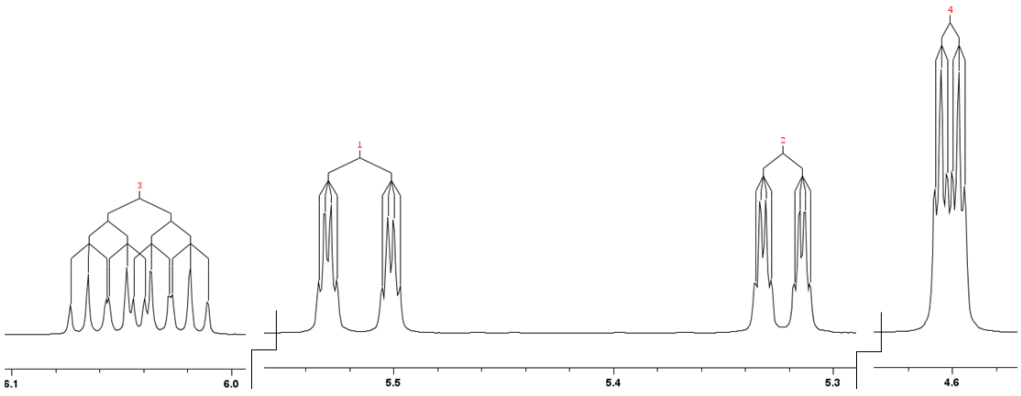

Figure 15: Selection of interesting splitting patterns in the (non-continuous) ^{1}H NMR spectrum of **6a**. ($CDCl_3$, 600 MHz)

It is difficult to accurately assign the different observed coupling constants, but an attempt was made: There are five different coupling constants observed (**Table 1),** and as shown in **Figure 16** are they not all assigned to each other, as indicated by the question marks behind the uncertain assignments. For instance, it is unclear whether the observed coupling constant of 1.4 Hz is the $^{2}J_{geminal}$ or the $^{4}J_{allylic}$ coupling. The most likely answer is that both couplings are present but have a similar coupling constant and is therefore overlapping. The observed multiplicity of the geminal protons on the sp^2-carbon (two doublet of quartets, dq) is most likely rather a doublet of doublet of doublets with the three coupling constants: $^{4}J_{allylic}$, $^{3}J_{cis\ /\ trans}$, and $^{2}J_{geminal}$, where $^{4}J \approx {}^{2}J < 2$ Hz.

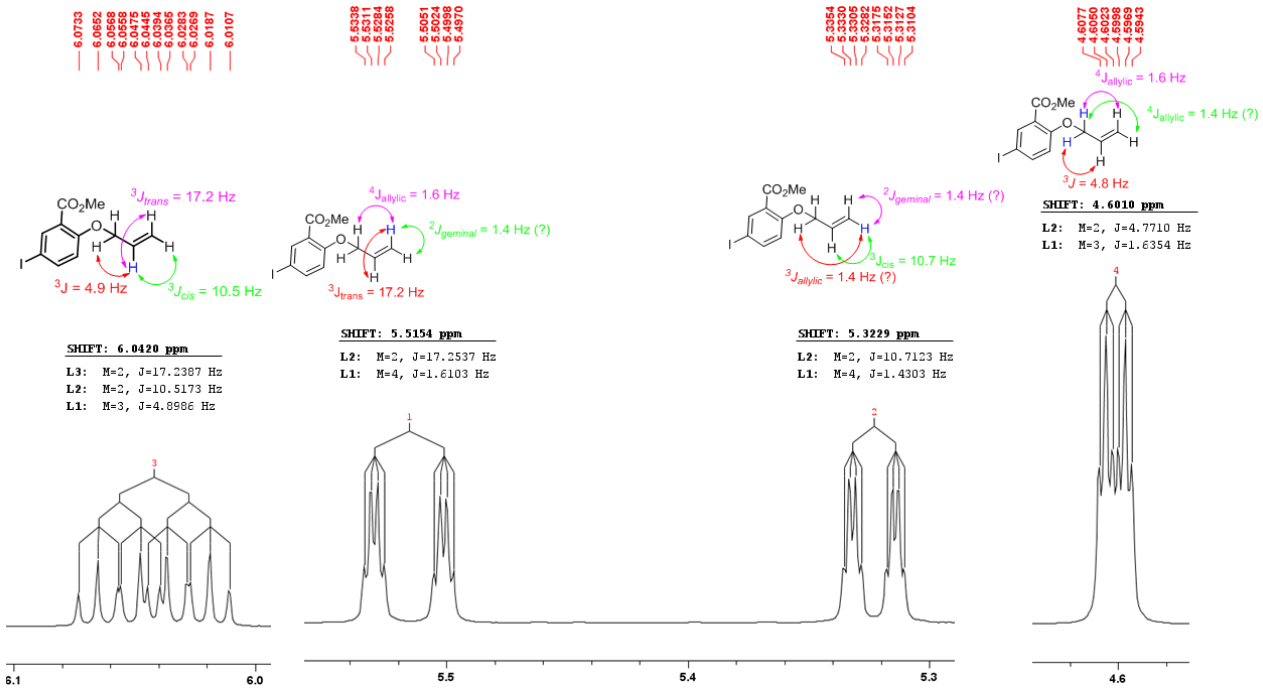

Figure 16: Attempt of assigning coupling constants for protons in the allylic system of **6a**.

Table 1: Approximate values for observed *J* - couplings in **6a**, together with the number of observed couplings.

J-coupling	Number of observed couplings
17 Hz	2
10 Hz	2
4.8 Hz	2
1.6 Hz	1
1.4 Hz	1

2.2.8 Synthesis of methyl 2-(n-propoxy)-4-iodobenzoate (7a)

n-Propyl ether **7a** was synthesized in similar manner as the previous analogues. Using n-propyl bromide, the first attempted synthesis resulted in a 65 % yield. The ^{1}H NMR spectrum showed the presence of silicon grease or some other impurity, so a second attempt to synthesize **7a** was performed. The second attempt yielded **7a** in a 93 % yield, but the ^{1}H NMR spectrum showed the presence of some unreacted starting material (< 1 % by NMR integrations). No attempts of purification were made. A ^{1}H NMR spectrum of **7a** is given in **Figure 17**.

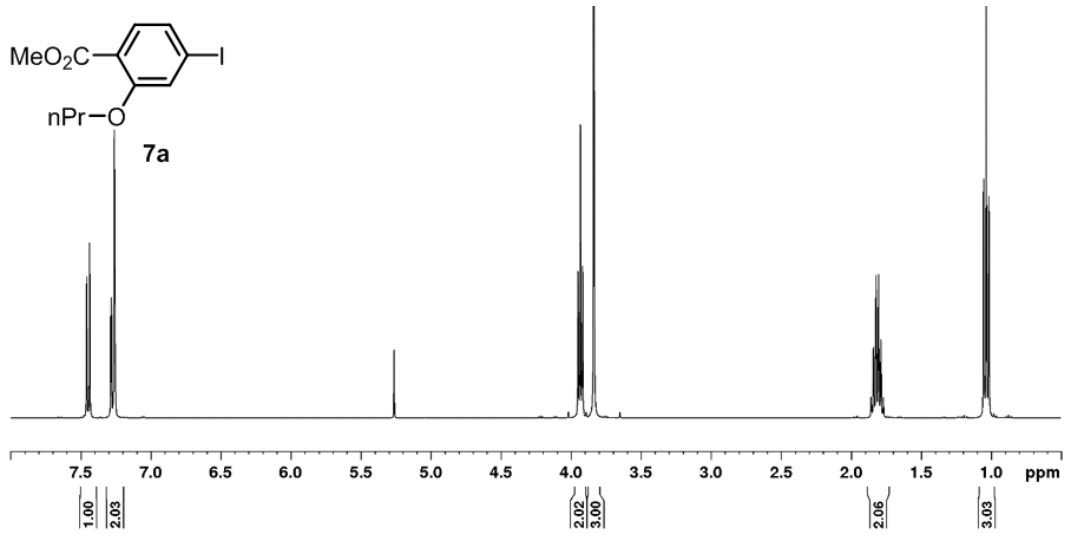

Figure 17 ^{1}H NMR spectrum of **7a**. (400 MHz, $CDCl_3$)

2.2.9 Synthesis of methyl 2-(benzyloxy)-4-iodobenzoate (8a)

In interest of broadening the scope of the alkylation reaction to analogues other than linear alkyl chains, an attempt to synthesize **8a** by the reaction with benzyl bromide was made. This resulted in a pale-yellow oil in 96 % yield. Some impurities were visible in the ^{1}H NMR (mainly benzyl bromide), which were tried removed by flash chromatography using a 10 % solution of ethyl acetate in hexanes as the eluent. This purification step removed most of the impurities, but some eluted together with the pure product. In order to remove the last visible impurities, the product was redissolved in diethyl ether and washed with a saturated solution of sodium bicarbonate, yielding an orange solid with a wax-like texture. The ^{1}H NMR spectrum of the purified product is given in **Figure 18**.

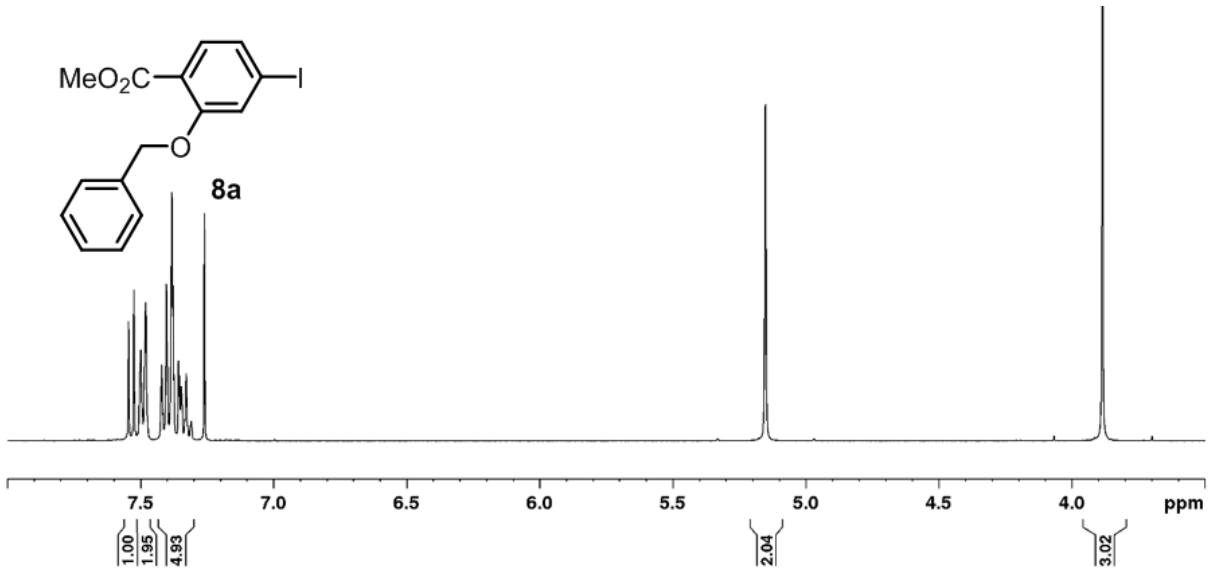

Figure 18: ^{1}H NMR spectrum of **8a** (400 MHz, $CDCl_3$)

2.2.10 Synthesis of methyl 2-(methylcyclohexyl)-4-iodobenzoate (9a)

Compound **9a** was synthesized using bromomethyl cyclohexane as the alkyl halide. The reaction was attempted twice, first time an impure product was obtained, with residual starting material and alkyl-bromide present. The second attempt yielded a relatively pure product in 98 % yield, with a ^{1}H NMR spectrum as shown in **Figure 19**.

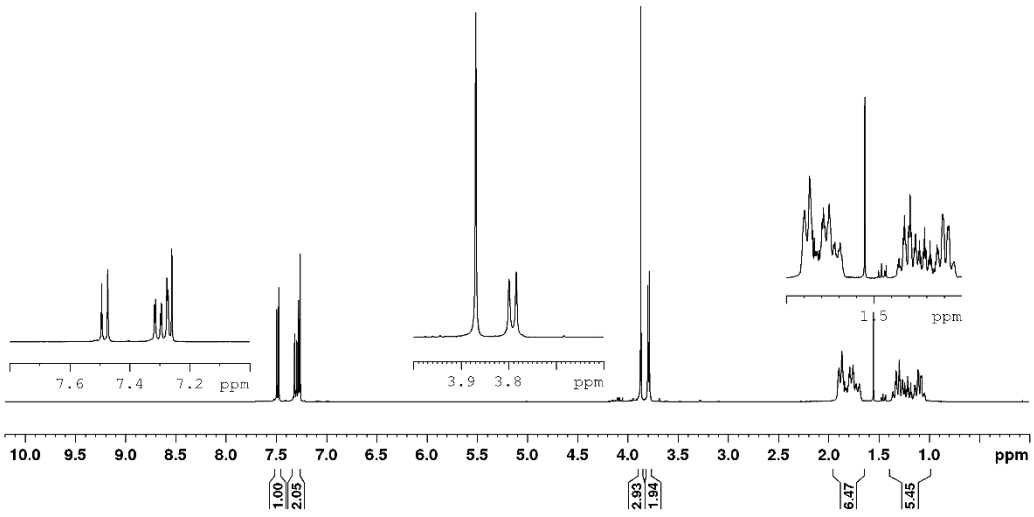

Figure 19 ^{1}H NMR of 9a. (400 MHz, $CDCl_3$)

2.2.11 Attempted synthesis of methyl 2-(t-butoxy)-4-iodobenzoate

An attempt of alkylating methyl 4-iodosalicylate with t-butyl bromide was made, despite the high probability of it not succeeding due to the assumed reaction pathway. Williamson's ether synthesis occurs by an S_n2-reaction pathway and as every introductory organic chemistry textbook claims: tertiary substrates do not undergo S_n2 substitution to any significant degree. This claim was (unsurprisingly) further proven by a mere 6 % yield in mass of the recovered material after working up the reaction, showing significant impurities in the ^{1}H NMR spectrum.

2.2.12 Characterization methyl 2-alkoxy-4-iodobenzoates

Like **Section 2.2.7** might indicate have all of these *O*-alkylated compounds been thoroughly characterized using NMR spectroscopy. Following is a more in-depth elucidation of these specific compounds, using the methyl alkylated analogue **1a** as an example. It is important to note that all of the compounds described in this chapter have been characterized in similar manner.

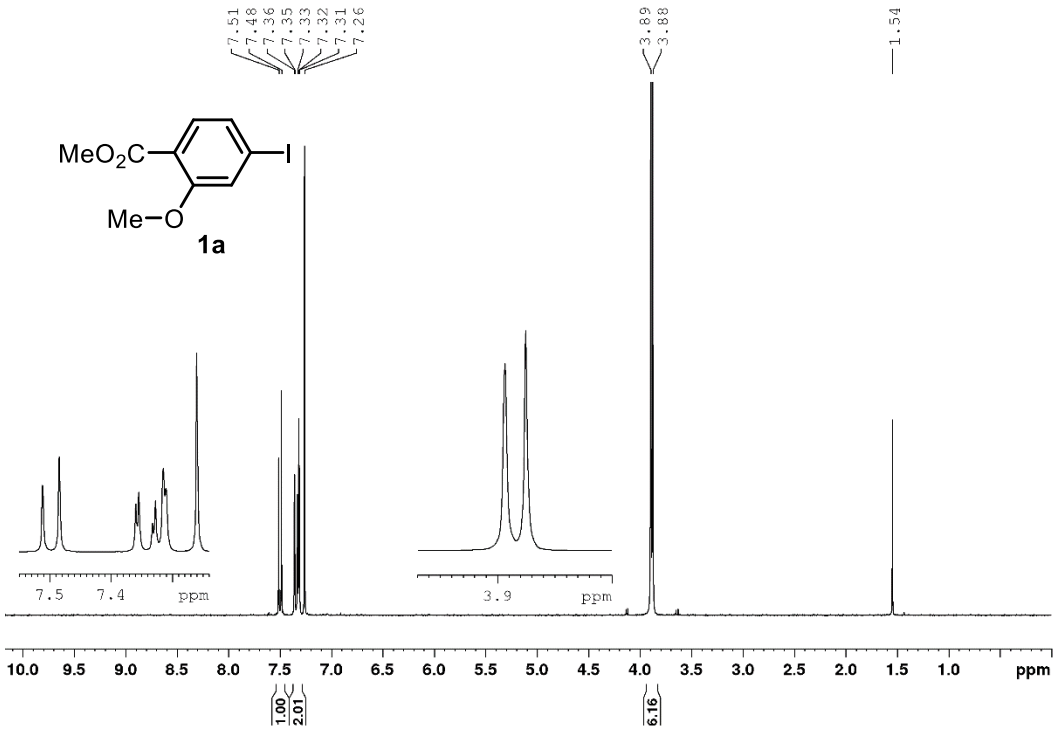

Figure 20 1H NMR spectrum of **1a**. (300 MHz, $CDCl_3$)

Looking at the ^{1}H NMR spectrum of **1a** (**Figure 20**), there are five signals visible from the product: three aromatic and two aliphatic. There are also two additional signals from residual $CHCl_3$ and H_2O in the NMR solvent (7.26 ppm and 1.54 ppm respectively). Two of the aromatic signals are partially overlapping and are generally poorly resolved. The aliphatic signals consist of two singlets almost appearing as a doublet. They integrate for three protons each, as expected from a methyl ester and a methoxy group. None of the signals can be assigned with absolute certainty from the ^{1}H NMR spectrum itself.

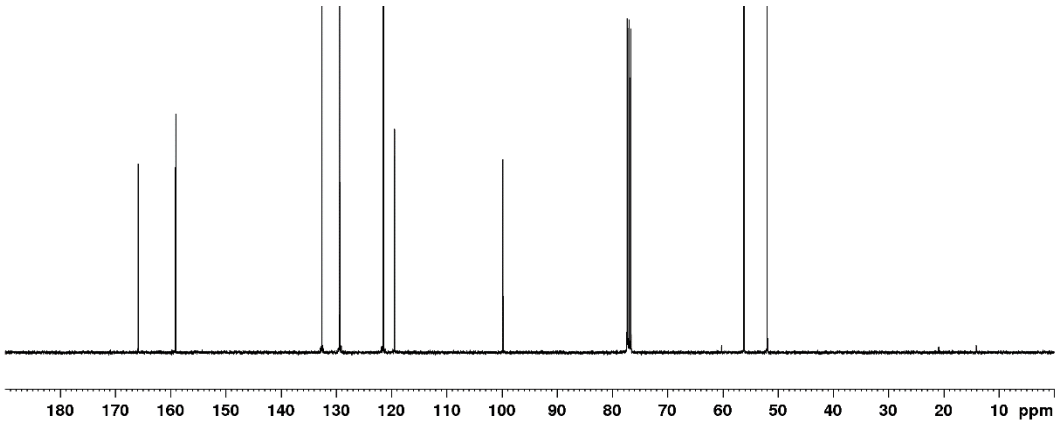

Figure 21 ^{13}C NMR spectrum of **1a**. (101 MHz, $CDCl_3$)

The ^{13}C NMR displays the eight carbon atoms present in **1a**, two aliphatic, six aromatic from the ring and one from the carboxylate. The iodinated carbon (**4**-I) is in all of the acquired ^{13}C NMR spectra for these types of compounds consistently located at around 100 ppm. Therefore, it is safe to assume that the peak at 99.8 ppm from the iodinated carbon (**4**). It is also relatively safe to assume that the signal with the highest chemical shift (166 ppm) is from the carboxylate.

In order to assign the peaks confidentially are 2D NMR techniques required: From the ^{1}H-^{13}C HMBC spectrum (**Figure 22**) can the correlations between the carboxylate carbon and the lower shifted singlet be assigned as the methyl ester group (CO_2**Me**). By the process of elimination is the other methyl singlet assigned to be the methoxy ether (**Me**O-Ar), which correlates to the 159 ppm carbon signal. Knowing the carboxylate carbon's chemical shift allows for the assignment of the **2**-H signal, which is the only aromatic proton that will correlate with the carboxylate. The doublet at 7.4 ppm in the ^{1}H NMR spectrum is therefore from the proton in the **2** position of **1a**, which makes sense in terms of coupling as it is too far away to couple with the proton in the **5** position.

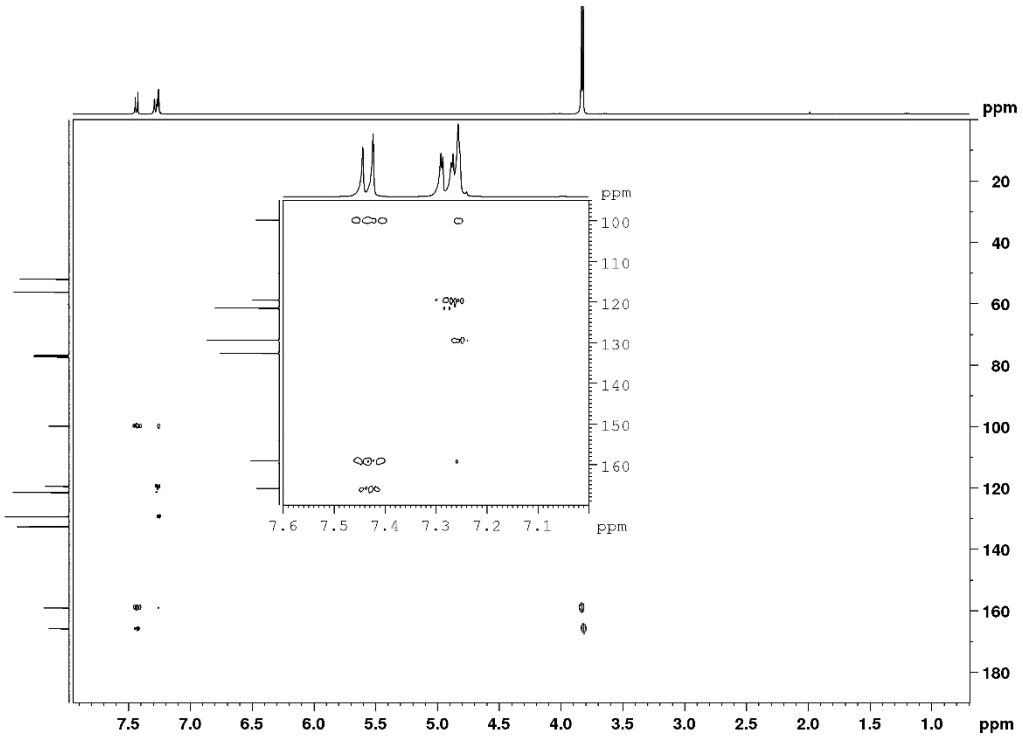

Figure 22 ^{1}H-^{13}C HMBC spectrum of **1a**. (400 - 101 MHz, $CDCl_3$)

Due to the aforementioned overlap of the other two aromatic peaks it is difficult to accurately assign but based on their multiplicities would it be expected for the 3-**H** to be a doublet of

doublets, consisting of a ^{3}J and a ^{4}J coupling. The remaining aromatic proton would be expected to be a doublet with a small ^{4}J coupling constant. These expected multiplicities are barely visible in the spectra.

By applying the knowledge gathered from the HMBC to the HSQC (**Figure 23**) is the carbon atom at 133 ppm assigned to be the carbon atom in position **2**.

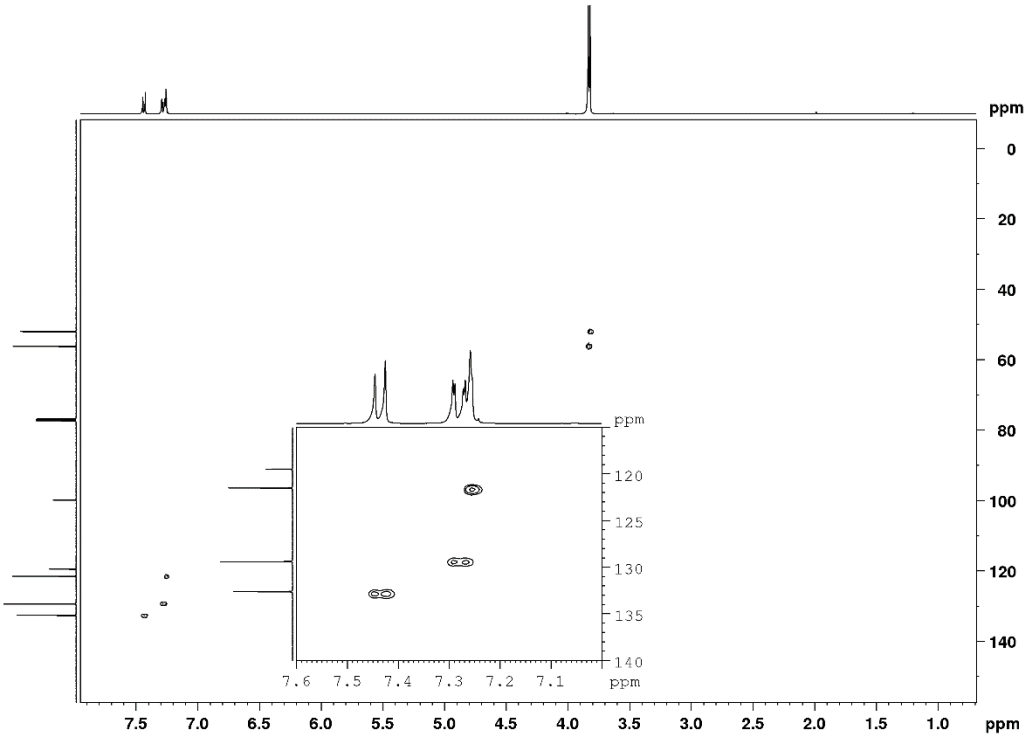

Figure 23 ^{1}H-^{13}C HSQC spectrum of **1a**. (400-101 MHz, $CDCl_3$)

All of these alkylated compounds have also been characterized using mass spectrometry (EI), where the expected molecular ion is present, together with a few shared, characteristic fragment ions such as m/z: 246 and m/z: 218, which probably is due to the presence of the following ions, or at least isomers of them. (**Figure 24**)

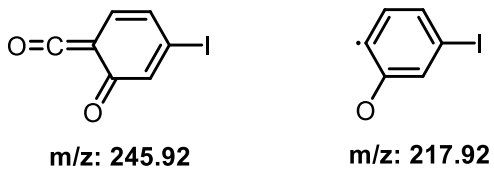

m/z: 245.92 **m/z: 217.92**

Figure 24 Probable structure of some fragment ions observed in the mass spectra of the alkylated salicylates.

2.2.13 Discussion and conclusions of the alkylation reactions

In this chapter, an effective, high-yielding procedure of O-alkylating methyl salicylates has been developed and thoroughly explored. The alkylated products have all been characterized by various techniques. The reactions are easily performed and require no demanding or time-consuming purification steps (such as flash chromatography). In some cases, starting material were present in the final product, but this was easily removed by washing the product with an alkaline solution. It could potentially also be solved by running the reaction for a longer time or adding a larger excess of the alkyl halide. The developed procedure has been shown to work with a handful of various analogues, spanning from a simple methyl group to large groups such as n-hexyl, phenyl or methyl cyclohexyl. The reaction procedure was not attempted optimized in regards of reaction time, it was usually left overnight and worked up next morning. It is highly possible that the reaction could in some cases be finished after 2 – 3 hours, but this was not investigated.

2.3 Homo coupling of methyl 2-alkyl-4-iodobenzoates

2.3.1 Motivation

The coupling of the alkylated benzoates was based on an article published by Nising *et al.* from 2004, where they report a palladium catalyzed cross coupling of aryl halides to form symmetric biaryl systems.[18] The reaction itself is a variation of the Suzuki-Miyuara reaction, but instead of adding 0.5 equivalents each of an aryl halide and an arylboronic acid or ester, is 0.5 equivalents of bis(pinacolato)diboron (B_2pin_2) added to make a boronic ester *in situ*. Due to this, is the reaction technically not a homo coupling, but a cross coupling reaction. For the sake of simplicity will this specific reaction be referred to as a homo coupling. Since all of the target molecules for this thesis are symmetric biaryls, Nising's method is sufficient for the next step of the synthetic path. The reaction conditions published in the aforementioned paper is given below in **Scheme 6**.

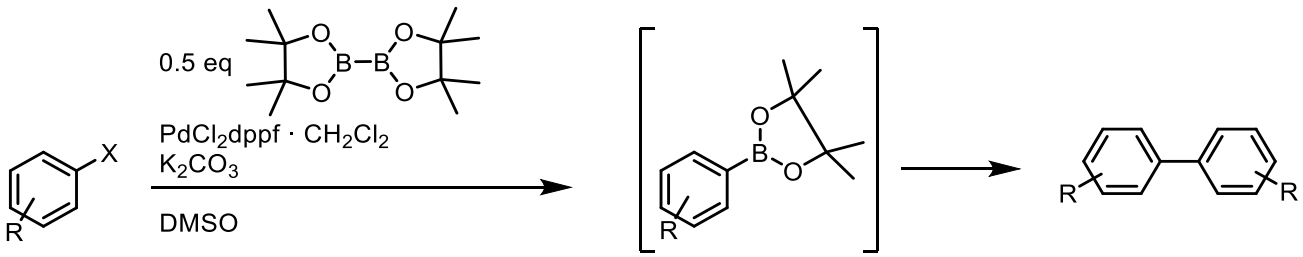

Scheme 6: General reaction conditions for the homo coupling reaction reported in Nising's paper.[18]

The *in situ* generation of the arylboronic ester shown above allows for the palladium catalyzed coupling reaction to occur. The reported catalyst loading is 4.0 mol % of the palladium compound.

2.3.2 Synthesis of dimethyl 3,3'-diethoxybiphenyl-4,4'-dicarboxylate (2b)

The reaction conditions for the first attempt of this coupling reaction is given shown below in **Scheme 7**.

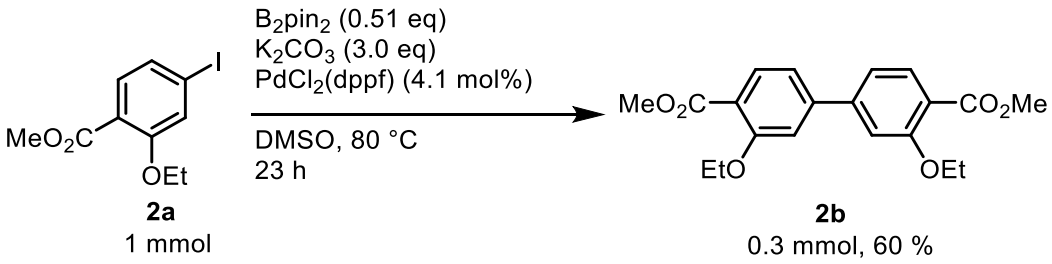

Scheme 7: Reaction conditions for the homo coupling of **2a**

The first attempt seemed promising, but after several replications and slight variations it was clear that there was little consistency in yield and purity. A handful of attempted variations are listed below in **Table 2**.

Table 2 Reaction conditions for syntheses of **2b**, divided into small and large scale.

Entry	2a (mmol)	B_2pin_2 (equiv.)	Catalyst (mol. %)	Concentration[d] (mol/L)	Yield[e] (%)
		Small scale (< 6 mmol)			
1	1.0	0.55	3.8	0.17	60 [f]
2	1.0	0.53	2.0	0.14	49 [f]
3	1.0	0.52	1.9	0.17	58 [f]
4	1.0	0.52	2.8	0.17	51 [f]
5	3.3	0.50	2.7	0.33	62 [g]
6	3.3	0.57	2.8	0.33	45 [g]
		Large scale (> 6 mmol)			
7	15	0.60	1.8	0.20	81[f]
8	17	0.60	1.8	0.23	73 [g]
9	16	0.60	1.9	0.16	72 [g]
10	8.6	0.60	1.9	0.17	73 [g]
11	16	0.44	1.7	0.20	66 [g]
12	6.5	0.55	2.7	0.33	41 [g]
13	6.6	0.55	2.7	0.33	69 [f]
14	6.6	0.55	2.8	0.33	59 [f]
15	6.6	0.52	1.9	0.22	50 [g]

[d] Concentration of **2a** in DMSO.

[e] Theoretical yield calculated from half of the amount of **2a**.

[f] Purified by flash chromatography (20:80 EtOAc in hexanes)

[g] Purified by silica filtration (silica plug) + recrystallization.

From this information it is possible to extract a series of conclusions: Firstly, there does not seem to be any clear correlation between catalyst loading and yield, at least not in any significant degree. Secondly, the yield seems to be mostly dependent on the skills of the operator doing the work-up. Most of the variations in yield are during the earlier attempts, or when attempting a new method of working the reaction up. The later attempts seem to be more consistent in both yield and purity, which leads into the third conclusion; that the method giving the best yield of **2a** seems to consist of filtering the raw product through a plug of silica, then recrystallizing the obtained product from ethanol. A more detailed description of the work up is given in the experimental section.

Purification by flash chromatography was also shown to be effective but can be problematic at larger scales (2 g or more). It is also far more time consuming and requires a large volume of solvent. It did however in one instance lead to the largest recorded yield (**Entry 7**, **Table 2**). A good eluent for flash chromatographic purification is a mixture of ethyl acetate in hexanes, in a 20:80 or 30:70 ratio.

2.3.3 Alternative syntheses of 2b

Due to issues with the workup of the reaction based on Nising's synthetic procedure was an alternative synthesis attempted. It is inspired by the success with changing the solvent from DMF to MeCN in the alkylation reaction, as discussed in **Section 2.2.3**. The motivation was that if the use of DMSO as a solvent in the coupling reaction could be avoided, a less intensive workup would be required and perhaps lead to a more consistent yield. Due to this, the coupling reaction was attempted by switching the DMSO out with acetonitrile and K_2CO_3 was switched out with Cs_2CO_3 for increased solubility. The lower boiling point of the solvent allows the reaction to be refluxed at approximately the same temperature as before (82 °C vs 80 °C).

The first attempt of this reaction yielded 68 % of relatively pure product and seemed promising. However, due to a lack of available cesium carbonate it was not reattempted until much later in the project, long after the reaction had already been optimized for running in DMSO. For the sake of completion, the synthesis was attempted at a later point to confirm it indeed was a viable method of synthesis; and the second attempt resulted in a 77 % yield of product **2b**.

During these reattempts a realization was made: The alkylation reaction and the coupling reaction both require the use of a carbonate base, refluxing acetonitrile and both are set to react overnight. Because of this, an attempt of combining the two first reaction steps into a one-pot synthesis was done. The first attempt was performed at a 1 mmol scale, and successfully yielded **2b** in 76 % yield after purification with flash chromatography. It was then repeated at a 10 mmol scale which yielded 78 % after both flash chromatography and recrystallization. The extensive purification was probably not necessary, when no difference in the ^{1}H NMR spectra between products of the one-pot reaction and the two-step reactions was observed. A summarizing scheme of the different alternative syntheses is shown in **Scheme 8**.

Another change to the original synthesis is the addition of catalytic amounts of 1,1'-bis(diphenylphosphino)ferrocene (dppf, the ligand of the palladium catalyst) to the reaction mixture. According to the original paper by Nising[18] they recommend the addition of dppf to electron rich or sterically hindered systems that require a longer reaction time, in order to prevent the decomposition of the catalyst. Although the addition of the dppf does not seem to increase the yield of the reaction, it does noticeably reduce the amounts of decomposed

palladium in the reaction mixture. This makes the work-up of the reaction easier as the black palladium species are prone to stick to the walls of glass containers.

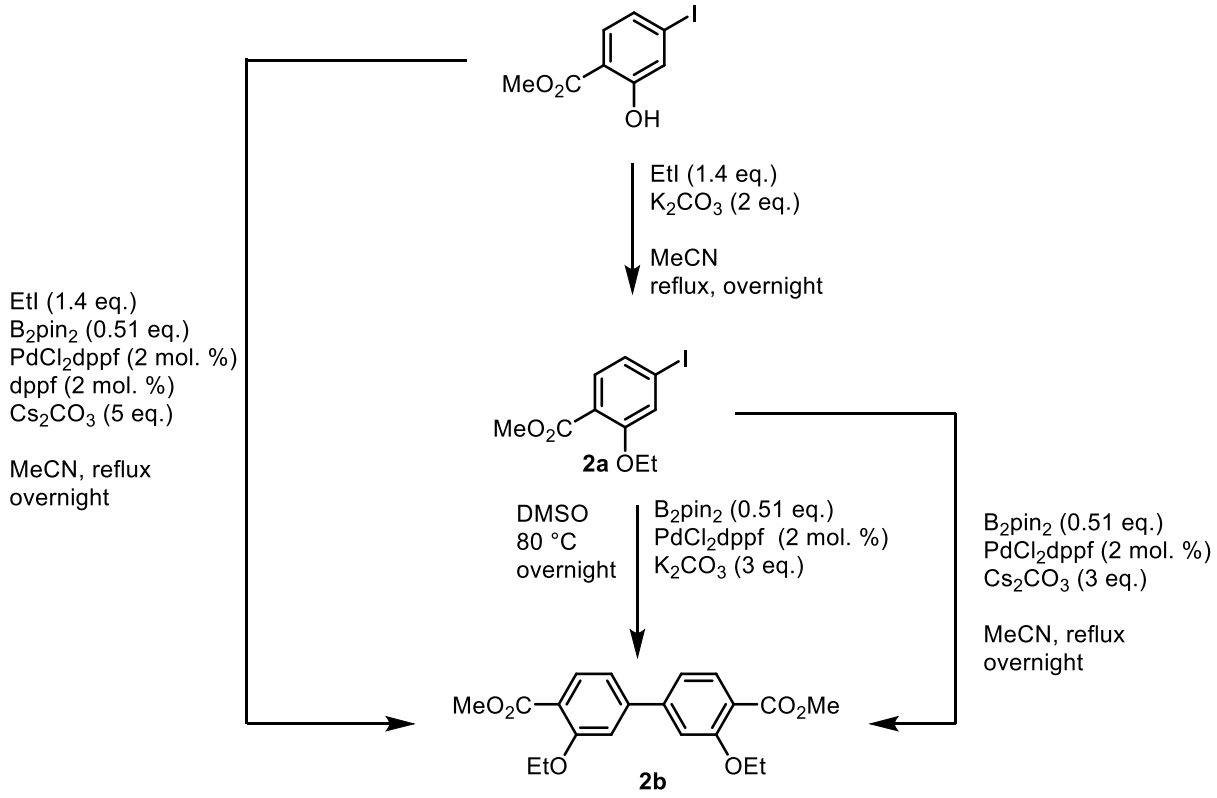

Scheme 8: Summary of alternative syntheses of **2b**.

2.3.4 Synthesis of dimethyl 3,3'-dimethoxybiphenyl-4,4'-dicarboxylate (1b)

The methyl functionalized analogue **1c** was not originally planned to be synthesized but due to the inconsistent results from the coupling of **2a**, it was desired to synthesize a simpler analogue in order to understand the system and the reaction better. Therefore, an attempt of coupling the methyl analogue **1a** under the same conditions as with **2a** was made. A summary of the experimental parameters for the homo coupling of **1a** is given below in **Table 3**.

Table 3 Summary of reaction conditions attempted for the homo coupling of **1a**.

Entry	1a (mmol)	B_2pin_2 (equiv.)	Catalyst (mol. %)	Concentration [h] (mol/mL)	Yield [i] (%)
1	0.98	0.53	6.4	0.16	75 [k]
2	1.0	0.51	1.8	0.17	72 [k]
3	3.5	0.50	1.8	0.19	78 [k]
4	34	0.60	1.9	0.17	69 [l]
5	15	0.60	1.8	0.17	81 [l]

[h] Concentration of **1a** in DMSO.

[i] Theoretical yield calculated from half of the amount of **1a**

[k] Purified by flash chromatography (20:80 ethyl acetate in hexanes)

[l] Purified by silica filtration (silica plug) + recrystallization.

It is clear from these results that the yields are more consistent and also overall higher than the yields reported in **Table 2** for the synthesis of **2b**. The reason behind the improved yields is not known, but it is clear that compound **1b** display significantly different solubility properties when compared to **2b**, despite the relative structural similarity. For instance, the solubility of **1b** in boiling ethanol is 0.025 mmol/mL *vs.* 1.0 mmol/mL for compound **2b**. The decreased solubility could hypothetically affect the yield positively due to less loss during the aqueous work up, but no evidence of any considerable solubility of **2b** in water is apparent.

2.3.5 Synthesis of dimethyl 3,3'-dihexyloxybiphenyl-4,4'-dicarboxylate (3b)

The coupling of hexyl analogue **3a** never gave rise to any major complications. The reaction yielded **3a** as a pure, crystalline product in relatively good yields (70 – 80 %). **3a** was purified either by recrystallization (ethanol), or by flash chromatography using acetone as the eluent.

2.3.6 Characterization of dimethyl 3,3-dialkoxybiphenyl-4,4'-dicarboxylates

The characterization of these compounds was mainly preformed using NMR techniques. In order to show how these techniques aid the characterization process is the characterization

of compound **2b** shown below as an example. It is important to note that all of compounds described in **Chapter 2.3** are characterized in the same manner.

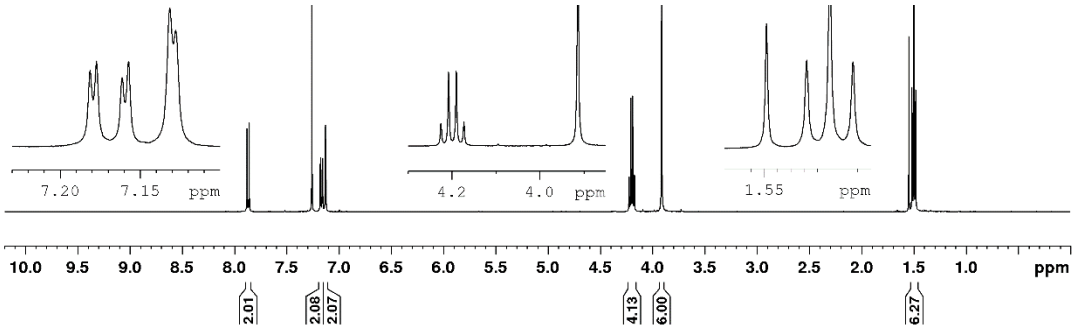

Figure 25: ^{1}H NMR spectrum of **2b**. ($CDCl_3$, 400 MHz)

The first and simplest method of characterization is the ^{1}H NMR spectrum (**Figure 25**). The spectrum is recorded in deuterated chloroform, and the residual solvent peak is therefore the singlet at 7.26 ppm. There is also some water present (in the NMR solvent mainly) giving rise to the peak at 1.55. All other peaks are from the compound itself. In the aliphatic region there are three peaks: a quartet, a singlet and a triplet present at 4.20, 3.91 and 1.50 ppm respectively. The ^{3}J coupling constants for the quartet and triplet are both at 6.98 Hz, indicating that they are coupled together (which is also confirmed by the COSY spectrum). Due to the integrals showing a 2:3 relationship between them, it is safe to assume these signals are due to the ethoxy groups in the molecule. Since the molecule has a C_2-symmetric axis only one set of signals shared from the two ethoxy groups is expected.

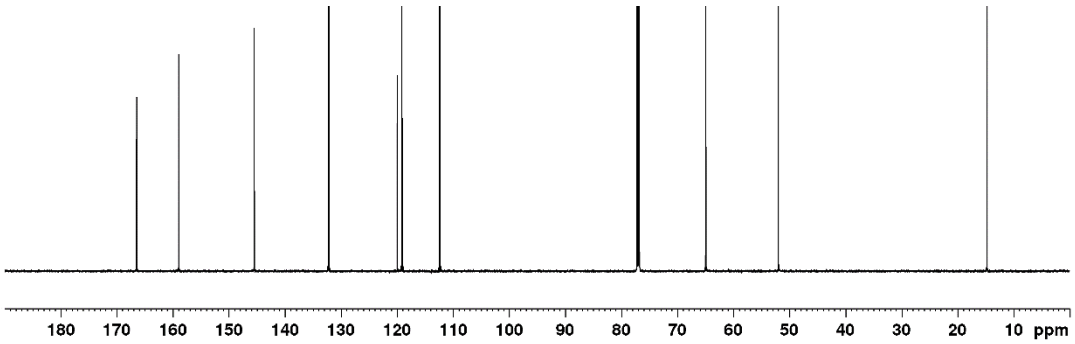

Figure 26: ^{13}C NMR of **2b**. ($CDCl_3$, 151 MHz)

The ^{13}C NMR spectrum (**Figure 26**) shows the expected ten signals from a total of twenty carbon atoms, again due to the C_2 symmetry of the molecule. Three aliphatic signals are visible, which can easily be assigned using 2D NMR techniques, for instance ^{1}H-^{13}C HSQC. (**Figure 27**). This NMR technique makes it simple to assign the signals in the ^{13}C spectrum

using the information we already have from the ^{1}H NMR spectrum. Hence, the carbon atoms giving the signals at 14.7, 52.0 and 64.9 ppm are assigned to be the -CH_2**C**H_3, -CO_2**Me** and -**C**H_2CH_3 signals respectively.

To further assign the aromatic peaks another 2D NMR technique is needed, ^{1}H-^{13}C HMBC (**Figure 28**). In the interest of simplification are all the observed correlations shown in **Figure 29**. By using HMBC can all signals from both ^{1}H and ^{13}C spectra be assigned. Due to the carbon atom in the 6,6'-position being the only carbon atom with no HMBC couplings, it is assigned using the method of elimination. A further proof of correct assignment is from the NOE correlation found between the -OC**H$_2$**CH_3 and the 2,2'-**H** (**Figure 30**). This simplifies the difficult assignment of the otherwise very similar 2,2' and 5,5'-carbons and hydrogens.

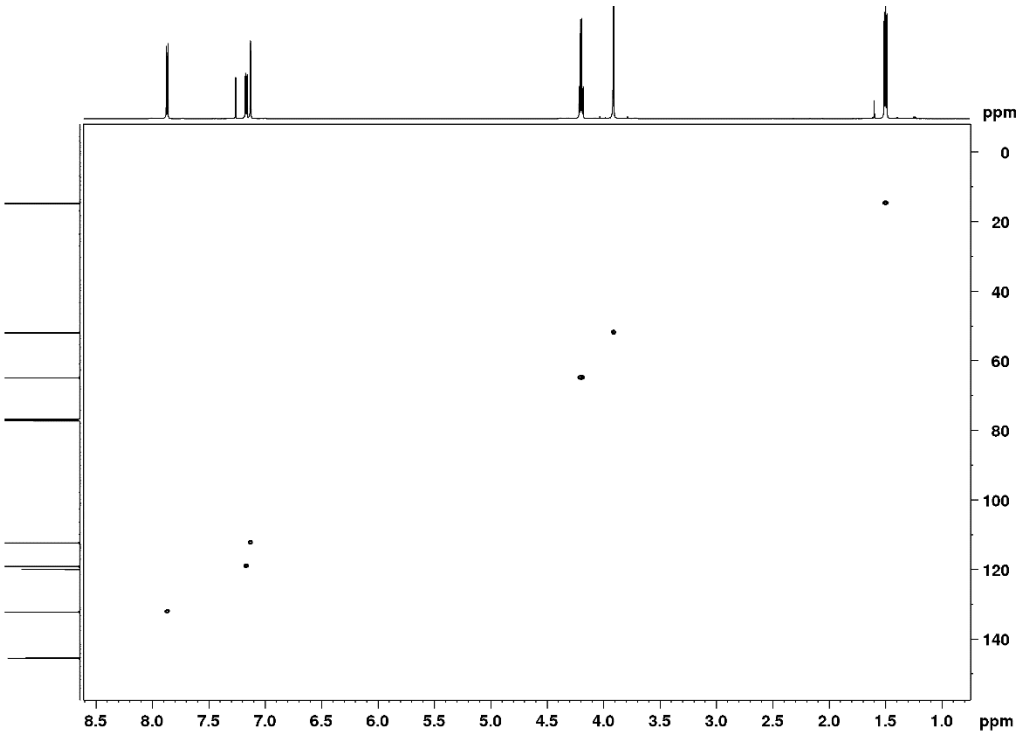

Figure 27: ^{1}H-^{13}C HSCQ spectrum of **2b**. ($CDCl_3$, 600 - 151 MHz)

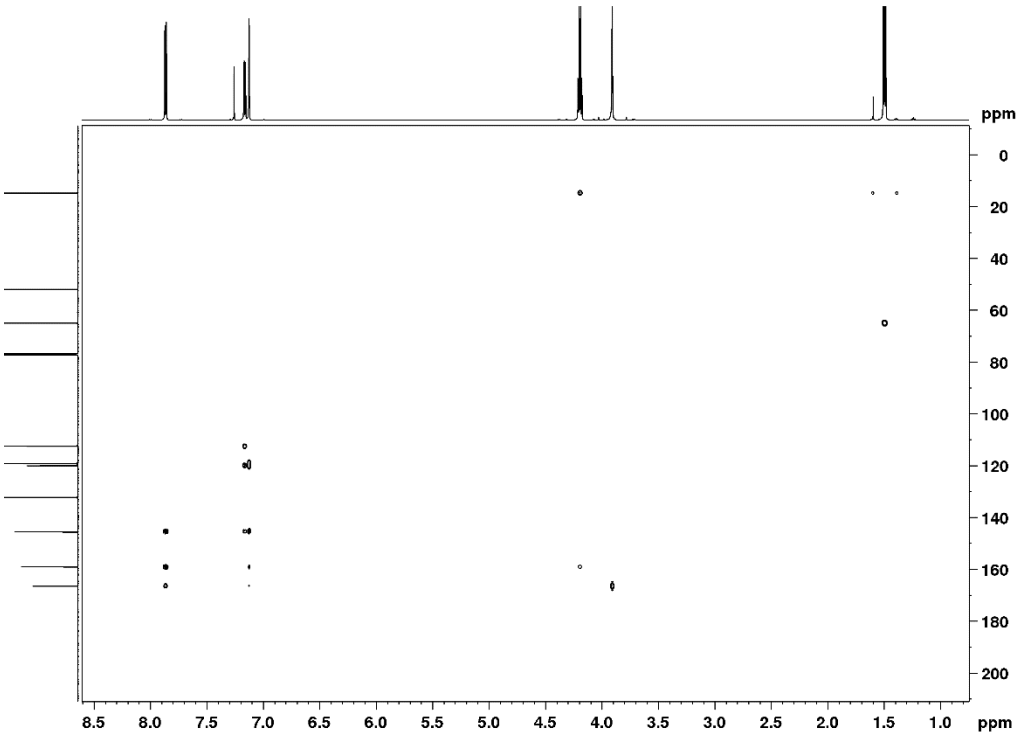

Figure 28: ^{1}H-^{13}C HMBC spectrum of **2b**. ($CDCl_3$, 600 - 151 MHz)

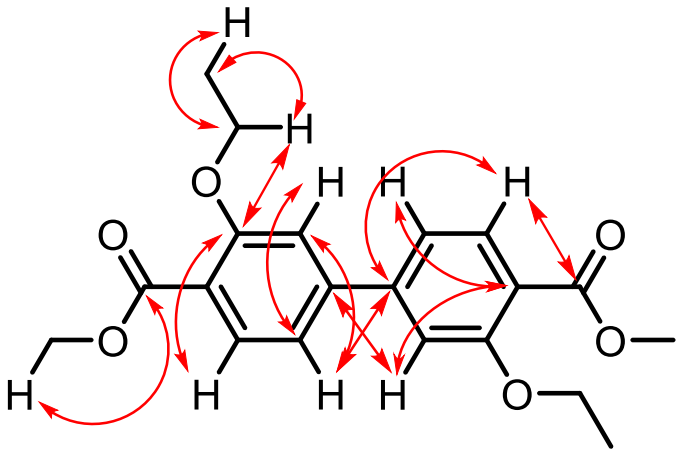

Figure 29: Observed ^{1}H-^{13}C HMBC correlations for compound **2b**.

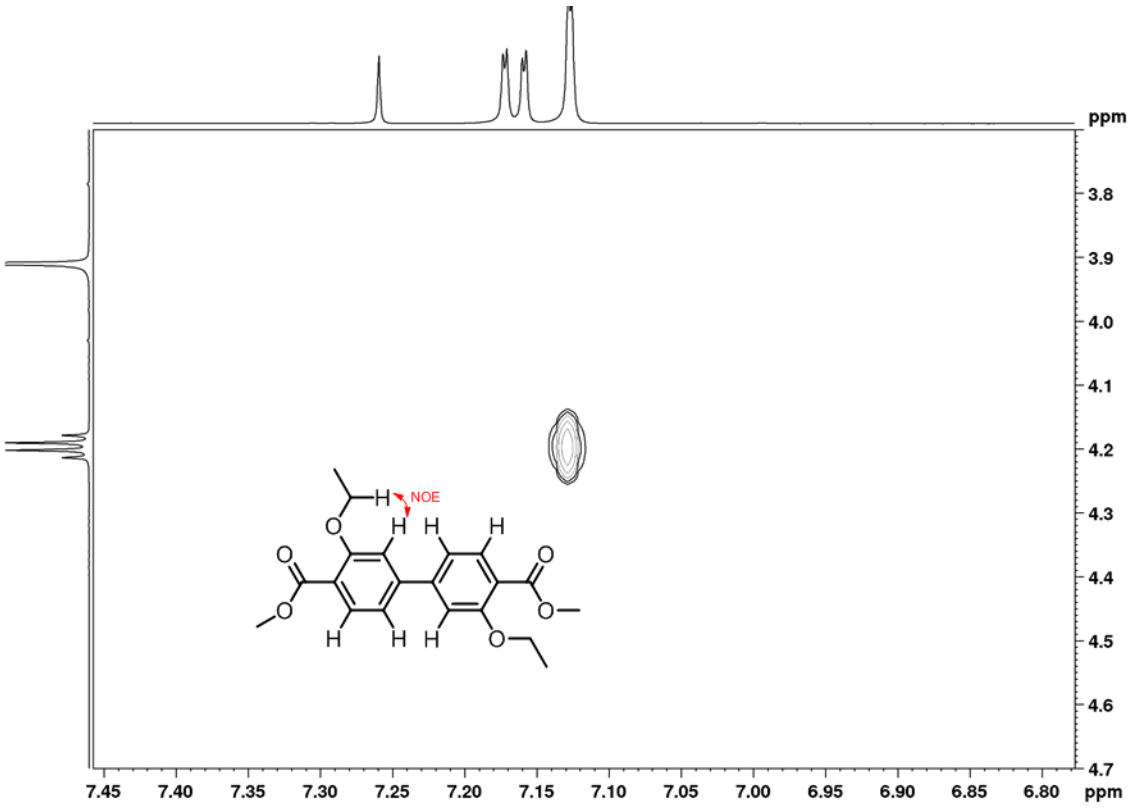

Figure 30: Selected NOESY correlation in **2b.** ($CDCl_3$, 600 MHz)

In addition to extensive NMR characterization were the compounds also characterized using EI mass spectrometry and melting point analysis. For these compounds, including **2b**, are a peak with a m/z of 238 is observed. A plausible reaction mechanism is described in "Interpretation of Mass Spectra" by Fred W. McLafferty [19] (page 245, 4th edition), as shown in **Figure 31**.

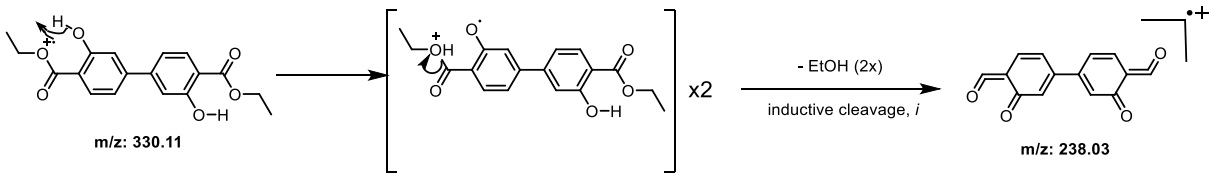

Figure 31: Possible mechanism for the formation of an ion with m/z = 238.

During an introductory course to single crystal X-ray crystallography was an opportunity to collect a crystal structure for compound **2b** (and **2b** only) available. The crystal structure is given in **Figure 32**.

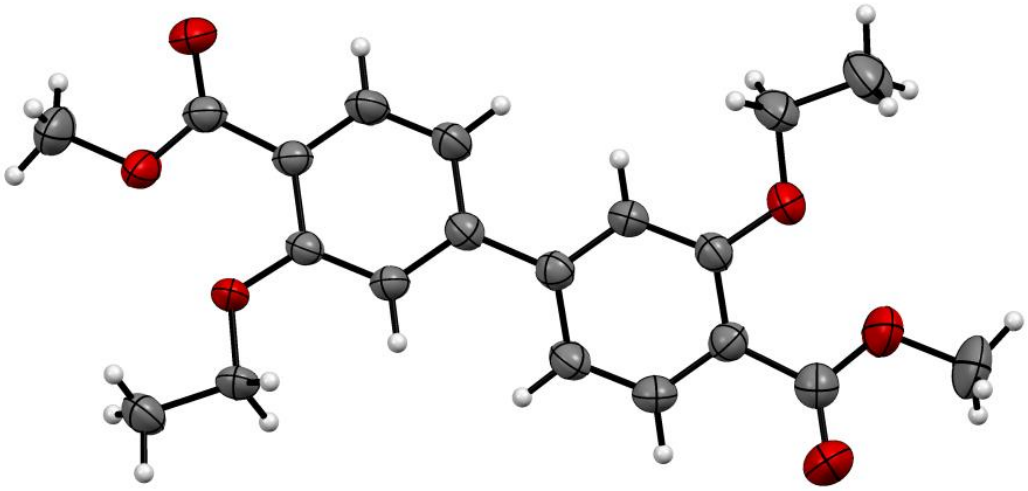

Figure 32 Crystal structure of compound **2b,** obtained by single crystal X-ray diffraction.

All bond angles and distances displayed by the crystal structure are within expected ranges. The two phenyl rings are not in plane but are twisted by roughly 30°. The carboxylic esters are also twisted off-plane in the opposite direction by another 30°, meaning they are roughly in-plane with the phenyl ring on the opposite side.

Due to SC-XRD not being particularly useful nor relevant for this type of work were no crystal structures of either **2a** or **2c** obtained.

2.3.7 Discussion and conclusions of the coupling reactions

The reaction conditions for the homo-coupling of methyl 2-alkoxy benzoates has gone under a large amount of optimization in order to be consistent in terms of yield and purity. The large amount of optimization has revealed a handful of small quirks about the reaction that has provided usefulness. For instance, the use of acetonitrile and cesium carbonate allows for the coupling to be done under water-free conditions, something that would have been difficult and very demanding to perform under the DMSO-conditions. The usage of dppf in order to prevent catalyst decomposition also made the reaction a lot more pleasant to work-up, which is something every chemist would appreciate even though it might not have been strictly necessary in terms of improving the reaction yield.

The ability to synthesize a dialkoxy functionalized dimethyl biphenyl-4,4'-dicarboxylate in a one-pot reaction starting from a cheap starting material is also a valuable discovery. This shortens the time it takes convert methyl 4-iodosalicylate into linker **1c**, **2c** or **3c** (or potentially other analogues) by a whole one day.

2.4 Hydrolysis of dimethyl 3,3'-dialkoxy-1,1'-biphenyl-4,4'-dicarboxylates

The hydrolysis reaction is based on a general procedure commonly used in the Catalysis group.[20] It is an alkaline ester hydrolysis that uses lithium hydroxide as a base. The reason for the use of lithium and not cheaper bases such as sodium or potassium hydroxide is due to previous problems with the presence of sodium ions when synthesizing a metal-organic framework. The actual mechanism behind these problems is not investigated, but as a pre-caution; is lithium hydroxide now used instead and the problems have disappeared.

The solvent system for the hydrolysis is a mixture of tetrahydrofuran, methanol and water (2:1:2 by volume). Traditionally has the reaction been run at ambient temperatures overnight, but for some cases in this work has there been some observed unreacted or semi-reacted starting material in the final product, so the hydrolysis reactions for this project are run at 50 °C overnight instead. The procedure for the saponification is shown in **Scheme 9**.

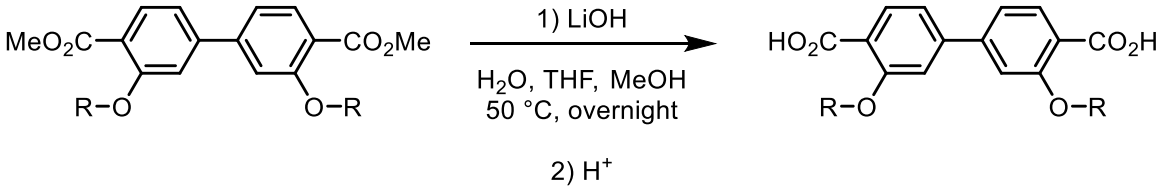

Scheme 9 General procedure for the hydrolysis of dimethyl biphenyl dicarboxylates.

2.4.1 Synthesis of 3,3'-diethoxybiphenyl-4,4'-dicarboxylic acid (2c)

The diethoxy-substituted compound **2b** was the first substrate to undergo hydrolysis in this project. The reaction is very straight forward, where the diester of the linker is stirred together with lithium hydroxide in the solvent system at 50 °C overnight. The following day are the volatile solvents removed using rotary evaporation, before the remaining aqueous solution is transferred to a beaker where it is diluted in water, and an acid is added to protonate the carboxylates. The acid used is either glacial acetic acid or concentrated hydrochloric acid. The protonated linker is insoluble in water, and therefore precipitates, then separated by vacuum filtration and dried in an oven at 130 °C overnight. The reaction is believed to go to completion, but the yielded product is often problematic to isolate quantitatively due to its consistency when wet, making it very hard to transfer after filtration, and when dry it is very difficult to remove from glassware due to some attractive forces between the glass and the dry product. In some cases, the isolated product was contaminated with filter paper due to the difficulties removing it from the Büchner funnel. This is especially prone to happen if hydrochloric acid is used for protonation, making the filter paper brittle from the acidic medium and therefore prone to break into small pieces. Using acetic acid prevents this, but it is surprisingly difficult to remove traces of the acetic acid in the final product, despite washing with copious amounts of water and drying at 130 °C.

2.4.2 Synthesis of 3,3'-dimethoxybiphenyl-4,4'-dicarboxylic acid (1c)

The hydrolysis of **1b** has in every case proven to be non-problematic with the exceptions of the aforementioned issues with the product sticking to filter paper. There has never been observed any non-hydrolyzed reactants in the final product, even when the reaction was performed at ambient temperatures.

2.4.3 Synthesis of 3,3'-dihexoxybiphenyl-4,4'-dicarboxylic acid (3c)

Compound **3c** was synthetized in the same manner as **1c** and **2c**. Because of the more lipophilic hexyl-groups the compound is more soluble in organic solvents. This allows for purification from recrystallization, something that has not been possible for the methoxy or ethoxy systems. A solubility of approximately 14 mg/mL in boiling acetone was crudely measured, which was sufficient for recrystallization.

2.4.4 Characterization of 3,3'-dialkoxy-1,1'-biphenyl-4,4'-dicarboxylic acids

The characterization of the finished linkers was done mostly by NMR, analogous to what is shown in **Section 2.2.12** and **Section 2.3.6**. The NMR spectroscopy will therefore not be covered in such a detail. Similarly, as with the two aforementioned chapters, it is important to note that the characterization described in this section has been performed on all of the compounds described in this chapter. Compound **3c** will be used as an example throughout this section.

The main difference in the NMR spectroscopy between the carboxylic acids and the dimethyl carboxylates is that the spectra are recorded in DMSO-d_6, and not chloroform-d_1. This is due to the insolubility of the diacids in less polar solvents. The ^{1}H NMR spectrum of hexyloxy linker **3c** is given below in **Figure 33**. The second most obvious difference, apart from the DMSO solvent peak at 2.5 ppm, is the appearance of the broad peak for the free carboxylic acids. Due to the acid protons rapidly exchanging with solvent molecules, it is broadened and does not integrate for the expected value of two protons. The appearance of this peak has been observed in various chemical shifts and broadness throughout the project.

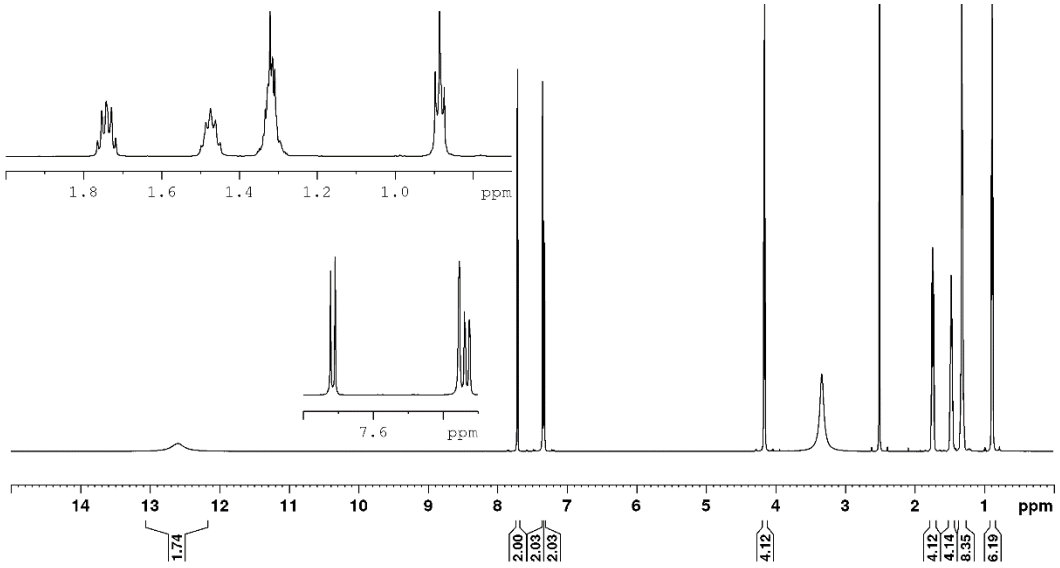

Figure 33 ^{1}H NMR spectrum of **3c**. (600 MHz, DMSO-d_6)

Another difference between the ^{1}H NMR spectra between the diester and the diacids is the switch in chemical shift of the 2,2' and 6,6'-protons. The 6,6' protons (dd) are observed having a higher chemical shift than the 2,2'-protons (d) in all of the diester compounds (in $CDCl_3$), which is something that changes when looking at the diacids compounds. This is most likely due to the change of solvent, as the same switch is observed in the ^{1}H NMR of the diester when dissolved in DMSO *vs* $CDCl_3$.

All three dialkoxy linkers (**1c, 2c** and **3c**) have also been analyzed using high-resolution mass spectrometry and elemental analysis, and the data acquired is given below in **Table 4** and **Table 5**.

Table 4 Results from high-resolution mass spectrometric analysis of linkers **1c**, **2c** and **3c**. (Positive ESI, MeOH)

	HRMS (calculated) [m/z]	**HRMS (measured) [m/z]**	**Error [ppm]**
1c	326.0683,	325.0683	0.0
2c	353.0996, $[C_{18}H_{18}O_6Na]^+$	353.0995	0.1
3c	465.2248, $[C_{26}H_{34}O_6Na]^+$	465.2247	0.1

Table 5 Results from elemental analysis of linkers **1c**, **2c** and **3c**. The largest error is reported, with a threshold of 0.4 %.

	Elemental analysis (calculated)			**Elemental analysis (measured)**			**Largest error**
	C [%]	**H** [%]	**O** [%]	**C** [%]	**H** [%]	**O** [%]	[%]
1c	63.58	4.67	31.76	62.93	4.76	31.29	**0.65** (C)
2c	65.45	5.49	29.06	65.19	5.5	28.87	0.26 (C)
3c	70.56	7.74	21.69	70.31	7.89	21.41	0.28 (O)

The high-resolution mass spectrometry shows the expected ions with the expected m/z value. For the elemental analysis are linker **2c** and **3c** within the commonly used threshold of a 0.4 % error, while linker **1c** is just outside. This error is due to the unfortunate timing of not having enough time to purify the sample before the samples were to be sent in for analysis.

It is not very easy to assay the purity of the finished linkers. Although all the NMR spectra show a pure product, it might not always be the case. Several batches of the obtained linkers have displayed a range of colors that might indicate that some residual palladium or iron might be present in the final product. This is especially prone to happen if the coupling product was purified by filtration through silica and then recrystallized. The final linkers have been isolated as white solids, so it is safe to assume that any discoloring is due to metal contaminations from the coupling reaction.

2.4.5 Discussion and conclusions of the hydrolysis reaction.

The hydrolysis reaction is on paper a very simple procedure but has a lot of practical issues as previously discussed. The inevitable losses due to the physical properties of the products are frustrating. But despite these problems have three linkers been synthesized and characterized. It would have been interesting to continue the analogization by coupling and hydrolyzing more analogues than just methyl, ethyl and hexyl, but there was not enough time to do so.

2.5 Synthesis of 3,3'-dihydroxy-1,1'-biphenyl-4,4'-dicarboxylic acid (1d) and its ester derivatives (2d and 3d)

2.5.1 Motivation

There were two main reasons to synthesize dihydroxy linker **1d**, the first reason which will be explained later in more detail (**Section 3.1.1**), was to troubleshoot the problems occurring with the MOF synthesis. The second reason is the potential of synthesizing a **UiO-67-1d** MOF, which would be an interesting structure by itself, but would also create another potential synthetic route to **UiO-67-dialkoxy** by post synthetic modification of the **UiO-67-1d** MOF.

The synthesis of the linker has been attempted throughout the project in several different ways as shown in **Scheme 10**. It is obvious from the number of attempted routes that the synthesis of **1d** has proved to be a difficult one. In most of the cases this was due to the insolubility of the compound in most solvents, and therefore a good method of purification was not found. There was always a small percentage of either starting material or the semi-

alkylated product present in the ^{1}H NMR spectra. For most other compounds, a solution to this would be to recrystallize the product or to purify it with flash chromatography, but as mentioned, the solubility issues of compound **1d** proved this difficult.

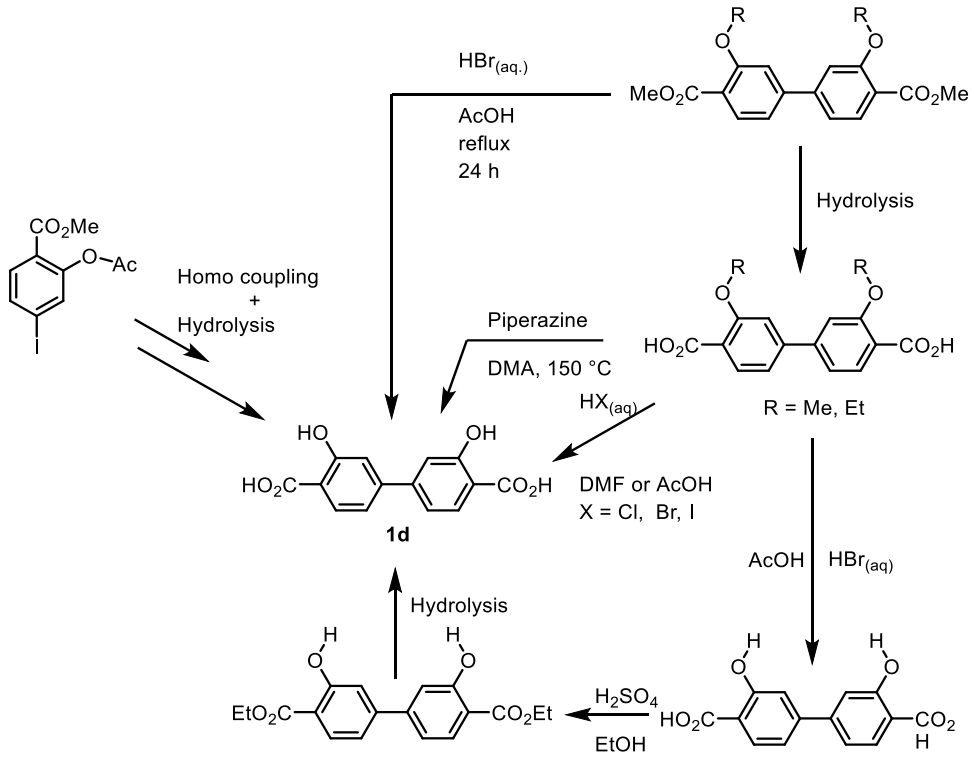

Scheme 10: A summary over different attempted synthetic routes to obtain compound **1d.**

2.5.2 Acid catalyzed dealkylation of 1c or 2c

As shown in **Scheme 10**, an acidic cleavage of the alkylated linkers was attempted using hydrohalic acids such as hydrobromic or hydroiodic acid. The general synthetic procedure was based a procedure from Liu *et al.* [21] The procedure calls for refluxing **1c** in glacial acetic acid with HBr (conc., aq.) added. However, whenever this was attempted a small amount of the partially dealkylated compound shown in **Figure 34** remains. The ^{1}H NMR spectrum of the isolated product is shown below in **Figure 35**. Note the peak at 3.9 ppm from the partially dealkylated product. There is also some residual acetic acid present.

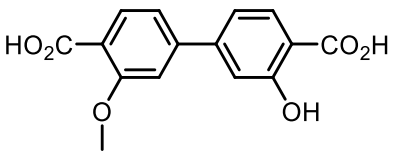

Figure 34: Partially dealkylated side product from the dealkylation of **1c**.

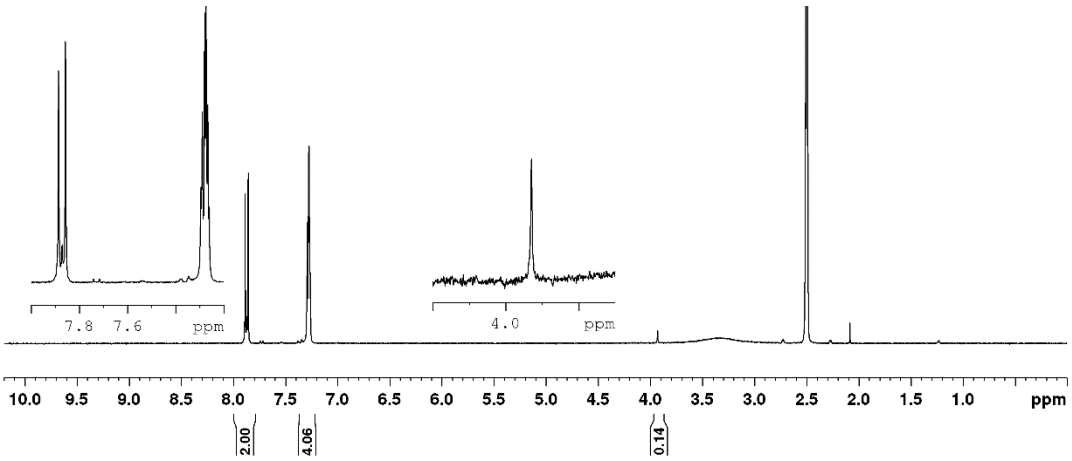

Figure 35: ^{1}H NMR spectrum of an attempted dealkylation of **1c**. (DMSO-d_6, 300 MHz)

2.5.3 One-pot hydrolysis and dealkylation of 2b

Partially inspired by the success of the one-pot alkylation and homo coupling described in **Section 2.3.3** and due to the acid catalyzed dealkylation proceeding at the optimal conditions for acid catalyzed ester hydrolysis, was an attempt of doing a one-pot synthesis from the methyl ester **2b** to dihydroxy linker **1d**. The procedure was identical to the acid catalyzed dealkylation done with compound **1c** and **2c**. The reaction resulted in product **1d** with an 85 % yield, with a comparable purity to the previous attempts of dealkylation. The success of a one-pot synthesis of **1d** from **2b**, combined with the one-pot synthesis from methyl 4-iodosalicylate to **2b**, now allows for a two-step synthesis to **1d** from what was previously a four-step synthetic route, as shown in **Scheme 11**.

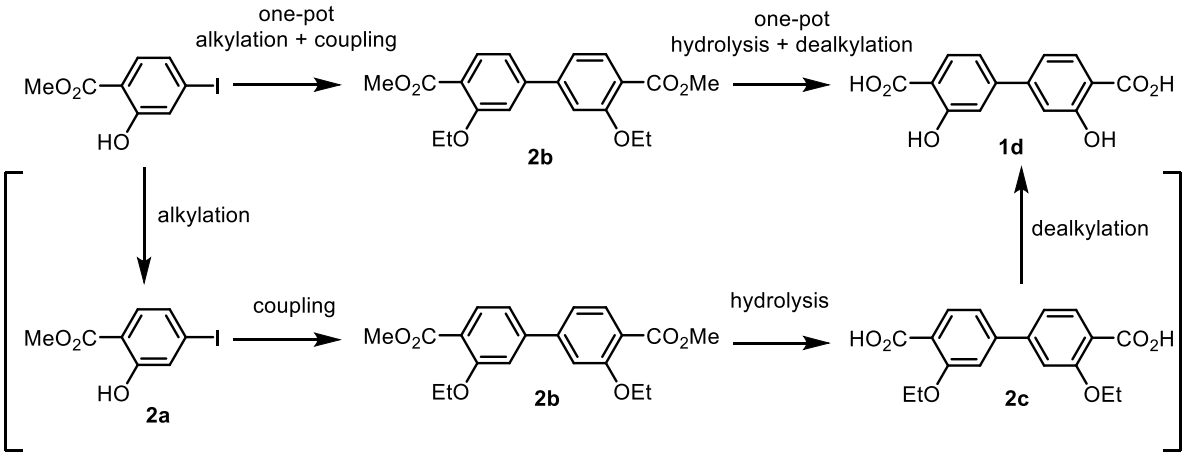

Scheme 11 Comparison of previous four-step synthesis of **1d** to the new, potential 2-step synthesis featuring two one-pot reactions)

Due to time limitations, this improved two-step reaction was never explored in any greater detail than what is described.

2.5.4 Alkyl amine assisted dealkylation of 1c

Due to the shear difficulty of purifying this compound was an alternative synthetic method using an alkyl amine assisted dealkylation published by Nishioka *et al.* in 2000 [22] attempted, after the reported success of obtaining **1d** by another group at the University of Oslo.[23] The synthetic procedure is given below in **Figure 36**. Just like with the acid catalyzed dealkylation did this method also result in small amounts of impurities, in addition to residual dimethylacetamide (DMA) which is very difficult to get remove, despite washings with hydrochloric acid, water or methanol.

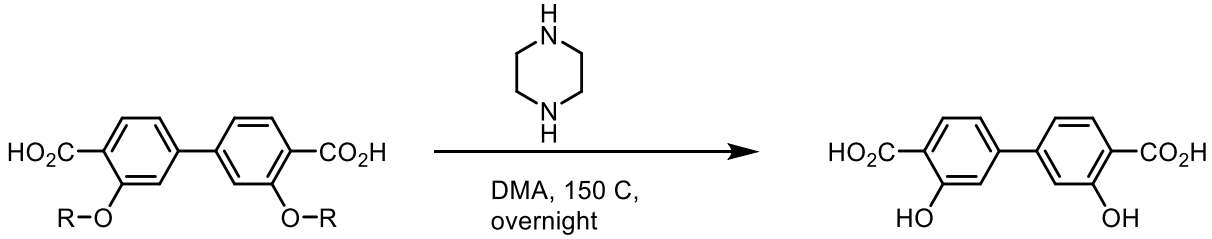

Figure 36: Synthetic procedure for alkyl amine assisted dealkylation.

2.5.5 Synthesis of 2d by homo coupling of 10a

The relevance of the synthesis of compound **2d** was something that was realized at two different occasions during this project, where compound **2d** would fill two different roles. The first occasion was during the problems optimizing the homo coupling of **2a** as discussed in **Section 2.3.2** where it was thought that if **2d** could be synthetized in an easier manner than what was experienced with **2a**, functionalization could occur post coupling. The other occasion was as a way of purifying the impure **1d** that was acquired through dealkylation of either **1c** or **2c**.

The first attempts of synthesizing **2d** was through the direct coupling of the starting material methyl 4-iodosalicylate. This gave no isolatable products, and the idea was quickly scrapped. It was clear that the free phenolic positions were causing troubles for the coupling reaction, and therefore had to be protected in order to succeed. Therefore, the starting material was acetylated in the phenolic position, giving product **10a**.

The synthesis of **10a** was done by acetylation with acetic anhydride, catalyzed by sulfuric acid as shown in **Scheme 12**. The reaction reaches completion within one hour and is relative pure. But there was in some cases some residual starting material that had to be removed by recrystallization from methanol. The obtained pure **10a** displayed a melting point range between 91 – 92 °C (observed for two different batches), which is not consistent with previously reported values in the literature. In 2010 Park *et al.* reported the melting point of **10a** to be 75 °C. [24]It is worth noting that Park is not reporting any purification of the compound, and present impurities might be a possible explanation of the discrepancy between the observed and reported melting points.

The idea was that compound **10a** could be coupled under the same coupling conditions used previously in this project, but this was not the case. Just as with the unprotected starting material, the homo coupling of **10a** yielded no isolatable product, probably due to the lability of the acetyl group in basic media with water present (which is present due to the hygroscopicity of DMSO). The coupling was later attempted under water-free conditions, using the alternative acetonitrile / Cs_2CO_3 coupling system described in **Section 2.3.3,** to no success.

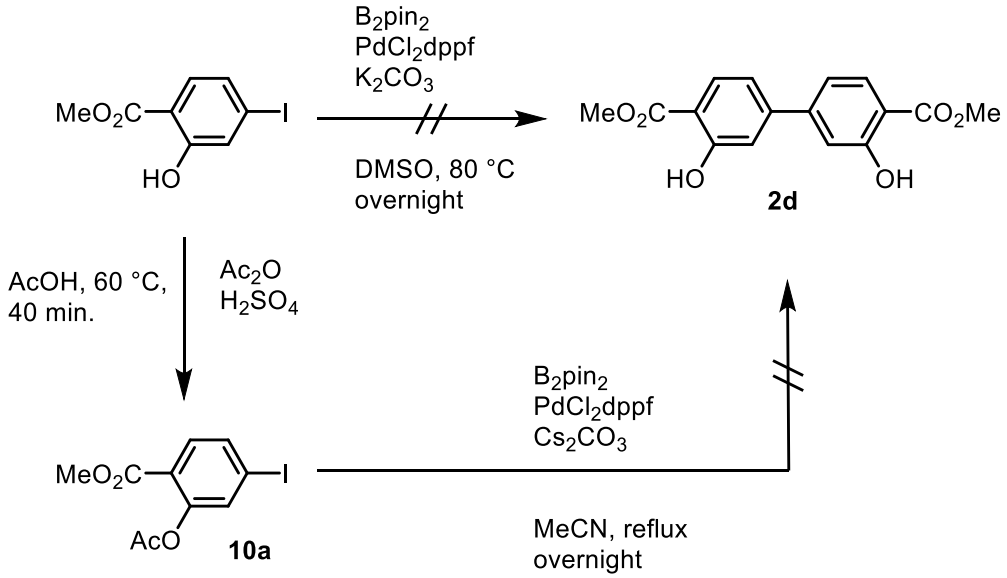

Scheme 12 Synthetic pathways to compound **2d**.

2.5.6 Synthesis of 2d and 3d by esterification.

Compound **1d** is practically insoluble in all available solvents, and purification of the compound is therefore practically impossible. A less efficient possibility to purify **1d** is to esterify the carboxylic groups to yield a more soluble and therefore a more easily purified compound

which can be hydrolyzed to yield **1d**. Since all compounds in the project, apart from **1c**, **2c**, **3c** and **1d**, are methyl esters, it only felt natural to continue the trend, and use methanol in the esterification shown in **Scheme 13**.

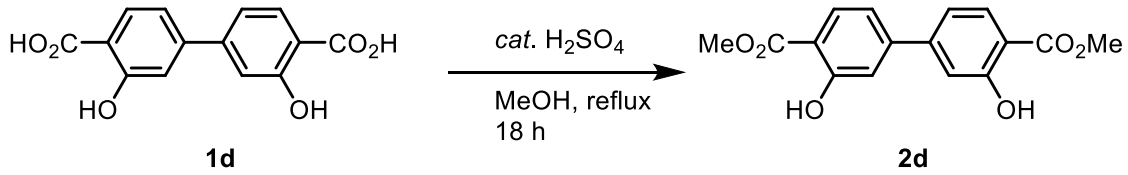

Scheme 13: Methyl esterification of **1d**.

The reaction was a success, but the obtained product **2d** is almost as insoluble as its precursor **1d**. It is relatively soluble in DMSO, and sparingly soluble in chloroform and practically insoluble in methanol.

In the process of characterizing this compound, an unexplained phenomenon appeared in the ^{1}H NMR (**Figure 37**).

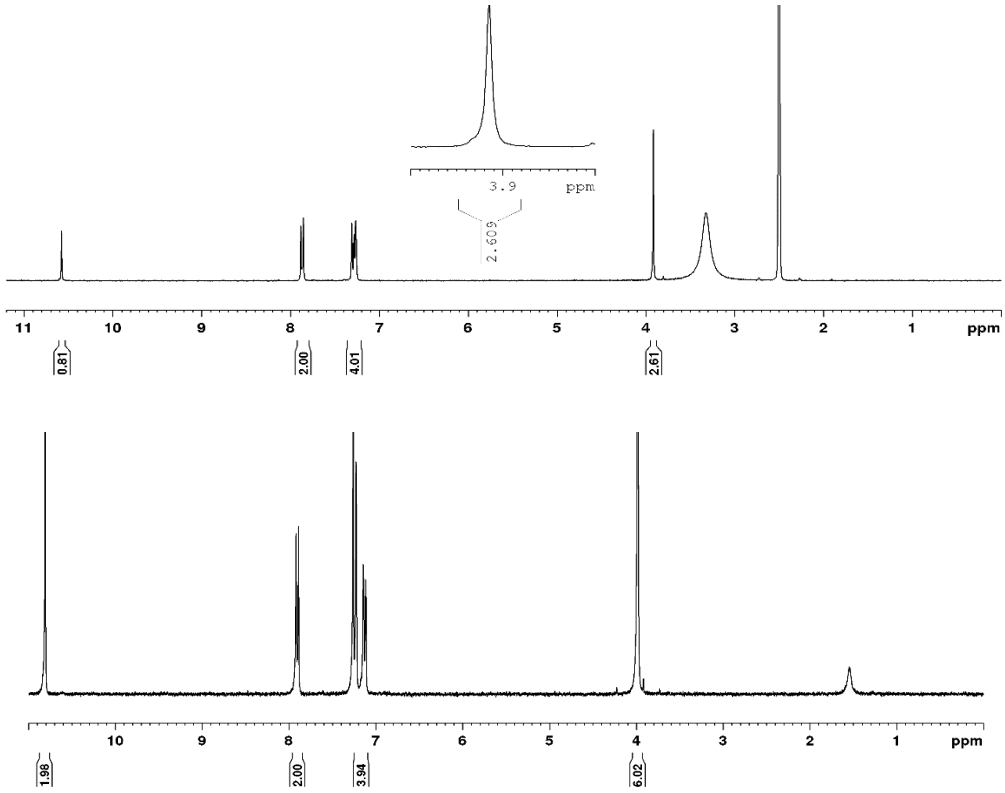

Figure 37: Comparison of ^{1}H NMR spectra of **2d** in DMSO-d_6 (top) and in chloroform-d_1 (bottom). (300 MHz)

When comparing the DMSO-spectrum (top) *vs.* the chloroform-spectrum (bottom), an inconsistency in the integrals is observed. The spectrum appears as to be expected when dissolved in deuterated chloroform, but when the compound is dissolved in DMSO, the methyl

ester peak (3.9 ppm) is integrating for less than half of what it ought to, something that is also observed in the phenolic signal (10.6 ppm). A discrepancy in the integral of a heteroatomic proton, such as a phenolic signal is not unheard of, and could be brushed off as normal due to the rapid exchange of the acidic protons. However, the discrepancy in the integration of the methyl peak is interesting. Compound **2d** has been previously reported in the literature and when comparing the spectroscopic data published by Cohen *et al.* in 2017, [25] the same phenomenon is observable. (**Figure 38**). The discrepancy might not be visible on first glance, due to the integrals of the aromatic signals being split up (for some reason). Disregarding the odd integration, it is obvious that the methyl peak is appearing half as intense as it should. In the article, the authors provide no explanation on the discrepancy.

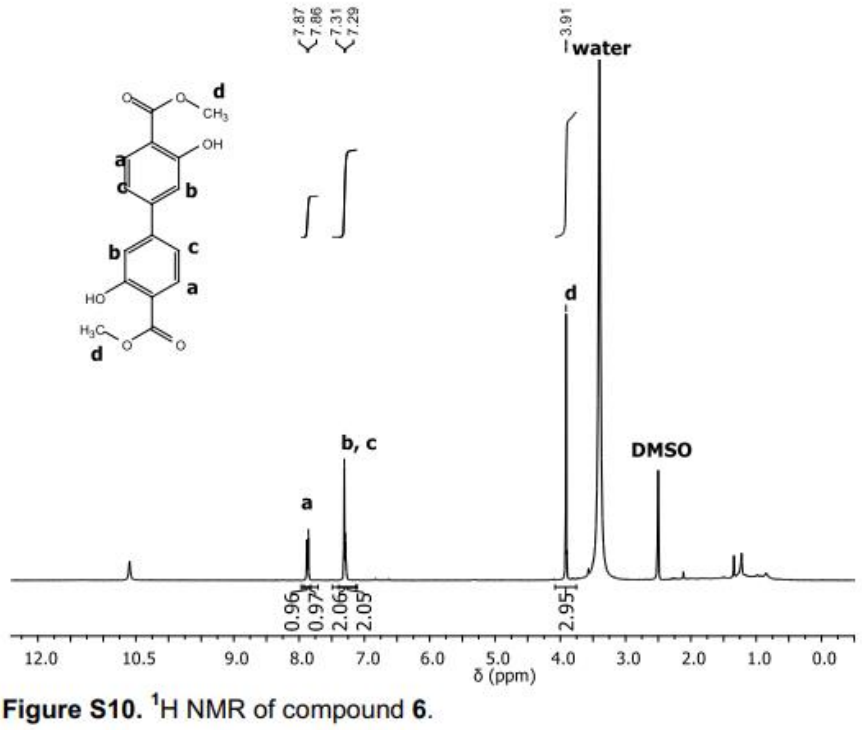

Figure S10. ^{1}H NMR of compound **6**.

Figure 38: Published ^{1}H NMR spectrum of compound **2d** from Cohen *et al.*(DMSO, 400 MHz) The spectrum is available in the supplementary information[25]

Due to the continued issues of insolubility it was decided to synthesize the ethyl ester (**3d**) instead, which displays much better solubility in common organic solvents. The ^{1}H NMR spectrum of the ethyl ester (**Figure 39**) displays the observable impurities in addition to the main product, **3d**. There are three visible phenolic signals (10.5 – 11 ppm). There is also one methyl signal visible (4 ppm, singlet), which is most likely from residual semi-alkylated linker. There is also one other ethoxy signal (4.35, q, C**H**$_2$-CH$_3$) overlapping with the main ethoxy

peak, which is from either semi-esterified product or the ethyl ester from the alkylated impurity. A review over the possible (by)-products is given in **Scheme 14**.

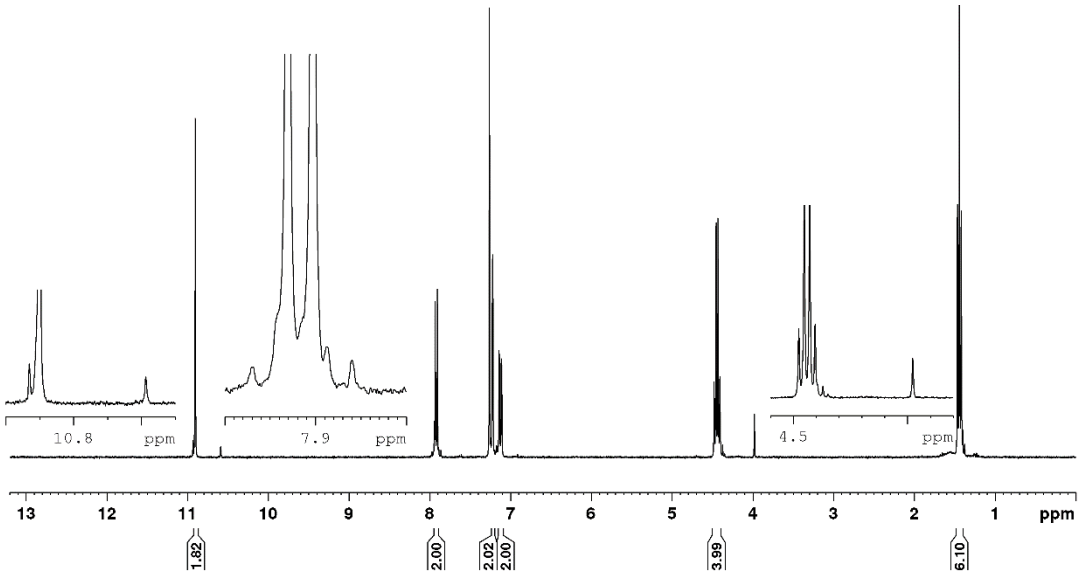

Figure 39: ^{1}H NMR of **3d** with its impurities. ($CDCl_3$, 300 MHz)

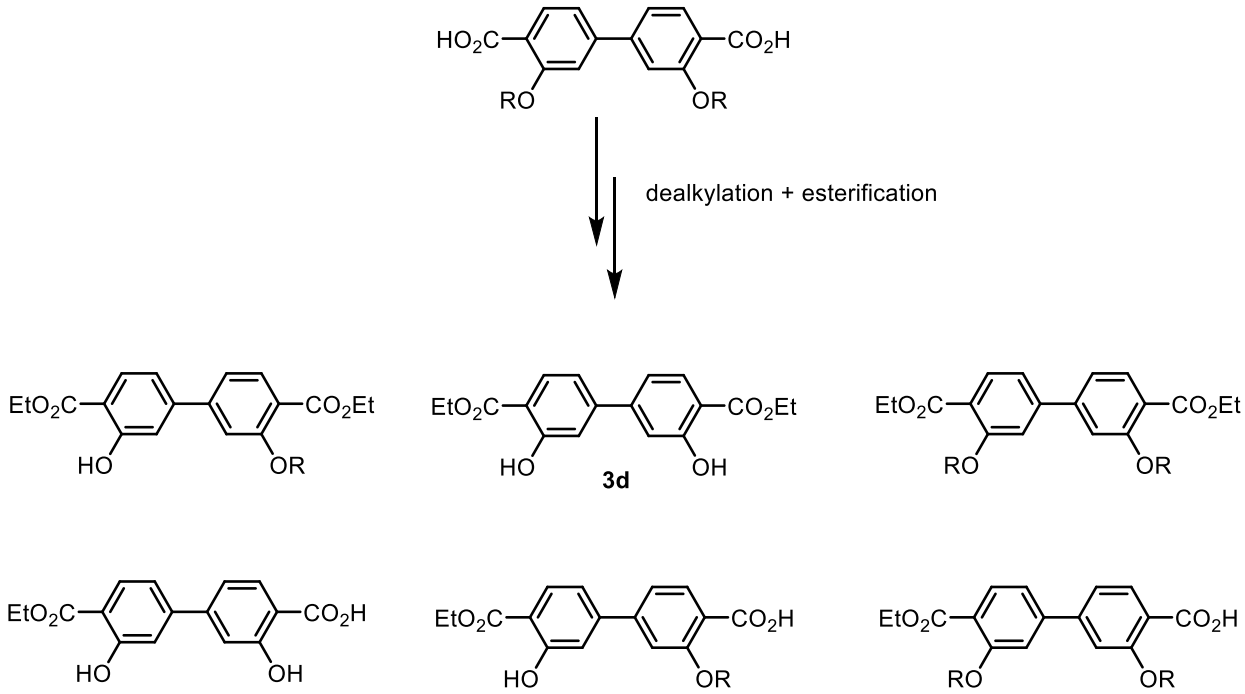

Scheme 14 Possible products and side products from the esterification of impure **1d**.

The spectrum in **Figure 39** was acquired after attempted purification using flash chromatography. Due to the spectrum showing obvious signs of impurities, another attempt using flash chromatography was made, and the spectrum shown in **Figure 40** was acquired. ¨

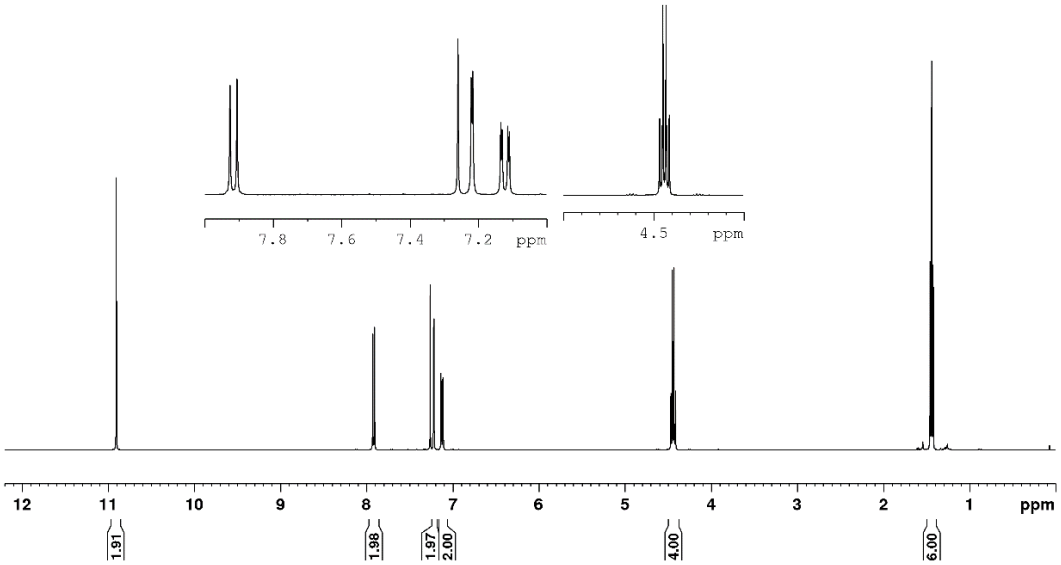

Figure 40: ^{1}H NMR spectrum of seemingly pure **3d**. ($CDCl_3$, 400 MHz)

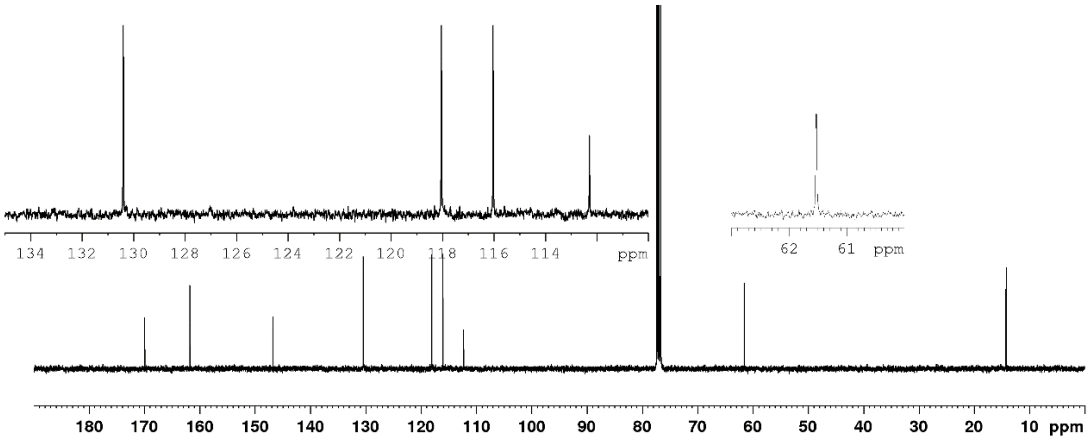

Figure 41: ^{13}C NMR spectrum of **3d**. ($CDCl_3$, 101 MHz)

The isolated product after the second run of flash chromatography is appearing nearly completely pure (in terms of purity assessed by NMR). The ^{13}C NMR spectrum is also indicating a pure product, as shown in **Figure 41**. There are only the expected signals from **3d** present in both spectra.

However, as with all compounds in the project, it was also characterized using mass spectrometry, more specifically GC-(EI)MS. In the gas chromatogram (**Figure 42**), an obvious minor peak is visible with a retention time of approximately 12.5 minutes. The major peak at

13.5 minutes is the fraction containing the main product, **3d**, as shown with the corresponding mass spectrum (**Figure 43**).

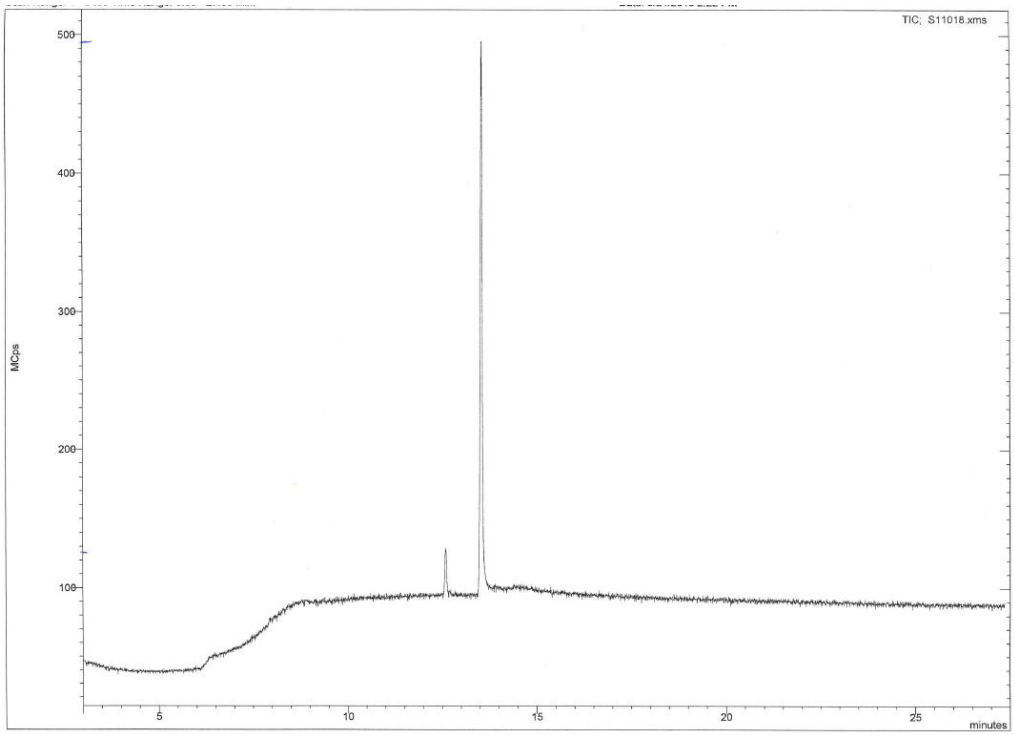

Figure 42: Gas-chromatogram of a sample containing **3d**.

Figure 43 shows the expected molecular ion peak at m/z = 330. When looking at the other mass spectrum for the minor peak in the chromatogram, it is clear that there is a side product present. (**Figure 44**)

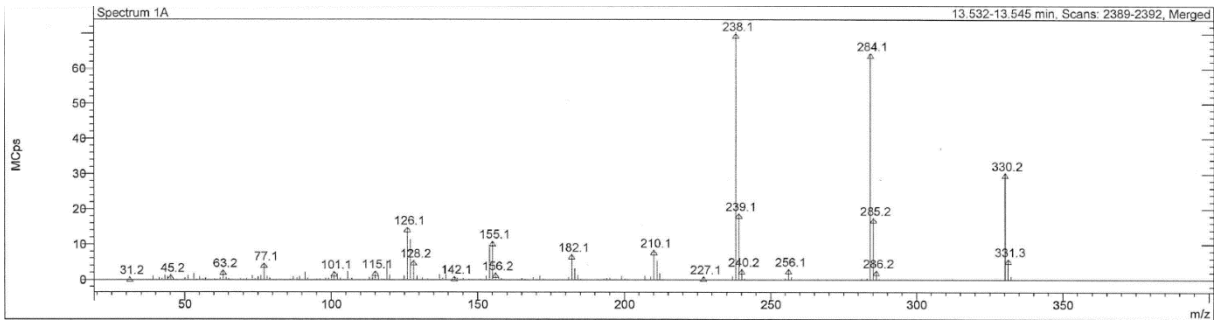

Figure 43: Electron-ionization mass spectrum of **3d**. ($CHCl_2$, 13.5 minutes)

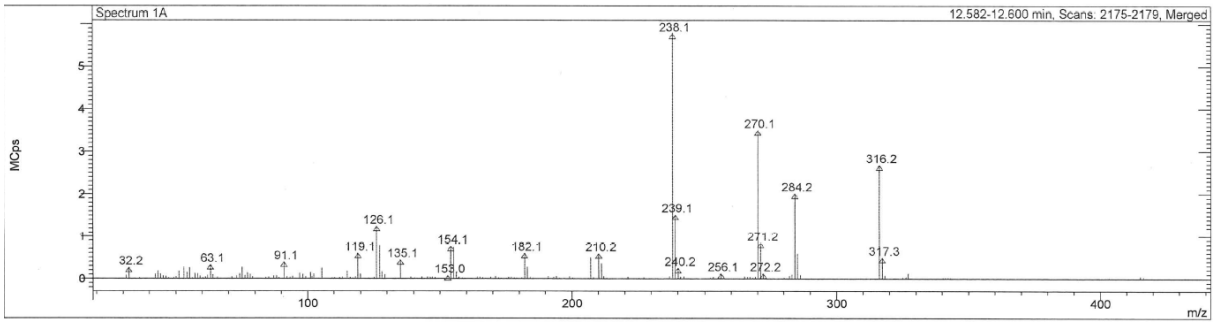

Figure 44: Electron-ionization mass spectrum of an impurity. ($CHCl_2$, 12.5 minutes)

The only logical possibilities of a molecular specie with m/z-value of 316, is the asymmetric specie shown in the bottom left of **Scheme 15**, or its isomer, with the methoxy group on the same side as the ethyl ester. This is a possibility because this particular batch of **1d** was synthesized from **1c**, which is the dimethyl linker. Also shown in **Scheme 15** is a possible explanation of the different m/z values observed in the different mass spectra. The mechanism behind the loss of alcohol and the formation of the β-ketoketene is described in McLafferty's "Interpretation of Mass Spectra". [19] This plausible mechanism describes why the peak of 270 is only visible in spectrum of the impurity, while the rest of the peaks are shared.

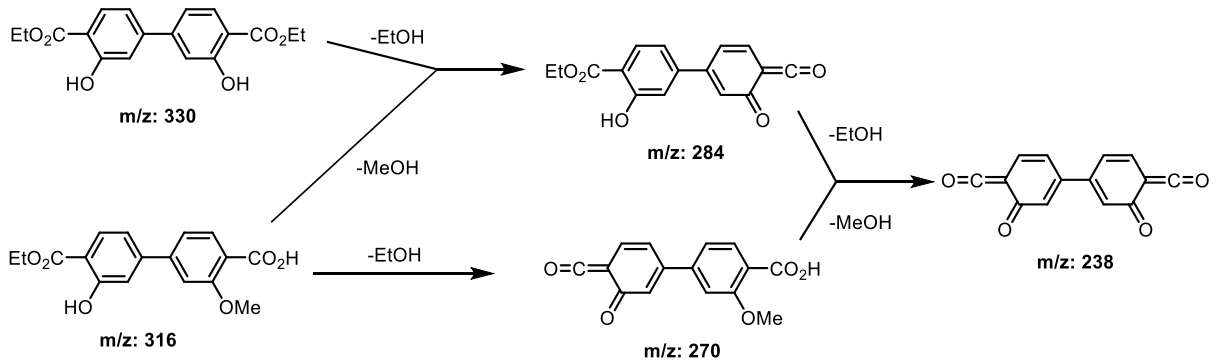

Scheme 15: Plausible reaction pathways to explain observed m/z-values in the mass spectra of **3d**.

After discovering this impurity, the same batch of **3d** was checked with ^{1}H NMR again, this time in DMSO-d_6 and not chloroform, and the impurity became visible in the aromatic region. (**Figure 45**)

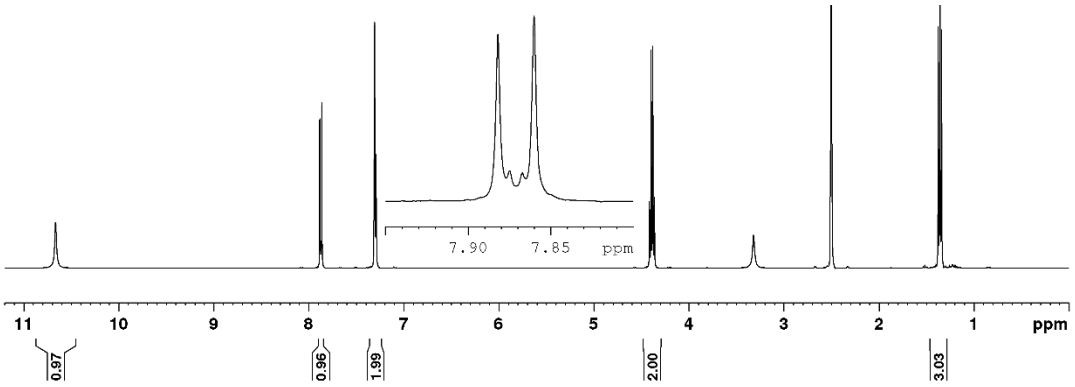

Figure 45: ^{1}H NMR of **3d**. Note the visible impurity, partially overlapping with the aromatic signal at 7.87 ppm. (DMSO-d_6, 400 MHz)

Due to not being able to fully purify **3d**, the esterification route reached a dead end. Just for the sake of completion, saponification of the batch of **3d** described above was attempted. As a test reaction, approximately 0.15 g of the ethyl ester **3d** was hydrolyzed using the same conditions as the other ester hydrolyses in this thesis, but with an extra two equivalents of base added to compensate for the free phenolic groups present. It was obvious that the reaction did not go to completion, based on the fact that there was a suspension of unreacted material in the reaction mixture. The resulting product contained large amounts of unreacted ester, according to ^{1}H NMR spectrum (**Figure 46**), even after leaving the reaction for 46 hours at 60 °C.

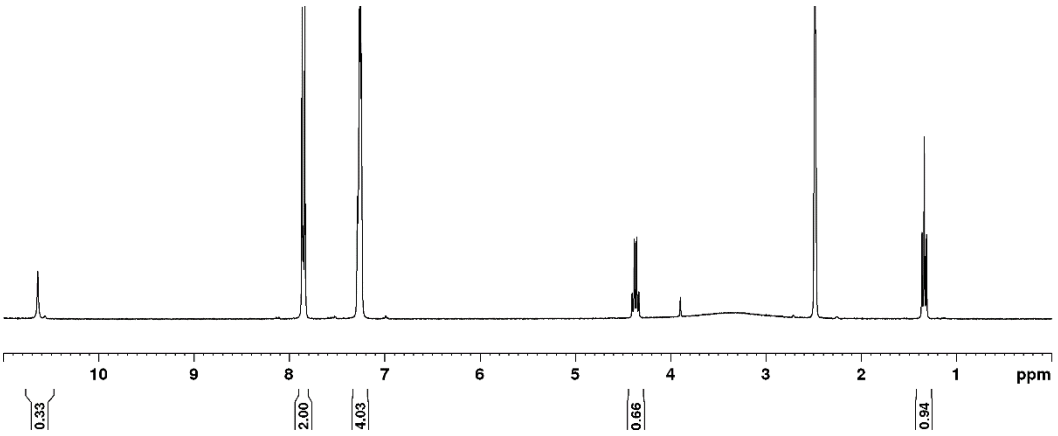

Figure 46 ^{1}H NMR spectrum from attempted hydrolysis of **3d**. (300 MHz, DMSO-d_6)

It is clear that for purification by esterification to be a viable step in obtaining pure **1d**, one would need to find a better protocol than just flash chromatography, as well as find a better hydrolysis procedure. Due to time constrictions, no further attempts to synthesize **2d** or **3d,** or to purify **1d** by esterification were made.

2.5.7 Discussion and conclusions of the synthesis of 1d

Despite all the attempts, no "perfect" synthetic route to **1d** was discovered. In all attempted cases, some residual mono-alkylated impurity was present. For the use as MOF linker, this tiny impurity is probably not to any concern, but due to time limitations no MOF synthesis using **1d** was explored.

The discovery of the one-pot hydrolysis and dealkylation discussed in **Section 2.5.3** does improve the otherwise long synthetic route dramatically. It is unfortunate that there was no extra time to really explore this synthetic pathway, and attempt making a dihydroxy-functionalized UiO-67. A completely different synthetic strategy to the alkoxy MOFs could be to explore the potential for post-synthetic alkylation of a dihydroxy UiO-67.

3 Synthesis of UiO-67 metal-organic frameworks

There is, and has been, a lot of research in the synthesis of metal-organic frameworks at the catalysis group of the University of Oslo. The research in the last decade has mainly been on the UiO-series (UiO-66, UiO-67 and UiO-68).

The main way of synthesizing standard UiO-67 metal-organic frameworks is based on the original synthesis published in 2008.[1] The synthesis is to this day still using zirconium (IV) tetrachloride and *N,N*-dimethylformamide, but also with the addition of a modulator, often benzoic acid, after the 2011 article by Behrens and co-workers reporting the influence of the addition of mono carboxylic acids to the metal-organic framework synthesis.[26] The original UiO-66 paper also reported the synthesis occurring under static conditions in an oven at 120 °C but has in later years also been synthetized using a traditional setup (for organic chemists, that is) with a round bottom flask in an oil bath with a reflux condenser and magnetic stirring. In this work, both methods were attempted.

3.1 Synthesis of UiO-67-dialkoxy metal-organic frameworks

As previously discussed (**Section 2.2.3)**, the diethoxy functionalized linker was from the beginning always thought of as being the starting point. Therefore, the first MOF to be attempted synthesized was the **UiO-67-2c**.

3.1.1 Attempted synthesis of UiO-67-1c and UiO-67-2c

The synthesis of a 3,3'-dimethoxy functionalized UiO-67 MOF was attempted in a similar fashion as previous UiO-67 MOFs has been synthesized before. The very first attempt of synthesizing **UiO-67-2c** was done without the addition of a modulator and resulted in a gel formation with no crystalline product present.

Later attempts consisted of parallel syntheses using linker **1c** and **2c.** Now with the addition of a modulator, the reactions resulted the yield of two crystalline products that both showed the UiO-67 crystallinity *via* PXRD. (**Figure 47**)

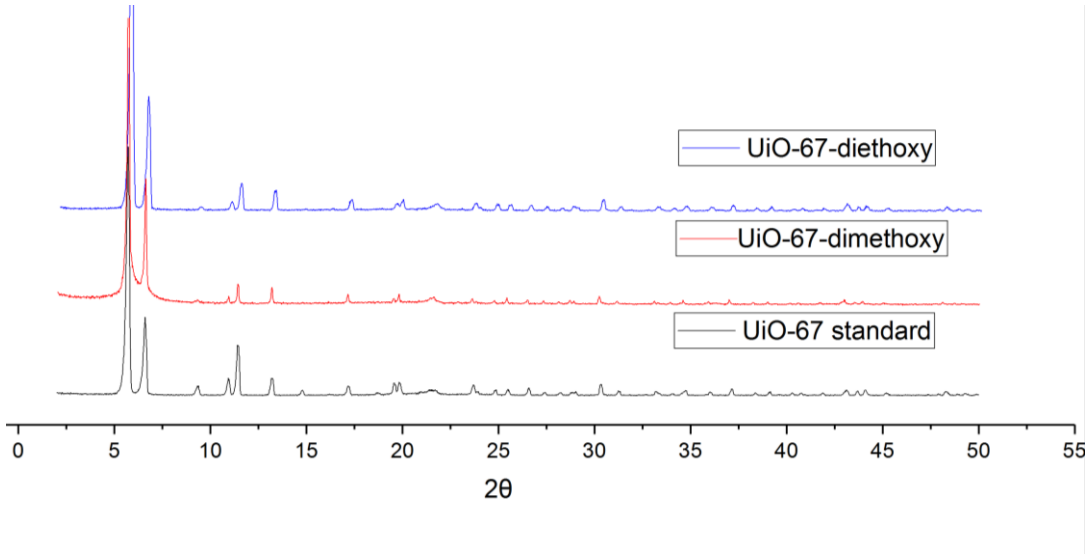

Figure 47: Powder diffractogram of obtained crystalline products, compared to the standard UiO-67 MOF.

The two crystalline samples were also characterized using thermogravimetric analysis (TGA), as shown in **Figure 48**. The dimethoxy sample seems to decompose at around 240 °C, while the diethoxy decomposes at around 300 °C.

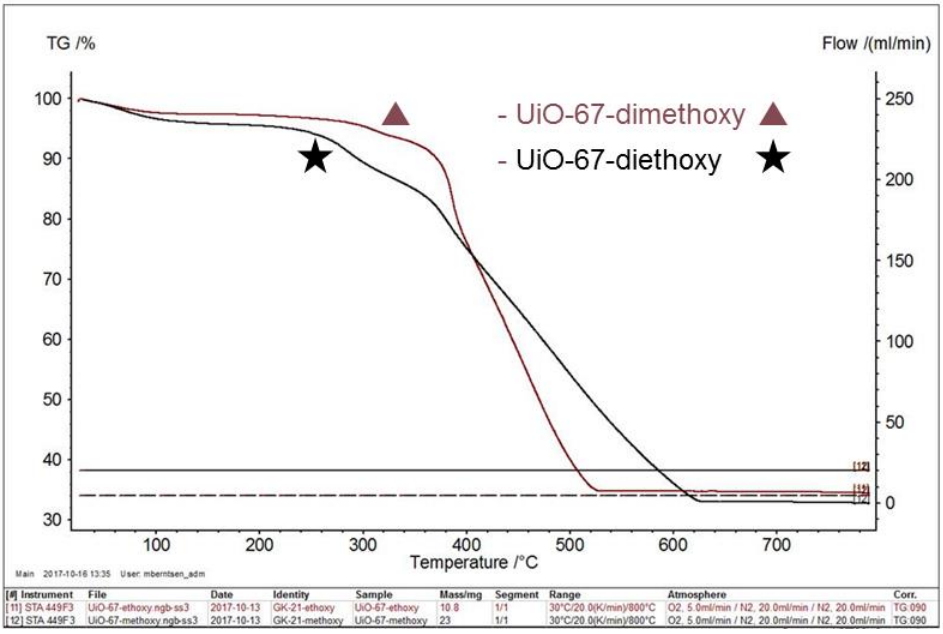

Figure 48 TGA-analysis of the two synthesized MOFs. The samples were heated (20 K/min) from 30 °C to 800 °C in a flowing O_2 and N_2 atmosphere (5.0 mL/min and 20 mL/min respectively)

The obtained crystalline products were imaged using scanning electron microscopy, resulting in the images below.

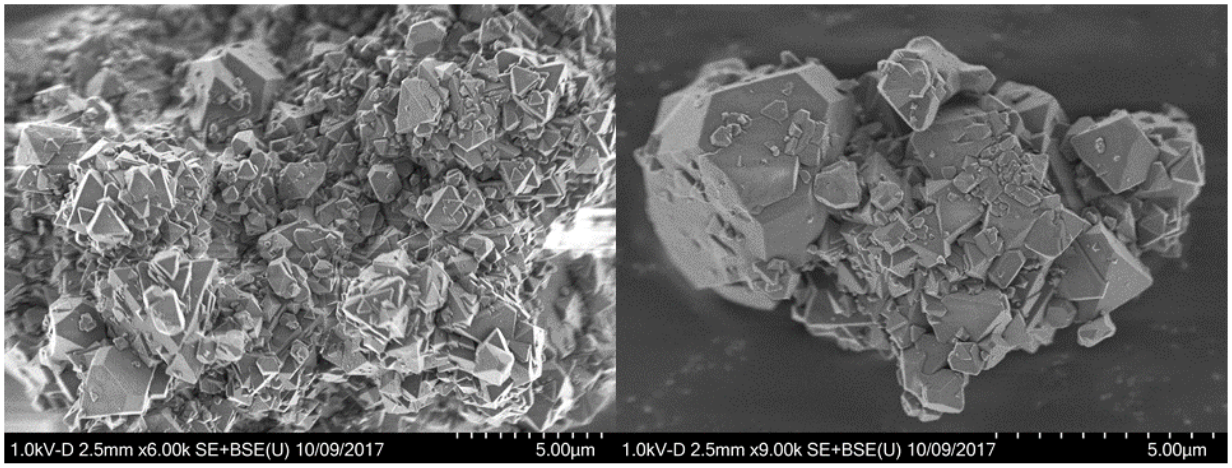

Figure 49 SEM images of **UiO-67-2c**.

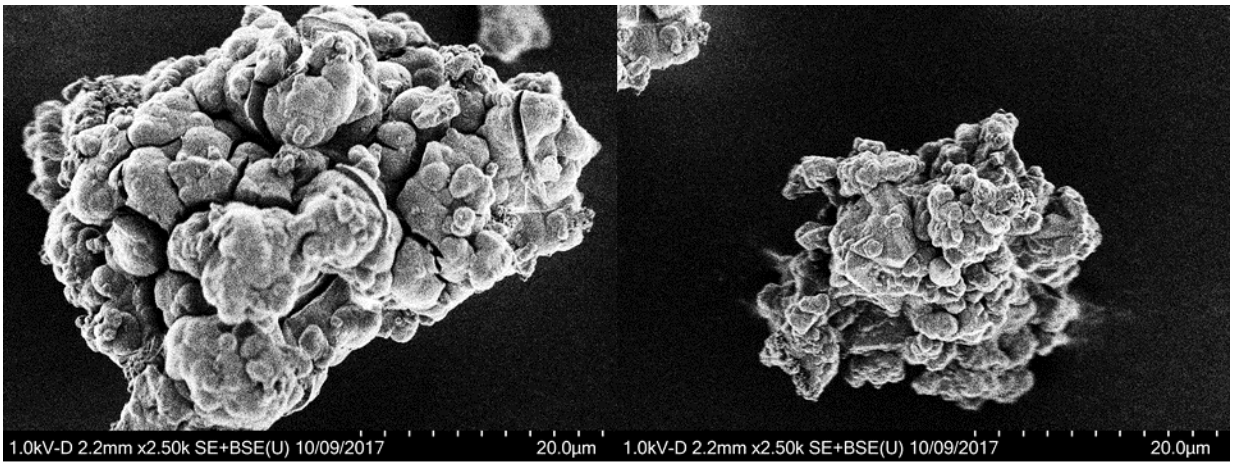

Figure 50 SEM images of **UiO-67-1c**.

When looking at the crystals from the ethoxy batch, shown in **Figure 49**, are there obvious signs of the octahedral crystallites associated with a UiO-structure. The crystallites are however very irregular in size and shape, which is a sign of poor quality. The quality is definitely better than in the methoxy batch, when comparing with the images in **Figure 50**. The latter displays no good sign of octahedral crystallites or other qualities.

Another common characterization method of metal-organic frameworks is NMR digestion. In order to see what organic compounds are present in the MOF product, the MOF is digested in a solution of sodium hydroxide in D_2O, in order to separate the inorganics (as insoluble zirconium hydroxide) and organics (mainly linkers in the form of carboxylate ions). The precipitate

is then separated by centrifugation and the remaining solution is analyzed using ^{1}H NMR spectroscopy. When digesting the obtained crystalline products shown in **Figure 47**, it became clear that the organic linker at some point undergoes decomposition.

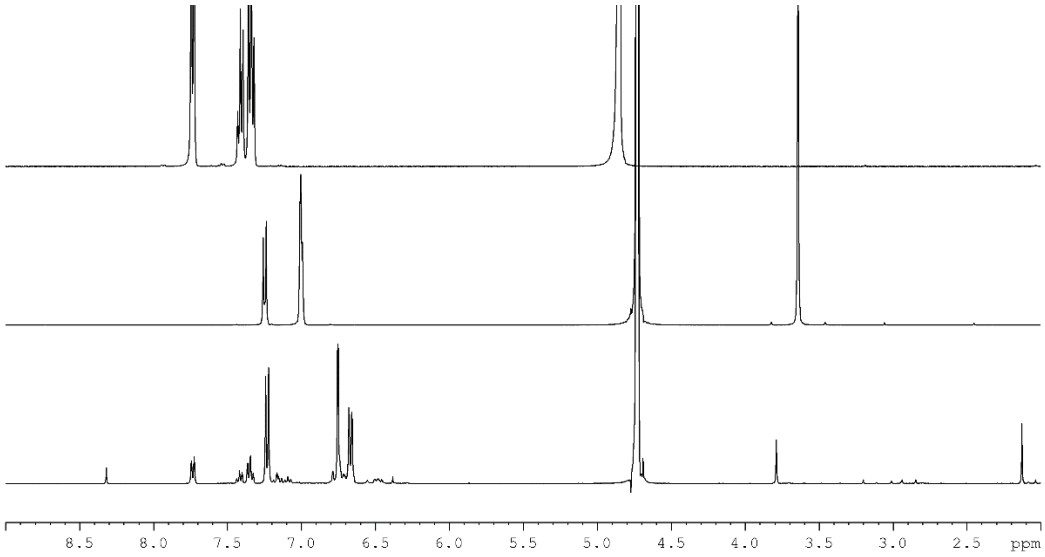

Figure 51: ^{1}H NMR spectra of digested UiO-67-dimethoxy MOF (bottom), **1c** linker (middle) and benzoic acid (top). (400 MHz, 1M NaOH in D_2O)

The figure above shows the ^{1}H NMR spectra for the following compounds that should be present in the sample, namely benzoic acid (added as a modulator) and **1c**. The bottom spectrum shows no visible signals from **1c**, but rather a different compound altogether.

The identity of this new compound was investigated. The main hypothesis was the potential cleavage of the methoxy ether. Alkyl ether cleavage is much more common in acidic medium, there is therefore logical to assume the decomposition would occur during the MOF synthesis, and not during the NMR-digestion. Additionally, if alkaline hydrolysis were to occur, it would be likely observed during the saponification step during the synthesis of the linker. To confirm decomposition during the MOF synthesis, a sample of **1c** was cleaved under acidic conditions (HBr (aq.), AcOH), and yielded the nearly pure dihydroxybiphenyl compound **1d**. (**Scheme 16**) as described in **Section 2.5.2**.

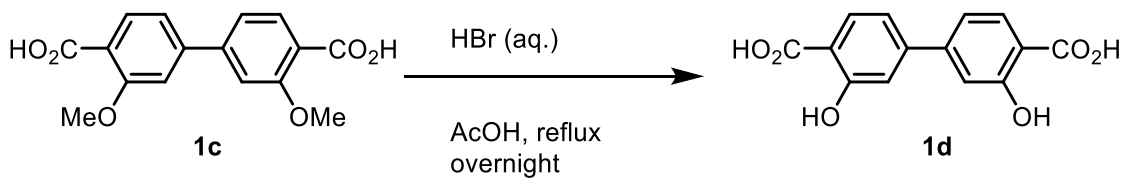

Scheme 16: Synthesis of **1d**. Reaction does not go to completion.

When comparing the ^{1}H NMR spectrum of **1d** with the digested MOF (**Figure 52**), it is clear that alkyl-cleavage is occurring.

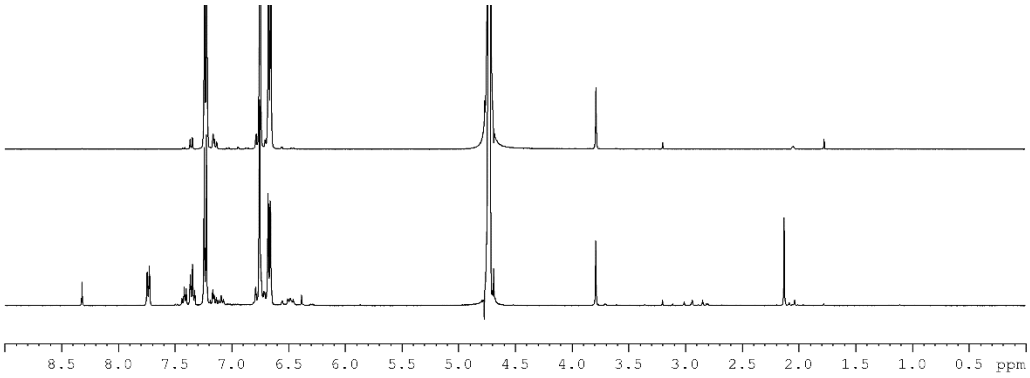

Figure 52: ^{1}H NMR spectra of digested UiO-67-dimethoxy MOF (bottom) and **1d** (top). Note the singlet located at 3.8 ppm from the mono-methoxy impurity. (400 MHz, 1M NaOH in D_2O)

It is worth noting that the cleavage reaction also does not proceed to completion, ^{1}H NMR showed approximately 7% of the mono-methoxy functionalized linker (singlet at 3.8 ppm). This small impurity proved rather useful for the investigation. To investigate if the cleavage could occur during the conditions of the MOF synthesis, an NMR-experiment mimicking the synthesis conditions for the MOF was designed. Linker **1c**, benzoic acid and concentrated HCl (aq.) was added to a J. Young NMR tube. Note that no zirconium (IV) chloride was added, but rather equimolar amounts of hydrochloric acid, which would be present due to the hydrolysis of $ZrCl_4$. A ^{1}H NMR spectrum was obtained before and after the tube was heated at 130°C for 22 h and is shown below. (**Figure 53**)

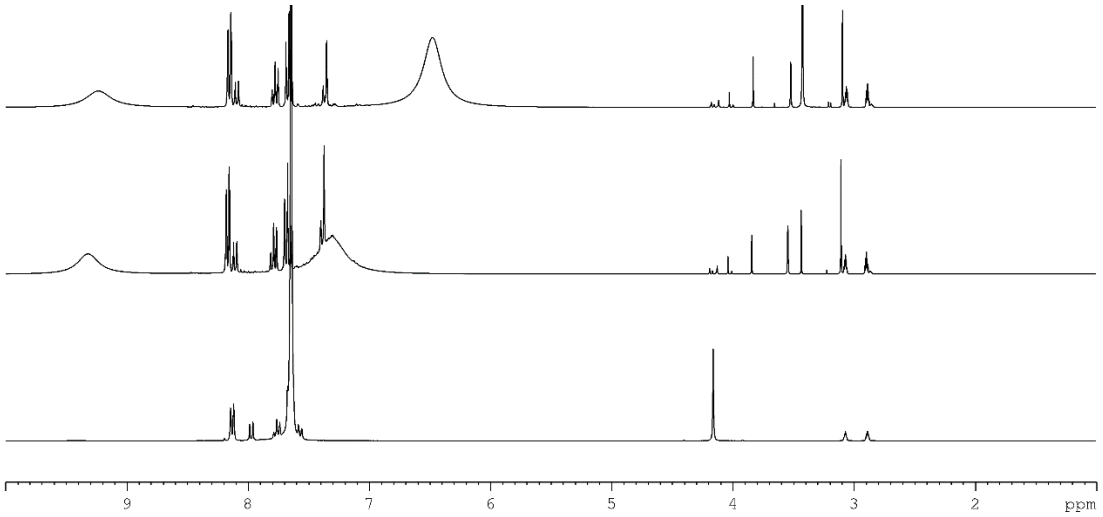

Figure 53: ^{1}H NMR spectra of linker **1c** under MOF-like conditions, before (bottom), after heating at 130°C for 22 h (middle) and after spiking the sample with methanol (top) (300 MHz, DMF-d_7)

Due to overlapping signals, it is difficult to draw any conclusions from the aromatic region, but in the aliphatic region several new singlets have appeared. The proposed mechanism behind the cleavage is shown in **Scheme 17**.

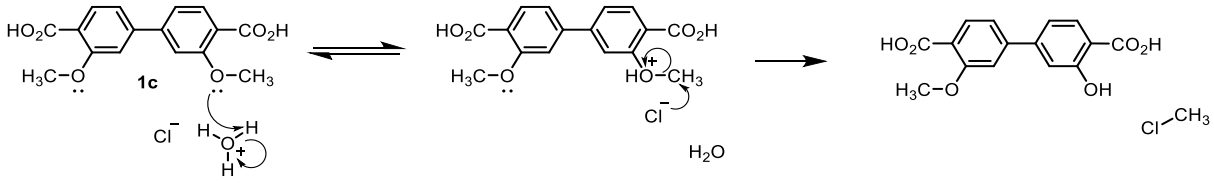

Scheme 17 Acid assisted cleavage of alkyl ethers.

The methyl chloride would then rapidly undergo substitution with water, and yield methanol. (**Scheme 18**)

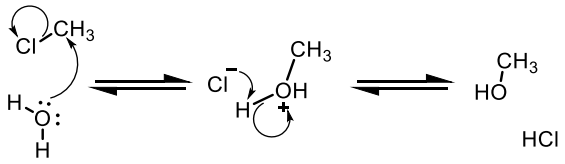

Scheme 18: Hydrolysis of methyl chloride.

The production of methanol in the cleaving reaction was confirmed by spiking the sample with methanol, which is shown in the top spectrum in **Figure 53**.

Further evidence was gathered by isolating the dissolved species in the sample by precipitation with water. The acquired compound yields the ^{1}H NMR spectrum shown in **Figure 54**.

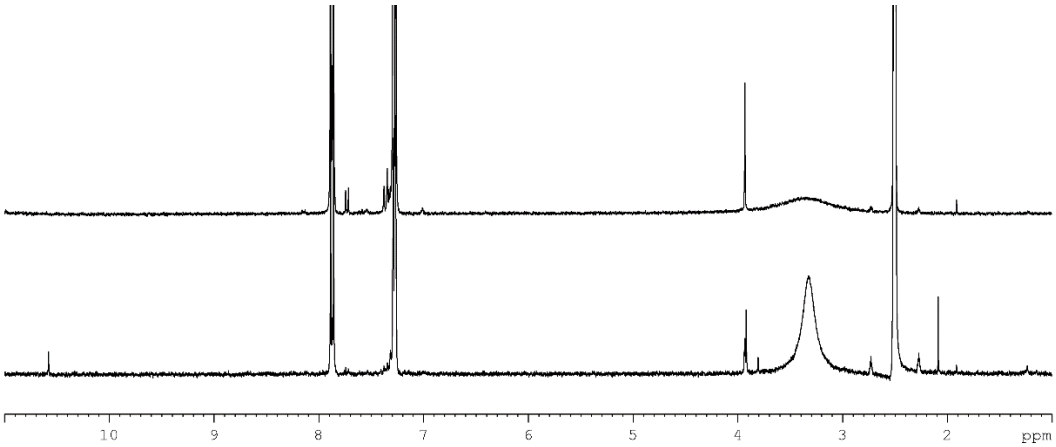

Figure 54: ^{1}H NMR spectra of **1d** (top) and isolated precipitate from the MOF-like NMR-experiment (bottom). Note the singlet at 3.9 ppm from the mono-methoxy impurity. (300 MHz, DMSO-d_6)

The conclusion from these experiments is that the lability of alkyl ethers (especially methoxy) is an issue when synthesizing UiO-67 MOFs under these conditions.

3.1.2 Optimizing reaction conditions for UiO-67-dialkoxy

Further experiments based on the results from **Section 3.1.1** were conducted in order to optimize the reaction conditions for the MOF syntheses. The degree of decomposition was investigated at lower reaction temperatures in order to find a suitable temperature that could maximize the formation of the MOF and minimize the decomposition of the linker.

All three linkers (**1c**, **2c** and **3c**) were heated separately in deuterated DMF, together with hydrochloric acid at 100 °C for 24 h. (**Figure 55**, **Figure 56** and **Figure 57**)

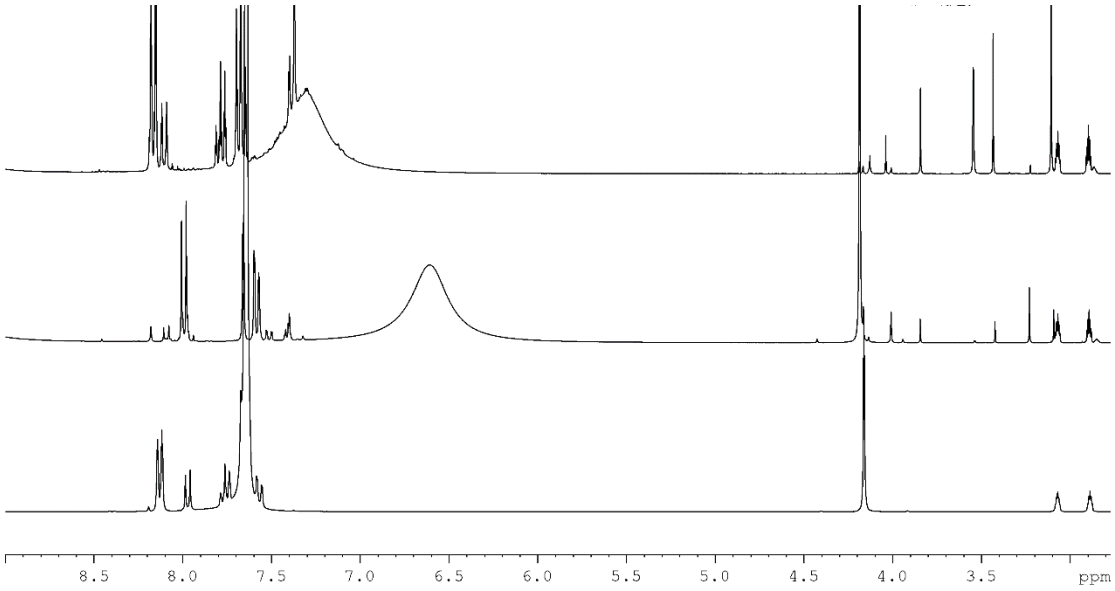

Figure 55: ^{1}H NMR spectra of **1c** in deuterated DMF with hydrochloric acid present. Bottom spectrum is before heating, middle spectrum is after 24 hours at 100 °C and top spectrum is at 130 °C for 24 hours. Note that the two top spectra are different, individual samples. (300 MHz, DMF-d_7)

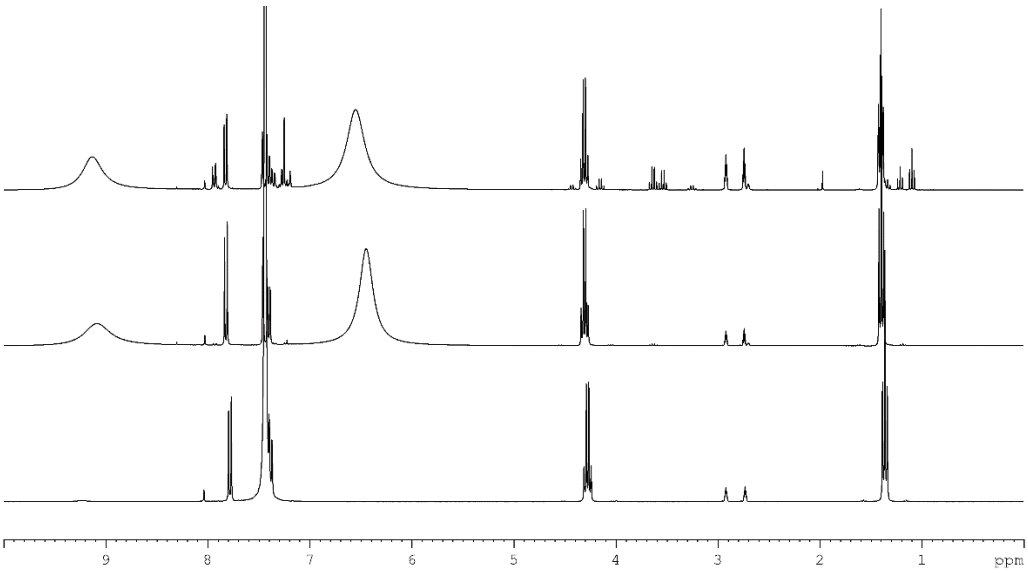

Figure 56: ^{1}H NMR spectra of **2c** in deuterated DMF with hydrochloric acid present. Bottom spectrum is before heating, middle spectrum is after 24 hours at 100 °C and top spectrum is at 130 °C for 24 hours. Note that the two top spectra are different, individual samples. (300 MHz, DMF-d_7)

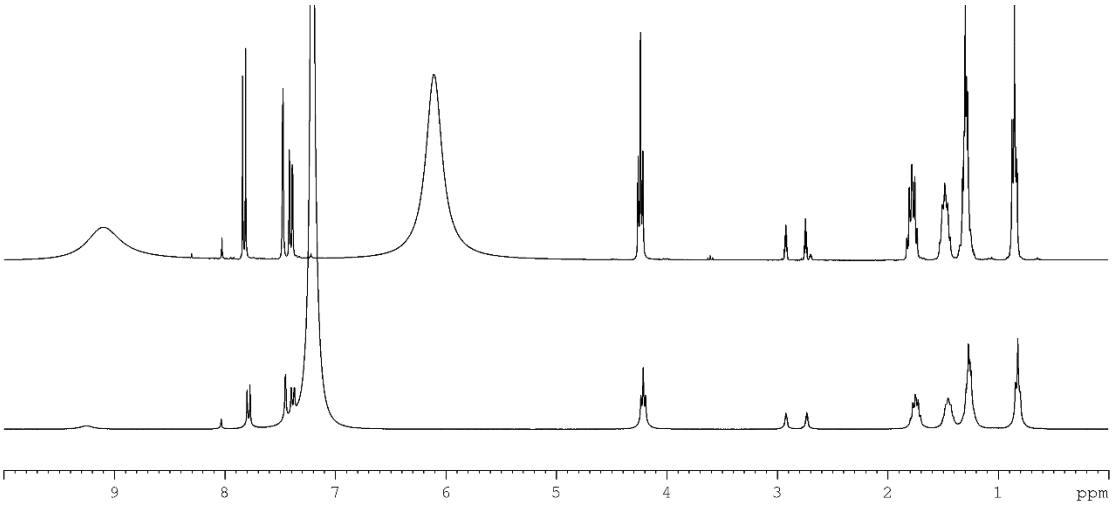

Figure 57 ^{1}H NMR spectra of **3c** in deuterated DMF with hydrochloric acid present. Bottom spectrum is before heating and top spectrum is after heating at 100 °C for 24 h. (300 MHz, DMF-d_7)

It is clear from the experiments that **2c** and **3c** barely hydrolyze at 100 °C after 24 hours, while **1c** still do to a significant degree.

3.1.3 Summary of attempted syntheses of UiO-67-2c

Based on the results from the optimization experiments in **Section 3.1.2**, several attempts on synthesizing **UiO-67-2c** were conducted. A summary over the different attempts of synthesizing **UiO-67-2c** is given in **Table 6**.

Table 6: Summary of attempted synthesis conditions for **UiO-67-2c**. Equivalents are given in respect to $ZrCl_4$. All entries were run with 3 equivalents of H_2O added, except **Entry 13** which had no water added.

Entry	$ZrCl_4$ (mg)	DMF (equiv.)	Modulator (type, equiv.)	Temperature	Time	Product
1	300	300	None	120 °C, static	4 d	Gel
2	500	50	BA [j], 3	130 °C, stirring	1 d	Crystalline
3	2000	50	BA, 3	130 °C, stirring	1d	Crystalline
4	500	50	BA, 3	100 °C, stirring	1 d	Gel
5	150	500	BA, 3	100 °C, stirring	1 d	Gel
6	100	500	BA, 3	100 °C, static	1 d	Gel
7	100	500	Nitro-BA [k], 3	100 °C, static	1 d	Gel
8	100	500	BA, 3	100 °C, static	2 h	Gel
9	71	500	Nitro-BA, 3	100 °C, static	10	Gel
10	71	500	BA, 10	100 °C, static	1 d	Gel
11	100	500	AcOH, 3	100 °C, static	2 d	Gel [l]
12	100	300	BA, 3	100 °C, static	1 d	Gel
13	100	60	HCO_2H, 124	100 °C, static	1d	Gel

[j] Benzoic acid

[k] 4-nitrobenzoic acid

[l] No gel-formation until 48 hours of reaction time.

Gel formation is, as **Table 6** shows, a frequent occurrence when attempting to synthesize **UiO-67-2c**. The two crystalline products (**Entry 2** and **Entry 3**) are the two samples discussed and characterized in **Section 3.1.1**. An example of a P-XRD diffractogram displaying the amorphic nature of the gel product is given in **Figure 58**.

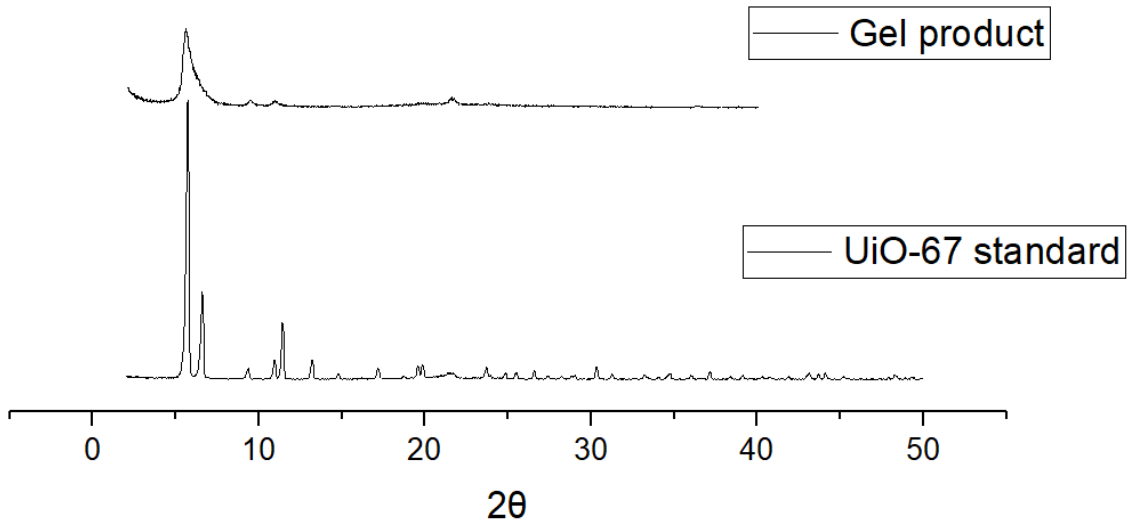

Figure 58 Comparing the P-XRD diffractograms of a standard UiO-67 sample, and a gel product from this work.

The lowered reaction temperature, as a measure to prevent linker decomposition, seems to facilitate the formation of a kinetic product that is the gel. Sadly, due to time constrains, no further attempts of synthesizing metal-organic frameworks were attempted.

3.1.4 Discussion and conclusions of the synthesis of UiO-67-dialkoxy metal-organic frameworks

Even though no successful synthesis of a UiO-67-dialkoxy MOF was reported in this work, there is a still some unexplored, potentially viable routes to such MOFs. One of them is the usage of post synthetic modification or post synthetic linker exchange, to obtain the desired MOF structure. The main issue with post synthetic modification, in this case being alkylation of **UiO-67-1d**, is the need of a base to deprotonate the phenol groups in order to alkylate. MOF structures, especially UiO-type MOFs, are sensitive to basic media, and quickly decomposes in the presence of base.

Another potentially viable route is the usage of hydrothermal synthesis. Zhao *et al.* reported in 2015[27] the synthesis of a 2,5-diethoxyterephtalic acid based UiO-66 MOF, using zirconium nitrate as the Zr-source, suspended in a water and acetic acid mixture under reflux. A water-based synthesis is great alternative to the DMF-based synthesis using zirconium chloride not only for the milder reaction conditions, but also for environmental and safety aspects. A green synthesis of UiO-type MOFs would be very important in a potential industrial production scheme.

4 Conclusion and future prospective

As described in the introduction is the primary aim of this thesis the synthesis and characterization of 3,3'-dialkoxy UiO-67 linkers. During the two years of this project three compounds that fit that description (compound **1c**, **2c** and **3c**) have been made, which are presented in this work with their synthetic routes thoroughly explained and explored. Some even have several synthetic pathways, including a more time-efficient one-pot synthesis. These three compounds have in addition been fully characterized using methods such as NMR spectroscopy, mass spectrometry, melting point analysis and elemental analysis. In addition to this, seven various analogues of alkylated salicylates have been synthesized and characterized, creating a huge potential for future coupled products. An in-depth exploration of the possible synthesis of a dihydroxy functionalized UiO-67 linker (**1d**) has also been performed, where as many as five different synthetic pathways were explored.

The secondary aim of this project is to synthesize UiO-67 MOFs with the aforementioned 3,3'-dialkoxy substituted linkers. Due to the discussed problems with linkers decomposing to the corresponding phenols during the MOF synthesis, a lot of time and effort was directed to the investigation of this decomposition and to find potential optimized reaction conditions. Although no successful synthesis is reported, a thorough explanation and investigation of the problems is presented instead.

Regarding future work, trying to further explore alternative synthetic conditions in order to obtain a UiO-67 MOF with either **1c**, **2c**, or **3c** would be interesting. The NMR-experiments discussed in **Section 3.1.1** indicate that the more sterically hindered **3c** undergoes dealkylation much slower than its methylated or ethylated analogue. Perhaps it is a better candidate to be put into a MOF than what has been attempted in this work. Another strategy in order to yield these MOFs could be to look into other zirconium precursors that allow for the synthesis to occur at less extreme conditions than the current $ZrCl_4$-based synthesis. There has been reported several syntheses of UiO-66 using hydrothermal (water-based) synthesis with zirconium nitrate[27] or zirconium sulfate tetrahydrate[28] as the zirconium source. This could, considering what has been discovered in this work, prove to be a potential way of synthesizing the target MOFs of this thesis.

There is also the possibility of introducing the alkyl groups post-synthetically, through the potential **UiO-67-1d**. The two-step synthetic pathway to **1d**, starting from the cheap and

readily available methyl 4-iodosalicylate, as discussed in **Section 2.5.3** would make this pathway especially interesting.

If a successful synthesis of **UiO-67-3,3'-dialkoxy** is discovered, then analogization in terms of synthesizing 2'2-dihydroxy, 2,2'-dialkoxy and corresponding UiO-67 MOFs of these would be an interesting project, for instance in terms of comparing the influence that the alkyl groups would bring in the 3,3' position *versus* the 2,2'-position.

Experimental

5 General

All chemicals were used as received. CH_2Cl_2, THF and MeCN used in reactions was dried with an MB SPS-800 solvent purification system from MBraun. Hexanes were distilled before use.

NMR-spectra were recorded using Bruker DPX200, DPX300, AVII400, AVIII400, AV600 and AVII600 spectrometers at ambient temperatures, and the chemical shifts are reported in ppm relative to the residual solvent signals ($CDCl_3$ (7.26 ppm for ^{1}H NMR and 77.0 ppm for ^{13}C NMR), DMSO-d_6 (2.50 ppm for ^{1}H NMR and 39.5 ppm for ^{13}C NMR), DMF-d_7 (2.94 ppm and 35.2 ppm for ^{13}C NMR) and D_2O (4.79 ppm for ^{1}H NMR)

Mass spectra were obtained by MicroMass Prospec Q (EI) and MicroMass QTOF 2W (ESI) by Osamu Sekiguchi. All ESI-spectra were run in positive ion mode, unless otherwise noted.

All reported melting points are uncorrected and were recorded using a Stuart SMP10 point apparatus

All elemental analysis was performed by Microanalytisches Laboratorium Kolbe, Mülheim an der Ruhr, Germany.

5.1 Linker syntheses

5.1.1 Synthesis of methoxy ether 1a

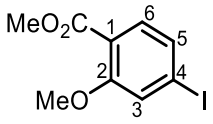

Methyl iodide (2.6 mL, 51 mmol, 1.4 equiv.) was added to a mixture of methyl 4-iodosalicylate (10 g, 36 mmol, 1.0 equiv.) and potassium carbonate (10 g, 73 mmol, 2.0 equiv.) in acetonitrile (100 mL). The slight yellow reaction mixture was refluxed under an argon atmosphere while stirring for 23 hours. The mixture was diluted in diethyl ether (300 mL) and transferred to a separatory funnel where it was washed with water (1 x 300 mL) and a solution of sodium chloride (1 x 300 mL, aq., sat.). The diethyl ether was dried using magnesium sulfate, then filtered and removed by rotary evaporation yielding **1a** (5.04g, 17.3 mmol, 95 %) as a colorless oil. **1a** was pure by ^{1}H NMR. (**Figure 59**)

^{1}H NMR (400 MHz, $CDCl_3$): 7.45 (d, 1H, 6-**H**, ^{3}J = 8.1 Hz), 7.29 (m, 2H, 3,5-**H**), 3.85 (s, 3H, **Me**O-2), 3.84 (s, 3H, **Me**-O_2C)

^{13}C NMR (101 MHz, $CDCl_3$): 165.9 (**C**O_2Me), 159.1 (**2**), 132.6 (**6**), 129.5 (**5**) 121.5 (**3**), 119.5 (**1**), 99.8 (**4**), 56.2 (**Me**-O-Ar), 52.0 (**Me**-O_2C)

MS (EI, CH_2Cl_2) m/z (rel. %): 292 (M^+, 58), 261 ([M-MeOH]$^+$, 100), 259 (68), 218 (22), 134 (26), 63 (18)

The spectroscopic data are in coherence with what is previously reported in the literature.[29-31]

5.1.2 Synthesis of dimethoxy ester 1b

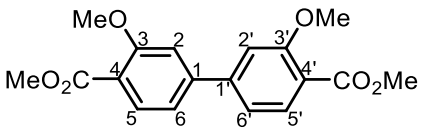

Potassium carbonate (6.38 g, 46.2 mmol, 3.02 equiv.) and bis(pinacolato)diboron (2.34 g, 9.22 mmol, 0.603 equiv.) were added to a round bottom flask containing **1a** (4.47 g, 15.3 mmol, 1.00 equiv.) dissolved in DMSO (90.0 mL). The green tinted mixture was bubbled through with argon for 10 minutes under stirring, before $Pd(dppf)Cl_2 \cdot CH_2Cl_2$ (0.225 g, 0.276 mmol, 1.80 mol %) was added, turning the reaction mixture red. The reaction mixture was heated at 80 °C, as the mixture turned black, and was left overnight while stirring under an argon atmosphere. The following day, the reaction mixture was poured into a mixture of 400 mL ice and 100 mL H_2O, and the raw product was filtered off. The raw product was re-dissolved in dichloromethane (400 mL) and washed with water (300 mL) and a sodium chloride solution (300 mL, aq., sat.). The dichloromethane was then dried using magnesium sulfate, before removed by rotary evaporation. The remaining brown, amorphous solid was purified by silica filtration (EtOAc) before being recrystallized (EtOH), yielding **1b** (2.05 g, 6.22 mmol, 81 %) as a white solid. **1b** was pure by ^{1}H NMR. (**Figure 70**)

^{1}H NMR (400 MHz, $CDCl_3$): 7.89 (d, 2H, 5,5'-**H**, ^3J = 8.0 Hz), 7.19 (dd, 2H, 6,6'-**H**, ^3J = 8.0 Hz, ^4J = 1.6 Hz), 7.14 (d, 2H, 2,2'-**H**, ^4J = 1.4 Hz), 3.98 (s, 6H, 3,3'-O**Me**), 3.91 (s, 6H, **Me**-O_2C)

^{13}C NMR (101 MHz, $CDCl_3$): 166.3 (MeO_2C), 159.5 (**3,3'**), 145.6 (**1,1'**), 132.3 (**5,5'**), 119.6 (**4,4'**), 119.2 (**6,6'**), 111.1 (**2,2'**), 56.2 (3,3'-O**Me**), 52.1 (**Me**-O_2C)

MS (EI, CH_2Cl_2) m/z (rel. %): 330 (M^+, 43), 299 ([M - OMe]$^+$, 100), 297 (42)

M_p: 173-174 °C

The spectroscopic data are in coherence with what is previously reported in the literature. [23, 25]

5.1.3 Synthesis of dimethoxy linker 1c

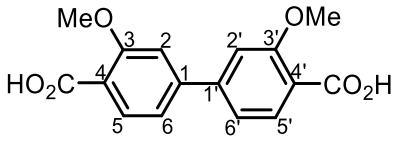

Water (53.0 mL) and methanol (27.0 mL) were added to a flask containing **1b** (3.77 g, 12.5 mmol, 1.00 equiv.) and lithium hydroxide (1.19 g, 49.6 mmol, 4.96 equiv.) dissolved in THF (53.0 mL). The reaction mixture was stirred at ambient temperature for 22 hours. The excess THF and MeOH were then removed *in vacuo*, and additional water (*ca* 200 mL) was added. The product was precipitated out of solution by adding glacial acetic acid until the pH was below 4. The precipitate was collected by vacuum filtration and washed several times with water, before dried in an oven at 130 °C for 24 hours yielding **1c** (4.08 g, 11.3 mmol, 90 %) as a grey-white solid. The product was pure by ^{1}H NMR. (**Figure 83**)

^{1}H NMR (400 MHz, DMSO-d_6): 12.68 (b.s, 2H, COO**H**), 7.74 (d, 2H, 5,5'-**H**,^{3}J = 7.9 Hz), 7.39 (d, 2H, 2,2'-**H**, ^{4}J = 1.4 Hz), 7.36 (dd, 2H, 6,6'-**H**,^{3}J = 7.9 Hz, ^{4}J = 1.4 Hz) 3.93 (s, 6H, 3,3'-O**Me**)

^{13}C NMR (101 MHz, DMSO-d_6): 167.0 (**C**OOH, 158.5 (**3,3'**), 143.9 (**1,1'**), 131.3 (**5,5'**), 120.8 (**4,4'**), 118.8 (**6,6'**), 111.1 (**2,2'**), 55.9 (3,3'-O**Me**)

MS (ESI, CH_3OH) m/z (rel. %): 627 ($[2M + Na]^+$, 8), 325 ($[M + Na]^+$, 100), 258 (21), 230 (51)

HRMS (ESI, CH_3OH): Measured m/z: 325.0683. Calculated m/z for $[C_{16}H_{14}O_6Na]^+$: 325.0683

Elemental analysis: Calculated for $C_{16}H_{14}O_6$: C, 63.58; H, 4.67; O, 31.76. Found: C, 62.93; H, 4.76; O, 31.29.

M_p: >290 °C (decomp.)

The spectroscopic data are in coherence with what is previously reported in the literature. [15, 23]

5.1.4 Synthesis of ethoxy ether 2a

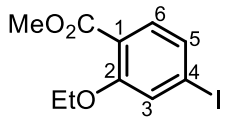

Ethyl iodide (2.0 mL, 25 mmol, 1.4 equiv.) was added to a mixture of methyl 4-iodosalicylate (5.05 g, 18.2 mmol, 1.0 equiv.) and potassium carbonate (5.03 g, 36.4 mmol, 2.0 equiv.) in acetonitrile (50 mL). The reaction mixture was refluxed under an argon atmosphere while stirring for 22 hours. The mixture was diluted in diethyl ether (250 mL) and transferred to a separatory funnel where it was washed with water (250 mL) and a saturated solution of sodium chloride (250 mL, aq.). The diethyl ether was dried using magnesium sulfate, then filtered and removed by rotary evaporation yielding **2a** (96-99 %) as a colorless oil. **2a** was pure by NMR. (**Figure 63**)

^{1}H NMR (400 MHz, $CDCl_3$): δ 7.48 (d, 1H, 6-**H**, ^{3}J = 8.2 Hz), 7.31 (m, 2H, 3,5-**H**), 4.09 (q, 2H, 2-OC**H$_2$**CH_3, ^{3}J = 7.0 Hz), 3.87 (s, 3H, 1-CO_2**Me**), 1.45 (t, 3H, 2-OCH_2C**H$_3$**, ^{3}J = 7.0 Hz).

^{13}C NMR (101 MHz, $CDCl_3$): δ 166.2 (**C**O_2Me), 158.7 (**2**), 132.7 (**6**), 129.4 (**5)**, 122.7 (**3**), 120.0 (**1**), 99.8 (**4**), 65.0 (O-**C**H_2-CH3), 52.0 (-CO_2**Me**), 14.6 (O-CH_2-**C**H3).

MS (EI, CH_2Cl_2) m/z (rel. %): 306 (M^+, 17), 291 (36), 246 (100), 218 (43), 63 (36).

M_p: 43-44 °C

The spectroscopic data are in coherence with what is previously reported in the literature.[17]

5.1.5 Synthesis of diethoxy ester 2b from 2a

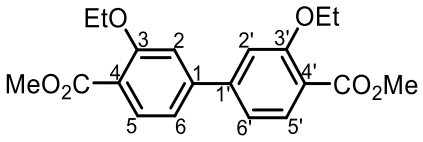

Potassium carbonate (1.35 g, 9.8 mmol, 3.0 equiv.) and bis(pinacolato)diboron (0.42 g, 1.7 mmol, 0.51 equiv.) was added to a round bottom flask containing **2a** (1.00 g, 3.3 mmol, 1.0 equiv.) dissolved in DMSO (30 mL). The green tinted mixture was bubbled through with argon for 10 minutes under stirring before Pd(dppf)Cl_2· CH_2Cl_2 (0.072 g, 0.098 mmol, 3 mol. %) was added, turning the reaction mixture red. The reaction mixture was heated at 80 °C, as the mixture turns black, and is left overnight while stirring under argon. The following day, the reaction mixture was poured into a mixture of 300 mL H_2O, and the raw product was filtered off. The raw product was re-dissolved in dichloromethane (300 mL) and washed with water (300 mL) and sodium chloride solution (300 mL, aq., sat.). The dichloromethane was then dried using magnesium sulfate, before removed by rotary evaporation. The remaining brown, amorphous solid was purified by silica filtration (EtOAc) before being recrystallized (EtOH), yielding **2b** (68-81 %) as a white solid. **2b** was pure by ^{1}H NMR. (**Figure 74**)

^{1}H NMR (400 MHz, $CDCl_3$): 7.87 (d, 2H, 5,5'-**H**, ^3J = 8.0 Hz), 7.17 (dd, 2H, 6,6'-**H** ^3J = 8.0 Hz, ^4J = 1.5 Hz), 7.13 (d, 2H, 2,2'-**H**, ^4J = 1.5 Hz), 4.20 (q, 4H, -OC**H$_2$**-CH_3, ^3J = 7.0 Hz), 3.91 (s, 6H, CO_2**Me**) 1.50 (t, 6H, -OCH_2-C**H$_3$**, ^3J = 7.0 Hz)

^{13}C NMR (101 MHz, $CDCl_3$): 166.4 (**C**O_2Me), 158.9 (**3,3'**), 145.4 (**1,1'**), 132.1 (**5,5'**), 119.9 (**4,4'**), 119.1 (**6,6'**), 112.4 (**2,2'**), 64.9 (O**C**H_2CH_3), 51.9 (CO_2**Me**), 14.7 (OCH_2**C**H_3)

MS (EI, CH_2Cl_2) m/z (rel. %): 358 (M^+, 58), 327 ([M - OMe]$^+$, 47), 325 (74), 311(100), 299 ([M - CO_2Me]$^+$, 31)

M$_p$: 122-123 °C

This compound has not been previously reported.

5.1.6 One pot synthesis of diethoxy ester 2b from methyl 4-iodosalicylate

Methyl 4-iodosalicylate (2.78 g, 10.0 mmol, 1.00 equiv.), B_2pin_2 (1.30 g, 5.13 mmol, 0.512 equiv.) and cesium carbonate (16.3 g, 50.1 mmol, 5.01 equiv.) were added to a dry two-necked round bottom flask containing acetonitrile (60.0 mL). The suspension was bubbled thoroughly with argon before adding ethyl iodide (1.1 mL, 13.9 mmol, 1.39 equiv.). After five additional minutes of bubbling, $Pd(dppf)Cl_2 \cdot CH_2Cl_2$ (0.163 g, 0.200 mol, 2.00 mol. %) and dppf (0.114 g, 0.203 mmol, 2.03 mol. %) were added to the reaction mixture, which was then heated to reflux for 20 hours under argon. The reaction mixture was then poured into water (600 mL) and the precipitate was vacuum filtered and washed with additional water. The precipitate was redissolved using CH_2Cl_2 (300 mL) and transferred to a separatory funnel where it was washed with water (300 mL) and a saturated solution of sodium chloride (300 mL, aq.). The dichloromethane layer was dried using magnesium sulfate and removed by rotary evaporation. The remaining brown solid was purified using flash chromatography (SiO_2, 20:80 EtOAc: Hexanes), yielding **2b** (1.28 g, 3.89 mmol, 77.8 %) as a white crystalline solid. **2b** was pure by ^1H NMR.

5.1.7 Synthesis of diethoxy linker 2c

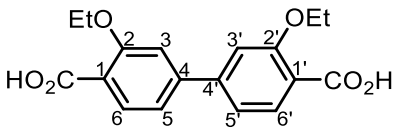

Water (6.0 mL) and methanol (3 mL) were added to a flask containing **2b** (0.503 g, 1.41 mmol, 1.0 equiv.) and lithium hydroxide (0.135 g, 5.65 mmol, 4.0 equiv.) dissolved in THF (6 mL). The reaction mixture was stirred at ambient temperature for 20 hours. The excess THF and MeOH were then removed *in vacuo*, and additional water (6.0 mL) was added. The product was precipitated out of solution by adding glacial acetic acid until pH was below 4. The precipitate was collected by vacuum filtration and washed several times with water, before dried in an oven at 115 °C for 24 hours yielding **2c** (0.41 g, 1.24 mmol, 88 %) as a grey-white solid. The product was pure by ^{1}H NMR. (**Figure 86**)

^{1}H NMR (400 MHz, DMSO-d_6): 12.61(b. s, 2H, COO**H**), 7.71(d,2H, 5,5'-**H**,^{3}J = 8.0 Hz), 7.36 (d, 2H, 2,2'-**H**, ^{3}J = 1.5 Hz) 7.33 (dd, 2H, 6,6'-**H** ^{3}J = 8.0 Hz, ^{4}J = 1.5 Hz), 4.22 (q, 4H, O-C**H$_2$**-CH$_3$, ^{3}J = 6.9 Hz), 1.36 (t, 6H, O-CH$_2$-C**H$_3$**, ^{3}J = 6.9 Hz)

^{13}C NMR (101 MHz, DMSO-d_6): 167.1(**C**OOH), 157.8 (**3,3'**), 143.8 (**1,1'**), 131.2 (**5,5'**), 121.3 (**4,4'**), 118.8 (**6,6'**), 112.2 (**2,2'**), 64.3 (O-C**H$_2$**-CH$_3$), 14.6 (O-CH$_2$-C**H$_3$**)

MS (ESI, CH$_3$OH) m/z (rel. %): 683 ([2M + Na]$^+$, 11), 353 ([M + Na]$^+$, 100).

HRMS (ESI, CH$_3$OH): Measured m/z: 353.0995. Calculated m/z for [C$_{18}$H$_{18}$O$_6$Na]$^+$: 353.0996

Elemental analysis: Calculated for C$_{18}$H$_{18}$O$_6$: C, 65.45; H, 5.49; O, 29.06. Found: C, 65.19; H, 5.50; O, 28.87.

M$_p$: 244-245 °C

The spectroscopic data are in coherence with what is previously reported in the literature.[32]

5.1.8 Synthesis of n-hexyloxy ether 3a

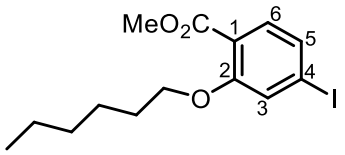

1-bromohexane (0.65 mL, 4.63 mmol, 1.3 equiv.) was added to a mixture of methyl 4-iodosalicylate (1.00 g, 3.59 mmol, 1.00 equiv.) and potassium carbonate (1.03 g, 7.46 mmol, 2.08 equiv.) in acetonitrile (10.0 mL). The reaction mixture was refluxed under an argon atmosphere while stirring for 22 hours. The mixture was diluted in dichloromethane (50 mL) and transferred to a separatory funnel where it was washed with water (25 mL), sodium hydroxide (25 mL, 3 M, aq.) and saturated sodium chloride (25 mL, aq.). The dichloromethane was dried using sodium sulfate, then filtered and removed by rotary evaporation yielding **3a** (1.13 g, 3.12 mmol, 87 %) as a slight yellow oil. **3a** was relatively pure, with some residual n-hexyl bromide observed in the ^{1}H NMR spectrum. (**Figure 67**)

^{1}H NMR (400 MHz, $CDCl_3$): δ 7.47 (d, 1H, Ph**H**, ^{3}J = 8.0 Hz), 7.29 (m, 2H, Ph**H**), 3.98 (t,2H, O-C**H$_2$**-CH_3-, ^{3}J = 6.5 Hz), 3.86 (s, 3H, -CO_2**Me**), 1.81 (p, 2H, O-CH_2-C**H$_2$**-CH_2-, ^{3}J = 6.5 Hz), 1.48 (m, 2H, O-CH_2-CH_2-C**H$_2$**-), 1.33 (m, 4H, CH_3-C**H$_2$**-C**H$_2$**-), 0.90 (m, 3H, C**H$_3$**-CH_2-).

^{13}C NMR (101 MHz, $CDCl_3$): δ 166.2 (**C**O_2Me), 158.7 (**2**), 132.6 (**6**), 129.1 (**5**), 122.4 (**3**), 119.7 (**1**), 99.7 (**4**), 69.1(O-**C**H_2-), 51.8 (-CO_2**Me**), 31.3 (CH_3-**C**H_2-CH_2- or CH_3-CH_2-**C**H_2-), 28.9 (O-CH_2-C**H$_2$**-CH_2-) 25.4 (O-CH_2-CH_2-**C**H_2-), 22.4 (CH_3-**C**H_2-CH_2- or CH_3-CH_2-**C**H_2-), 13.9 (**C**H_3-CH_2-).

MS (EI, CH_2Cl_2) m/z (rel. %): 362 (M^+, 4.4), 278 ([M-C_6H_{13}], 54), 246 (100), 43 (30).

This compound has not been previously reported.

5.1.9 Synthesis of di(n-hexyloxy) ester 3b

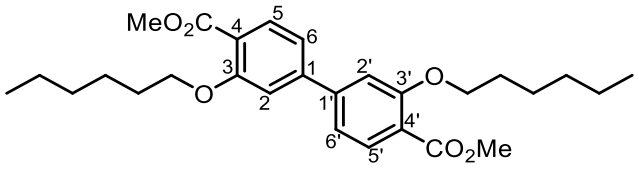

Potassium carbonate (3.43 g, 24.9 mmol, 3.01 equiv.) and bis(pinacolato)diboron (1.25 g, 4.92 mmol, 0.594 equiv.) were added to a round bottom flask containing **3a** (3.00 g, 8.29 mmol, 1.00 equiv.) dissolved in DMSO (50.0 mL). The orange tinted mixture was bubbled through with argon for 10 minutes under stirring before $Pd(dppf)Cl_2 \cdot CH_2Cl_2$ (0.121 g, 0.165 mmol, 2 mol. %) was added, turning the reaction mixture red. The reaction mixture was heated at 80 °C and was left for 22 h while stirring under argon. The reaction mixture was then poured into *ca.* 150 mL water and ice. The precipitated raw product was filtered off, and redissolved in *ca.* 150 mL CH_2Cl_2, which was washed with a saturated sodium chloride solution (150 mL), dried using sodium sulfate and filtered. Excess dichloromethane was removed by rotary evaporation. The product was purified by flash chromatography (CH_2Cl_2) yielding **3b** (1.57 g, 3.34 mmol, 67.9 %) as a slight yellow solid with a wax-like consistence. **3b** was pure by NMR. (**Figure 79**)

^{1}H NMR (400 MHz, $CDCl_3$): 7.87 (d, 2H, 5,5'-**H**, ^3J = 8.0 Hz), 7.16 (dd, 2H, 6,6'-**H**, ^3J = 8.0 Hz, ^4J = 1.3 Hz), 7.12 (d, 2H, 2,2'-**H**, ^4J = 1.3 Hz), 4.11 (t, 4H, 3,3'-OC**H**$_2$, ^3J = 6.5 Hz), 3.91 (s, 6H, **Me**O_2C), 1.86 (p, 4H, -OCH_2C**H$_2$**, ^3J = 7.0 Hz), 1.52 (m, 4H, OCH_2CH_2C**H$_2$**), 1.36 (m, 8H,C**H$_2$**C**H$_2$**CH_3) , 0.91 (m, 6H, -CH_2C**H$_3$**)

^{13}C NMR (101 MHz, $CDCl_3$): 166.7 (MeO_2**C**), 159.1 (**3,3'**), 145.5 (**1,1'**), 132.2 (**5,5'**), 119.9 (**4,4'**), 119.0 (**6,6'**), 112.2 (**2,2'**), 69.2 (-O**C**H_2CH_2), 52.0 (**Me**O_2C), 31.5 (-CH_2**C**$H_2CH_2CH_3$), 29.2 (-OCH_2**C**H_2), 25.7 (OCH_2CH_2**C**H_2), 22.6 (**C**H_2CH_3), 14.0 (-CH_2**C**H_3)

MS (EI, CH_2Cl_2) m/z (rel. %): 470 ([M^+], 19), 367 (27), 302 ([M-2(C_6H_{13})]$^+$, 32), 270 ([M2(OC_6H_{13})]$^+$, 100), 237 (31)

This compound has not been previously reported.

5.1.10 Synthesis of di(n-hexyloxy) linker 3c

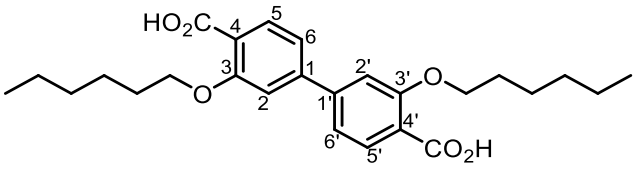

Water (15.0 mL) and methanol (8.0 mL) were added to a flask containing **3b** (1.42 g, 3.02 mmol, 1.0 equiv.) and lithium hydroxide (0.30 g, 12.5 mmol, 4.1 equiv.) dissolved in THF (15.0 mL). The reaction mixture was stirred at ambient temperature for 22 hours. The excess THF and MeOH were then removed *in vacuo*, and additional water (*ca.* 30 mL) was added. The product was precipitated out of solution by adding glacial acetic acid until the pH was below 4. The precipitate was collected by vacuum filtration and washed several times with water, before dried in an oven at 120 °C for 24 hours yielding **3c** (1.23 g, 2.78 mmol, 91.9 %) as a grey solid. The product was pure by ^{1}H NMR. (**Figure 90**)

^{1}H NMR (600 MHz, DMSO-d_6): 12.59 (b.s, 2H, -CO_2**H**), 7.71 (d, 2H, 5,5'-**H**, ^{3}J = 8.0 Hz), 7.35 (d, 2H, ^{3}J = 1.3 Hz) 7.32 (dd, 2H, 2,2'-**H**, 6,6'-**H**, ^{3}J = 7.95 Hz, ^{4}J = 1.5 Hz) 4.16 (t, 4H, O-C**H$_2$**-, ^{3}J = 6.3 Hz), 1.73 (p, 4H, O-CH_2C**H$_2$**-,^{3}J = 6.9 Hz) , 1.47 (m, 4H, O-CH_2CH_2C**H$_2$**-), 1.31, (m, 8H, -C**H$_2$**C**H$_2$**CH_3), 0.87 (t, 6H,-CH_2C**H$_3$**, ^{3}J = 6.7 Hz.)

^{13}C NMR (151 MHz, DMSO-d_6): 167.2 (**C**O_2H), 157.9 (**3,3'**), 143.8 (**1,1'**), 131.2 (**5,5'**), 121.2 (**4,4'**), 118.7 (**6,6'**), 112.1 (**2,2'**), 68.4 (O-**C**H_2CH_2), 30.9 (-CH_2**C**$H_2CH_2CH_3$), 28.6 (O-CH_2**C**H_2-,) 25.1 (O-CH_2CH_2**C**H_2-), 22.1 (-**C**H_2CH_3), 13.9 (-CH_2**C**H_3)

MS (ESI, MeOH) (rel. %): 907 ([M+Na]$^+$, 5), 686 (4), 553 (10), 465 ([M+Na]$^+$,100), 441 (8),413 (25)

HRMS (ESI, CH_3OH): Measured m/z: 465.2247. Calculated m/z for [$C_{26}H_{34}O_6Na$]$^+$: 465.2248

Elemental analysis: Calculated for $C_{26}H_{34}O_6$: C, 70.56; H, 7.74; O, 21.69. Found: C, 70.31; H, 7.89; O, 21.41.

M_p: 184-185 °C

This compound has not been previously reported.

5.1.11 Synthesis of dihydroxy linker 1d by acid catalyzed dealkylation

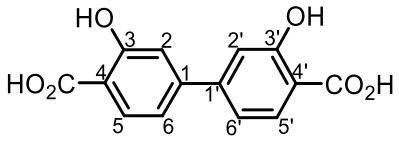

2c (0.444g, 1.34 mmol, 1.00 equiv.) was added to a round bottom flask containing glacial acetic acid (25.0 mL). Hydrobromic acid (10 mL, 8.9 M, aq.) was then added to the suspension and the reaction mixture was refluxed for 20 hours. The reaction mixture was then poured into 200 mL of water. The white precipitate was filtered off, washed with copious amounts of water and dried in an oven at 120 °C, yielding **1d** (0.330 g, 1.20 mmol, 89.6 %). The isolated product had approximately 1 % semi-alkylated byproduct visible by ^{1}H NMR. (**Figure 96**)

^{1}H NMR (400 MHz, DMSO-d_6): 7.87 (d, 2H, 5,5'-**H**, ^{3}J = 8.6 Hz), 7.27 (m, 4H, 2,2'-**H**, 6,6'-**H**)

^{13}C NMR (101 MHz, DMSO-d_6): 171.6 (**C**O_2H), 161.3 (**3**,**3'**), 145.5 (**1**,**1'**), 130.9 (**5**,**5'**), 117.9 (**6**,**6'** or **2**,**2'**), 115.2 (**6**,**6'** or **2**,**2'**), 112.8 (**4**,**4'**)

MS (Positive-ESI, MeCN) m/z (rel. %): 637 (17), 313 (35), 341 (100), 319 ([M – H + 2Na]$^{+}$, 99)

MS (Negative-ESI, MeCN) m/z (rel. %): 301 (5), 273 ([M-H]$^{-}$, 100), 255 (8), 136 ([M-2H]$^{2-}$, 2)

HRMS (Positive ESI, MeCN): Measured m/z: 319.0189. Calculated m/z for $C_{14}H_9Na_2O_6$: 319.0189.

HRMS (Negative ESI, MeCN): Measured m/z: 273.0405. Calculated m/z for $C_{14}H_9O_6$: 273.0405.

The spectroscopic data are in coherence with what is previously reported in the literature. [23, 33]

5.1.12 Synthesis of dihydroxy linker 1d by alkyl-amine assisted dealkylation

1c (0.302 g, 1.00 mmol, 1.00 equiv.) was suspended in *N,N*-dimethylacetamide (10 mL) together with piperazine (0.521 g, 6.06 mmol, 6.06 equiv.) and heated at 150 °C for 22 hours. The red-brown solution was then cooled in an ice-bath and HCl (conc., aq.) was added until pH was below 2. The precipitated product was then filtered and washed with copious amounts of water before dried in an oven yielding impure **1d**. ^{1}H NMR showed presence of both unreacted starting material and semi-alkylated byproduct, so no yield is reported.

The spectroscopic data are in coherence with what is previously reported in the literature. [23, 33]

5.1.13 One pot synthesis of 1d from dimethyl ester 2b

2b (0.155 g, 0.433 mmol, 1.00 equiv.) was dissolved in glacial acetic acid (6.0 mL). Concentrated hydrobromic acid (4.0 mL) was added, and the reaction mixture was left stirring under reflux for 23 hours before poured into 250 mL of water. The product was separated by vacuum filtration, and washed with water, then methanol, yielding **1d** (0.101 g, 0.370 mmol, 85.5 %) as a white solid. The isolated product contained approximately 2 % of an alkylated impurity, according to ^{1}H NMR.

The spectroscopic data are in coherence with what is previously reported in the literature. [23, 33]

5.1.14 Synthesis of dimethyl dihydroxy ester 2d

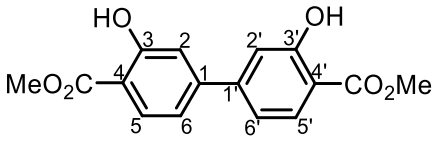

Impure **1d** (0.320 g, 1.17 mmol, 1.00 equiv.) was suspended in a solution of methanol (20 mL) and sulfuric acid (*ca.* 1 mL, conc.). The reaction mixture was then heated under reflux for 23 hours, before poured into 200 mL of water. The precipitate was isolated by vacuum filtration, yielding **2d** (0.307 g, 1.02 mmol, 87.2 %) as a white solid. (**Figure 100**)

^{1}H NMR [d] (300 MHz, $CDCl_3$): 10.8 (s, 2H, -O**H**), 7.91 (d, 2H, 5,5'-**H**, ^3J = 8.3 Hz), 7.23 (b.s, 2H), 7.13 (d, 2H, 6,6'-**H**, ^3J = 8.3 Hz) 3.98 (s, 6H, CO_2**Me**).

MS (ESI, CH_2Cl_2) (rel. %): 627.1 ($[2M+Na]^+$, 12), 413.3, 355.3 (9), 325.1 ($[M+Na]^+$, 100), 279.2 (13), 165 (14)

The spectroscopic data are in coherence with what is previously reported in the literature. [25]

[d] Less soluble in $CDCl_3$ than in DMSO-d_6 but displays expected integrals in chloroform. See **Section 2.5.5**.

5.1.15 Synthesis of diethyl dihydroxy ester 3d

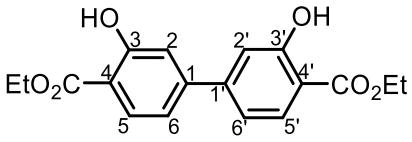

Impure **1d** (0.320 g, 1.17 mmol, 1.00 equiv.) was suspended in a solution of ethanol (20 mL) and sulfuric acid (ca. 1 mL, conc.). The reaction mixture was then heated under reflux for 23 hours, before poured into 200 mL of water. The precipitate was isolated by vacuum filtration, yielding **3d** (0.307 g, 1.02 mmol, 87.2 %) as a white solid. Compound **3d** was attempted purified by flash chromatography followed by recrystallization, but residual impurities were still visible in the ^{1}H NMR and GC-MS. (**Figure 101**)

^{1}H NMR (400 MHz, $CDCl_3$): 10.90 (s, 2H, O**H**), 7.92 (d, 2H, 5,5'-**H**, ^{3}J = 8.3 Hz, 7.22 (d, 2H, 2,2'-**H**, ^{4}J = 1.7 Hz, 7.12 (dd, 2H, 6,6'-**H**, ^{3}J = 8.3 Hz, ^{4}J = 1.8 Hz), 4.44 (q, 4H, OC**H$_2$**CH_3, ^{3}J = 7.1 Hz), 1.44 (t, 6H, OCH_2C**H$_3$**, ^{3}J = 7.1 Hz)

^{13}C NMR (101 MHz, $CDCl_3$): 169.9 (**C**O_2Et), 161.8 (**3,3'**), 146.7 (**1,1'**), 130.4 (**5,5'**), 118.0 (**6,6'**), 116.0 (**2,2'**), 112.3 (**4,4'**), 61.5 (O**C**H_2CH_3), 14.2 (OCH_2**C**H_3)

MS (EI, CH_2Cl_2) m/z (rel. %): 330 (M^+, 43), 284 ([M - EtOH]$^+$, 91), 238 ([M – 2EtOH]$^+$, 100)

This compound has not been previously reported.

5.1.16 Synthesis of isopropyl ether 4a

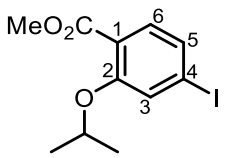

Isopropyl iodide (0.47 mL, 4.70 mmol, 1.3 equiv.) was added to a mixture of methyl 4-iodosalicylate (1.01 g, 3.62 mmol, 1.0 equiv.) and potassium carbonate (1.03 g, 7.48 mmol, 2.1 equiv.) in acetonitrile (10 mL). The reaction mixture was refluxed under an argon atmosphere while stirring for 22 hours. The mixture was diluted in dichloromethane (50 mL) and transferred to a separatory funnel where it was washed with water (25 mL) and saturated sodium chloride (25 mL, aq.). The dichloromethane was dried using sodium sulfate, then filtered and removed by rotary evaporation yielding **4a** (1.06 g, 3.32 mmol, 92 %) as a slight orange oil. ^{1}H NMR shows small amounts of starting material (ca. 1.6 % by integration). In order to remove this, the oil was redissolved in diethyl ether (50 mL) and washed with NaOH (50 mL, 1M, aq.), water (50 mL) and saturated sodium chloride solution (50 mL). The diethyl ether was then dried using magnesium sulfate before removed by rotary evaporation. The purified **4a** was clean by ^{1}H NMR. (**Figure 103**)

^{1}H NMR (400 MHz, $CDCl_3$): δ 7.46 (d, 1H, 6-**H**, ^{3}J = 8.1 Hz), 7.31 (m, 2H, 3-**H**, 5-**H**), 4.56 (sept, 1H, $(CH_3)_2$C**H**O-, ^{3}J = 6.0 Hz), 3.86 (s, 3H, -CO_2**Me**), 1.37 (d, 6H, (C**H$_3$**)$_2$CHO-, ^{3}J = 6.0 Hz).

^{13}C NMR (101 MHz, $CDCl_3$): 166.4 (**C**O_2Me), 157.8 (**2**), 132.7 (**6**), 129.5 (**3** or **5**), 124.8 (**3** or **5**), 121.2(**1**), 99.4 (**4**-I), 72.3 ((CH$_3$)$_2$**C**HO-), 52.0 (-CO_2**Me**), 21.9 (**C**H$_3$)$_2$CHO).

MS (EI, CH_2Cl_2) m/z (rel. %): 320 (M^+, 3.6), 278 ([M – ^{i}Pr]$^+$, 64), 246 ([M - MeO^{i}Pr]$^+$, 100), 218 (24), 63 (15)

The spectroscopic data are in coherence with what is previously reported in the literature.[34]

5.1.17 Synthesis of n-butyl ether 5a

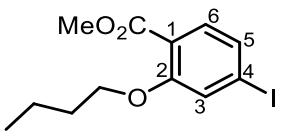

1-bromobutane (0.5 mL, 4.6 mmol, 1.3 equiv.) was added to a mixture of methyl 4-iodosalicylate (1.00 g, 3.60 mmol, 1.0 equiv.) and potassium carbonate (1.06 g, 7.68 mmol, 2.1 equiv.) in acetonitrile (10 mL). The reaction mixture was refluxed under an argon atmosphere while stirring for 19 hours. The mixture was diluted in dichloromethane (50 mL) and transferred to a separatory funnel where it was washed with water (25 mL) and saturated sodium chloride (25 mL, aq.). The dichloromethane was dried using sodium sulfate, then filtered and removed by rotary evaporation yielding **5a** (0.96 g, 2.86 mmol, 80 %) as a slight yellow oil. (**Figure 106**)

^{1}H NMR (400 MHz, $CDCl_3$): 7.48 (d, 1H, 6-**H**, ^{3}J = 8.1 Hz), 7.31 (dd, 1H, 5-**H**, ^{3}J = 8.1 Hz, ^{4}J = 1.5 Hz), 7.29 (d, 1H, 3-**H**, ^{4}J = 1.4 Hz), 4.01 (t, 2H, -OC**H$_2$**CH_2, ^{3}J = 6.4 Hz), 3.87 (s, 3H, CO_2**Me**), 1.81 (pent., 2H, -OCH_2C**H$_2$**, ^{3}J = 7.0 Hz), 1.53 (sext., 2H, C**H$_2$**CH_3, ^{3}J = 7.4 Hz), 0.98 (t, 3H, -CH_2C**H$_3$**, ^{3}J =7.4 Hz)

^{13}C NMR (101 MHz, $CDCl_3$): 166.3 (**C**O_2Me, 158.8 (**2**), 132.7 (**6**), 129.3 (**5**), 122.6 (**3**), 119.8 (**1**), 99.8 (**4**), 68.9 (O**C**H_2CH_2), 52.0 (CO_2**Me**), 31.1 (OCH_2**C**H_2), 19.1 (**C**H_2CH_3), 13.8 (CH_2**C**H_3)

MS (EI, CH_2Cl_2) m/z (rel. %): 334 ([M^+], 8), 278 ([M^+ - Bu], 33), 246 ([M^+ -Bu & MeOH], 100)

This compound has not been previously reported.

5.1.18 Synthesis of allyl ether 6a

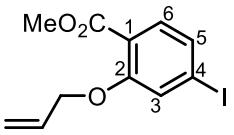

Allyl bromide (0.2 mL, 2.3 mmol, 1.3 equiv.) was added to a mixture of methyl 4-iodosalicylate (0.50 g, 1.80 mmol, 1.0 equiv.) and potassium carbonate (0.53 g, 3.83 mmol, 2.1 equiv.) in acetonitrile (5 mL). The slight yellow reaction mixture was refluxed under an argon atmosphere while stirring for 23 hours. The mixture was diluted in dichloromethane (25 mL) and transferred to a separatory funnel where it was washed with water (13 mL) and saturated sodium chloride (13 mL, aq.). The dichloromethane was dried using sodium sulfate, then filtered and removed by rotary evaporation yielding **6a** (0.40 g, 1.24 mmol, 69 %) as an orange-red solid. **6a** was pure by NMR. (**Figure 111**)

^{1}H NMR (400 MHz, $CDCl_3$): δ 7.49 (d, 1H, 6-**H**, ^{3}J = 8.2 Hz), 7.32 (dd, 1H, 5-**H**, ^{3}J = 8.2 Hz, ^{4}J = 1.5 Hz), 7.28 (d,1H, 3-**H**, ^{4}J = 1.5 Hz) , 6.02 (q.t, 1H,CH_2C**H**=CH_2,$^{3}J_{trans}$ = 17.2 Hz, $^{3}J_{cis}$ = 10.6 Hz, ^{3}J = 4.9 Hz), 5.50(dq, 1H, *(E)*-C**H**$_2$=CH-CH_2-O,$^{3}J_{trans}$ = 17.2 Hz, ^{2}J = 1.6 Hz) , 5.30(dq, 1H, *(Z)*-C**H**$_2$=CH-CH_2-O,$^{3}J_{cis}$ = 10.6 Hz, ^{2}J = 1.5 Hz) , 4.58(m, 2H,O-C**H**$_2$), 3.86 (s, 3H, -CO_2**Me**)

^{13}C NMR (101 MHz, $CDCl_3$): δ 166.1 (**C**O_2Me), 158.3 (**2**), 132.9 (**6**), 132.1 (OCH_2**C**HCH_2), 129.8 (**5**), 123.1 (**3**), 120.0 (**1**), 117.8 (CH=**C**H_2), 99.8 (**4**), 69.7 (O-**C**H_2), 52.1 (CO_2-**Me**)

MS (EI, CH_2Cl_2) m/z (rel. %): 318 ([M^+],55), 286 (100), 271 (32), 258 (65),103 (40), 77 (23)

Mp: 62 °C

This compound has not been previously reported.

5.1.19 Synthesis of n-propyl ether 7a

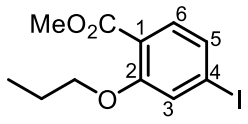

1-bromopropane (2.5 mL, 27.4 mmol, 1.3 equiv.) was added to a mixture of methyl 4-iodosalicylate (5.90 g, 21.2 mmol, 1.0 equiv.) and potassium carbonate (5.88 g, 42.6 mmol, 2.0 equiv.) in acetonitrile (60 mL). The reaction mixture was refluxed under an argon atmosphere while stirring for 20 hours. The mixture was diluted in dichloromethane (300 mL) and transferred to a separatory funnel where it was washed with water (100 mL) and saturated sodium chloride (100 mL, aq.). The dichloromethane was dried using sodium sulfate, then filtered and removed by rotary evaporation yielding **7a** (6.31 g, 19.7 mmol, 93 %) as a colorless oil. (**Figure 117**)

^{1}H NMR (400 MHz, $CDCl_3$): 7.45 (d, 1H, 6-**H**, ^3J = 8.0 Hz), 7.27 (m, 2H, 3-**H**, 5-**H**), 3.93 (t, 2H, OC**H**$_2$$CH_2CH_3$, ^3J = 6.4 Hz), 3.84 (s. 3H, CO_2**Me**), 1.82 (sext., 2H, OCH_2C**H**$_2$$CH_3$, ^{3}J = 6.0 Hz), 1.03 (t, 3H, OCH_2CH_2C**H**$_3$, ^{3}J = 7.4 Hz)

^{13}C NMR (101 MHz, $CDCl_3$): 166.0 (**C**O_2Me), 158.6 (**2**), 132.5 (**6**), 129.1 (**3** or **5**), 122.4 (**3** or **5**), 119.7 (**1**), 99.6 (**4**), 70.5(O**C**$H_2CH_2CH_3$), 51.8 (CO_2**Me**), 22.3 (OCH_2**C**H_2CH_3), 10.3 (OCH_2CH_2**C**H_3)

MS (EI, CH_2Cl_2) m/z (rel. %): 320 (M^+, 10), 291 ([M – Et]$^+$, 20) 278 ([M – ^{n}Pr]$^+$, 27), 246 ([M – MeO^{n}Pr]$^+$, 100), 218 (23)

This compound has not been previously described spectroscopically in the literature.

5.1.20 Synthesis of benzyl ether 8a

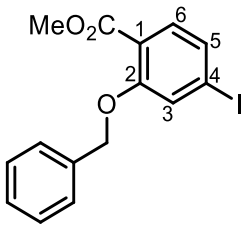

Benzyl bromide (1.4 mL, 11.8 mmol, 1.3 equiv.) was added to a mixture of methyl 4-iodosalicylate (2.59 g, 9.34 mmol, 1.0 equiv.) and potassium carbonate (2.51 g, 18.1 mmol, 1.9 equiv.) in acetonitrile (25 mL). The reaction mixture was refluxed under an argon atmosphere while stirring for 20 hours. The mixture was diluted in ethyl acetate (125 mL) and transferred to a separatory funnel where it was washed with water (60 mL) and saturated sodium chloride (60 mL, aq.). The ethyl acetate was dried using sodium sulfate, then filtered and removed by rotary evaporation yielding **8a** (2.69 g, 7.32 mmol, 78 %) as an off-white solid, with a wax-like texture. The product was washed with water and dried in an oven at 45 °C overnight. Some benzyl bromide was seen in the ^{1}H NMR. (**Figure 122**)

^{1}H NMR (400 MHz, $CDCl_3$): 7.53 (d, 1H, 6-**H**, ^{3}J = 8.1 Hz) 7.49 (m, 2H), 7.35 (m, 5H), 5.13 (s, 2H, Ph-C**H**$_2$-O), 3.87 (s, 3H, **Me**O_2C-Ar)
^{13}C NMR (101 MHz, $CDCl_3$): 166.2 (**C**O_2Me), 158.3 (**2**), 136.1 (***o-Ph***), 132.9, 130.0, 128.6, 128.0, 126.9, 123.3, 120.3, 99.8 (**4**), 70.9 (O**C**H_2Ph), 52.1 (CO_2**Me**)
MS (EI, CH_2Cl_2) m/z (rel. %): 368 (M^+, 1.7), 336 ([M-MeOH]$^+$, 8.3), 246 ([M – MeOBn]$^+$, 1.9), 91 ($C_7H_7^+$, 100), 65 ($C_5H_5^+$, 9.7) 39 ($C_3H_3^+$, 1.8)

The spectroscopic data are in coherence with what is previously reported in the literature.[33]

5.1.21 Synthesis of methyl cyclohexyl ether 9a

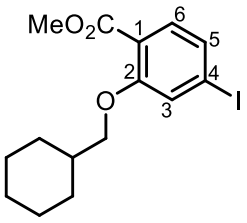

(Bromomethyl)cyclohexane (0.65 mL, 4.66 mmol, 1.30 equiv.) was added to a mixture of methyl 4-iodosalicylate (1.01 g, 3.60 mmol, 1.00 equiv.) and potassium carbonate (1.00 g, 7.26 mmol, 2.0 equiv.) in acetonitrile (10 mL). The reaction mixture was refluxed under an argon atmosphere while stirring for 22 hours. The mixture was diluted in diethyl ether (80 mL) and transferred to a separatory funnel where it was washed with water (2 x 80 mL) and a saturated solution of sodium chloride (80 mL, aq.). The diethyl ether was dried using magnesium sulfate, then filtered and removed by rotary evaporation yielding **9a** (1.32 g, 3.52 mmol, 98 %) as a clear oil. **9a** was pure by ^{1}H NMR. (**Figure 126**)

^{1}H NMR (400 MHz, $CDCl_3$): 7.49 (d, 1H, 6-**H**, ^{3}J = 8.2 Hz), 7.31 (dd, 1H, 5-**H**, ^{3}J = 8.1 Hz ^{4}J = 1.5 Hz), 7.28 (d, 1H, 3-**H**, ^{4}J = 1.4 Hz), 3.87 (s, 3H, CO_2**Me**), 3.79 (d, 2H, O**Me**Cy, ^{3}J = 6.0 Hz), 1.80 (m, 6H, Cy-**H**), 1.21 (m, 5H, Cy-**H**)

^{13}C NMR (101 MHz, $CDCl_3$): 166.4 (**C**O_2Me), 159.0 (**2**), 132.8 (**6**), 129.2 (**5**), 122.5 (**3**), 119.7 (**1**), 99.9 (**4**), 74.5 (O**Me**Cy), 52.0 (CO_2**Me**), 37.6 (**Cy**), 29.7 (**Cy**), 26.5 (**Cy**), 25.8 (**Cy**)

MS (EI, CH_2Cl_2) m/z (rel. %): 374 (M^+, 9.7), 342 ([M - MeOH]$^+$, 1.6), 278 ([M - MeCy]$^+$, 100), 246 ([M – MeOMeCy]$^+$, 92), 96 (37), 81 (56), 55 (89)

This compound has not been previously reported.

5.1.22 Synthesis of acetyl ester 10a

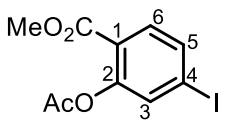

Methyl 4-iodosalicylcate (2.00 g, 7.17 mmol, 1.00 equiv.) was suspended in a solution of acetic anhydride (4.0 mL, 42 mmol, 5.9 equiv.) dissolved in acetic acid (20 mL). Five drops of concentrated sulfuric acid were added, and the reaction mixture is heated to 60 °C for 40 minutes, before it was poured into a beaker with ice. The precipitated product was filtered and washed thoroughly with water then dried in an oven, yielding **10a** (2.08 g, 6.50 mmol, 91.0 %) as a white solid. Due to the presence of approximately 2 % starting material (quantified by ^{1}H NMR), **10a** was recrystallized from methanol. The recrystallized product was clean by NMR. (**Figure 130**)

^{1}H NMR (400 MHz, $CDCl_3$): 7.71 (d, 1H, 6-**H**, ^{3}J = 8.3 Hz), 7.67 (dd, 1H, 5-**H**, ^{3}J = 8.3 Hz, ^{4}J = 1.6 Hz), 7.50 (d, 1H, 3-**H**, ^{4}J = 1.6 Hz), 3.86 (s, 3H, CO_2**Me**), 2.34 (s, 3H, O**Ac**)

^{13}C NMR (101 MHz, $CDCl_3$): 169.3 (2-O**C**OCH_3), 164.4 (**C**O_2Me), 150.6 (**2**), 135.3 (**5**), 133.0 (**3**), 132.6 (**6**), 122.7 (**1**), 99.7 (**4**), 52.3 (CO_2**Me**), 20.8 (2-OCO**C**H_3)

MS (EI, CH_2Cl_2) m/z (rel. %): 320 (M^+, 3), 278 ([M –Ac]$^+$, 100), 247 (19), 246 ([M-MeOAc]$^+$, 74)

M_p: 91-92 °C

The spectroscopic data are in coherence with what is previously reported in the literature.[24] However, the melting point is not. (See **Section 2.5.5**)

5.2 MOF syntheses

5.2.1 Attempted synthesis of UiO-67-2c

Water (0.46 mL, 26 mmol 3.0 equiv.) and zirconium chloride (2.0 g, 8.6 mmol, 1.0 equiv.) was dissolved in DMF (33 mL) at room temperature. The clear solution was then heated to close to the boiling point before adding benzoic acid (3.1 g, 25 mmol, 3.0 equiv.). The clear solution was then transferred to a suitable round bottle flask, and linker **2c** (2.8 g, 8.5 mmol, 1.0 equiv.) was added, stirred and dissolved. The flask was put in an oil bath and heated at 138 °C for 24 h in a reflux setup. The following day the white precipitate was filtered off, and first washed with warm DMF, then with acetone. The precipitate was then dried in an oven at 150 °C overnight, yielding 2.5 g (66 %) of a crystalline solid with a UiO-67 crystal structure, confirmed by P-XRD.

5.2.2 Attempted synthesis of UiO-67-1c

Water (0.46 mL, 26 mmol 3.0 equiv.) and zirconium chloride (2.0 g, 8.6 mmol, 1.0 equiv.) was dissolved in DMF (33 mL) at room temperature. The clear solution is then heated to close to the boiling point before adding benzoic acid (3.1 g, 25 mmol, 3.0 equiv.). The clear solution was then transferred to a suitable round bottle flask, and linker **1c** (2.6 g, 8.5 mmol, 1.0 equiv.) was added, stirred and dissolved. The flask was put in an oil bath and heated at 138 °C for 24 h in a reflux setup. The following day the white precipitate was filtered off, and first washed with warm DMF, then with acetone. The precipitate was then dried in an oven at 150 °C overnight, yielding 1.5 g (42 %) of a crystalline solid with a UiO-67 crystal structure, confirmed by P-XRD.

Appendix

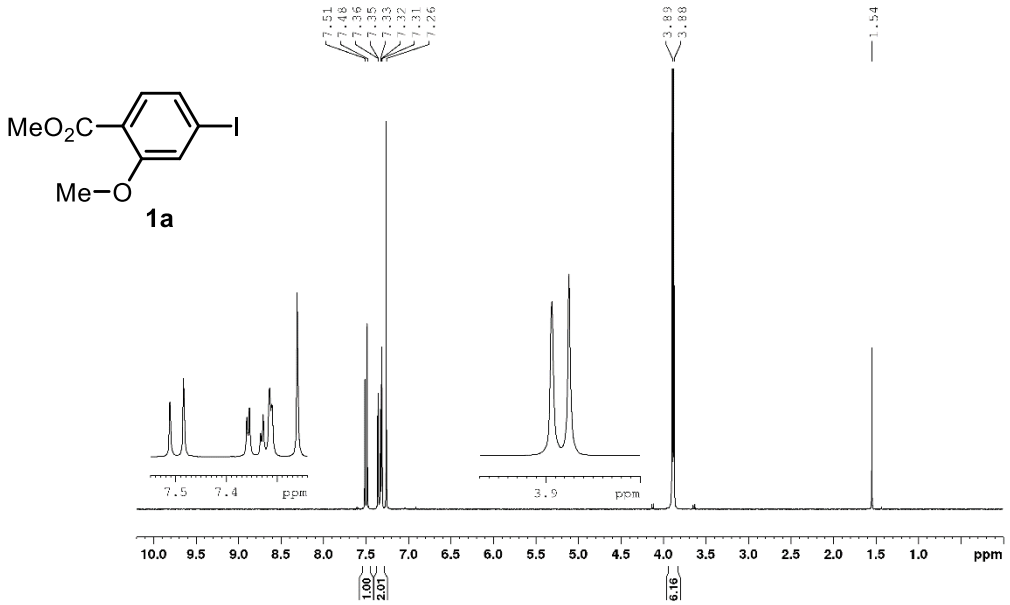

Figure 59 ^{1}H NMR spectrum of **1a** (300 MHz, $CDCl_3$)

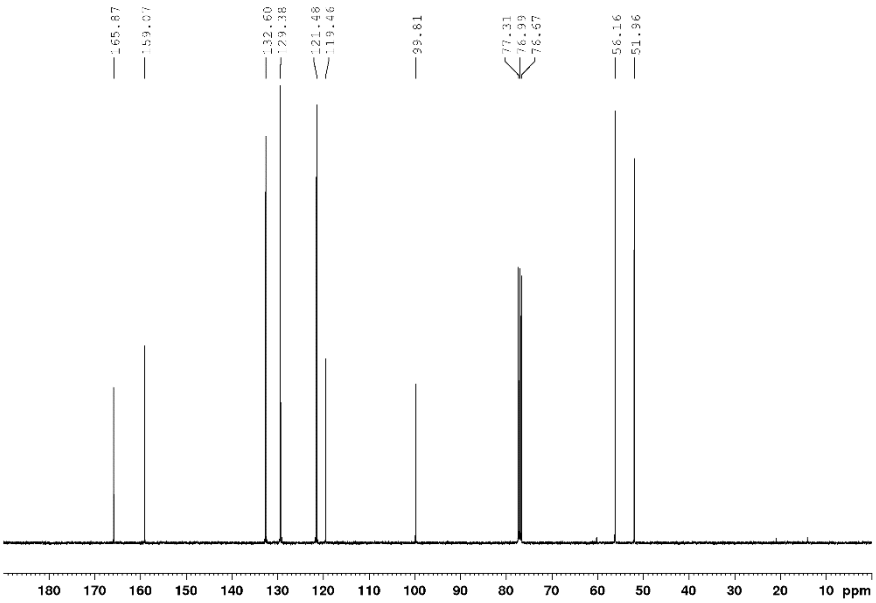

Figure 60 ^{13}C NMR spectrum of **1a** (101 MHz, $CDCl_3$)

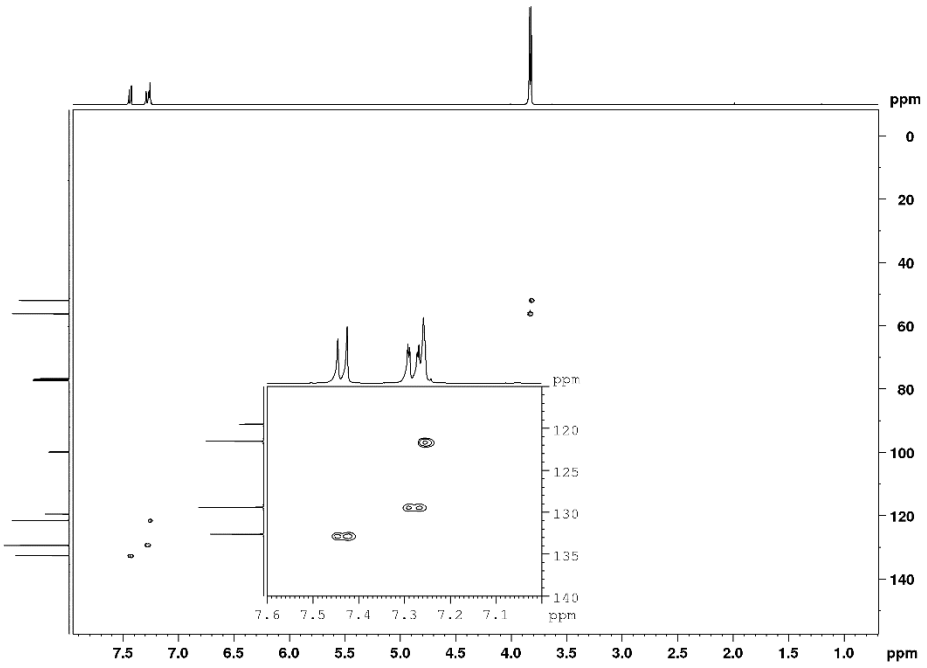

Figure 61 ^{1}H-^{13}C HSQC spectrum of **1a** (400-101 MHz, $CDCl_3$)

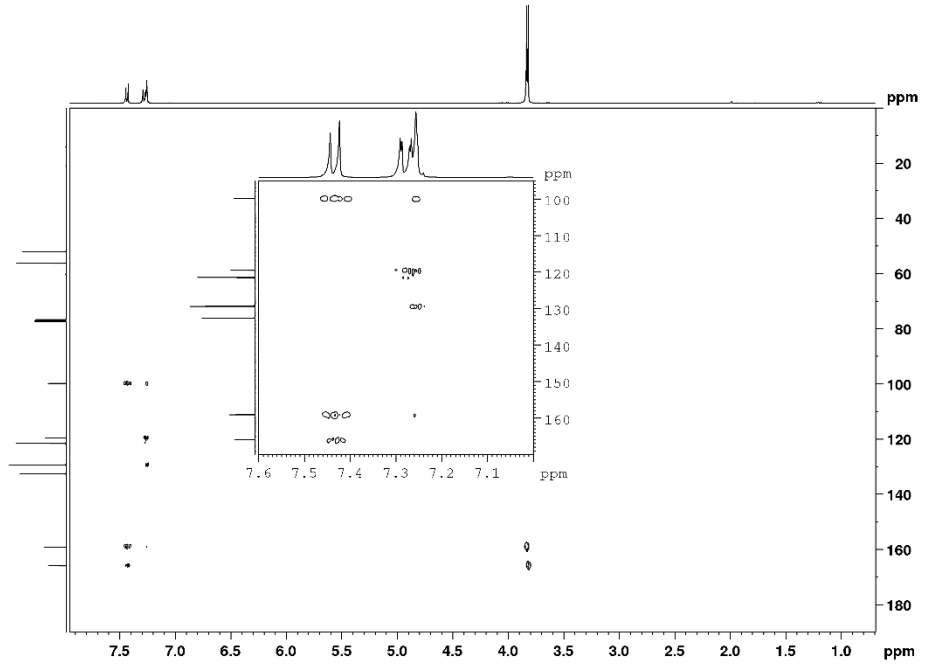

Figure 62 ^{1}H-^{13}C HMBC spectrum of **1a** (400-101 MHz, $CDCl_3$)

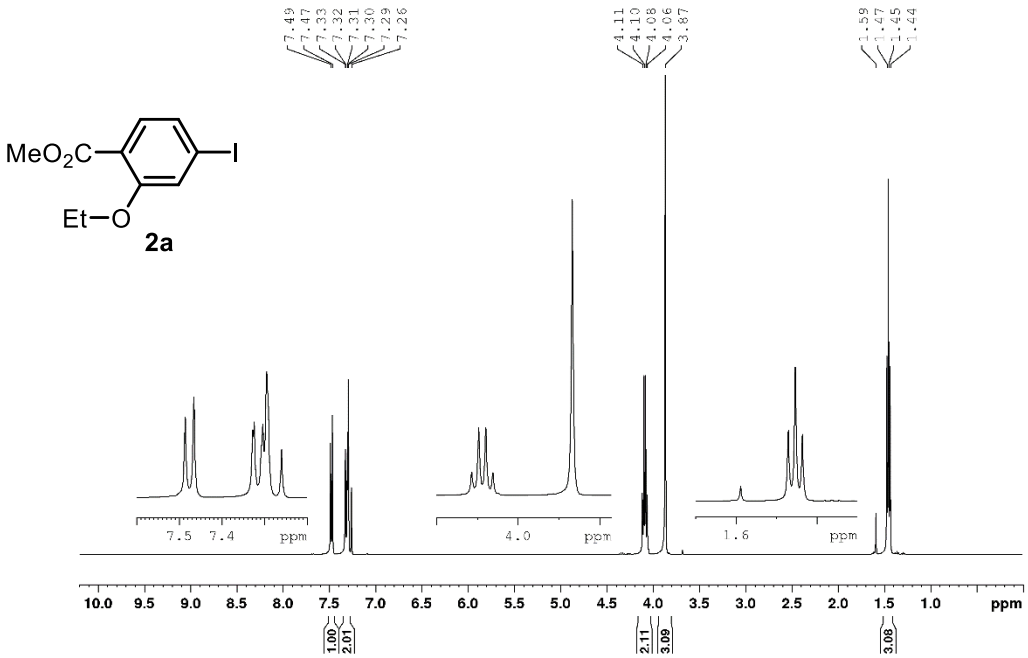

Figure 63 ^{1}H NMR spectrum of **2a** (400 MHz, $CDCl_3$)

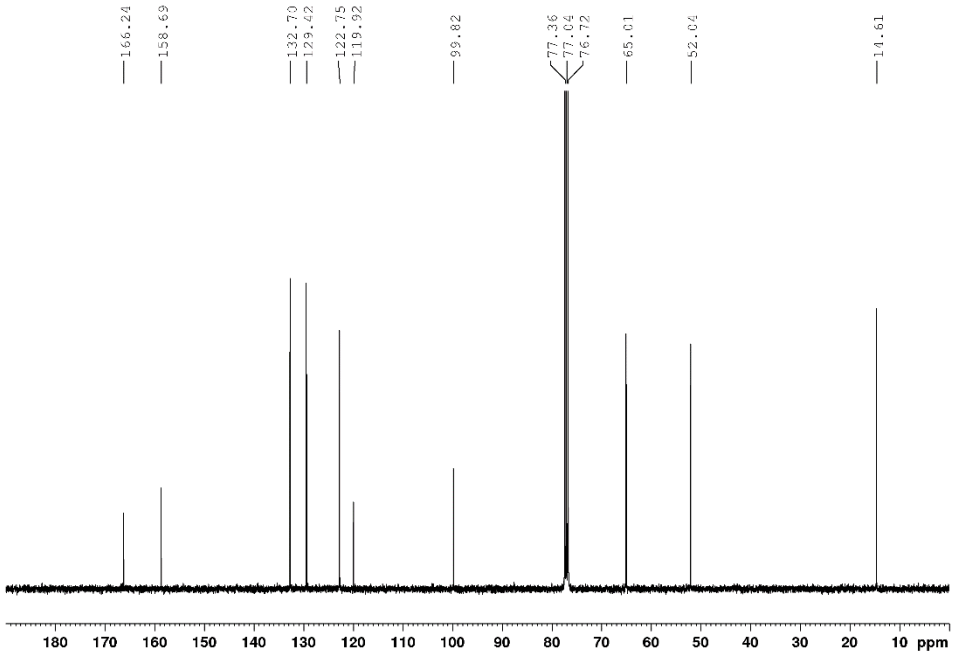

Figure 64 ^{13}C NMR spectrum of **2a** (101 MHz, $CDCl_3$)

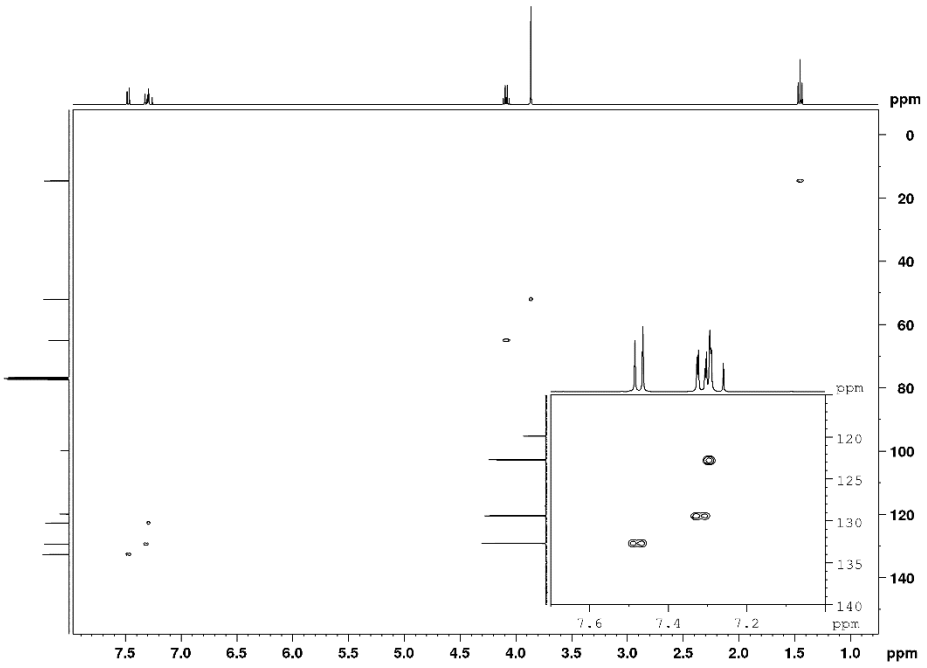

Figure 65 ^{1}H-^{13}C HSQC spectrum of **2a** (400-101 MHz, $CDCl_3$)

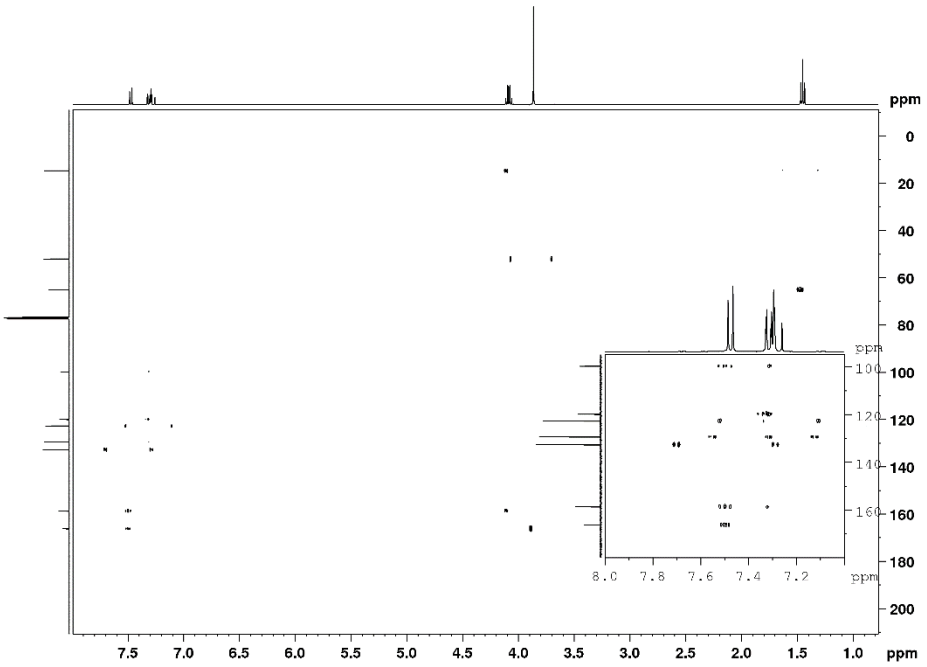

Figure 66 ^{1}H-^{13}C HMBC spectrum of **2a** (400-101 MHz, $CDCl_3$)

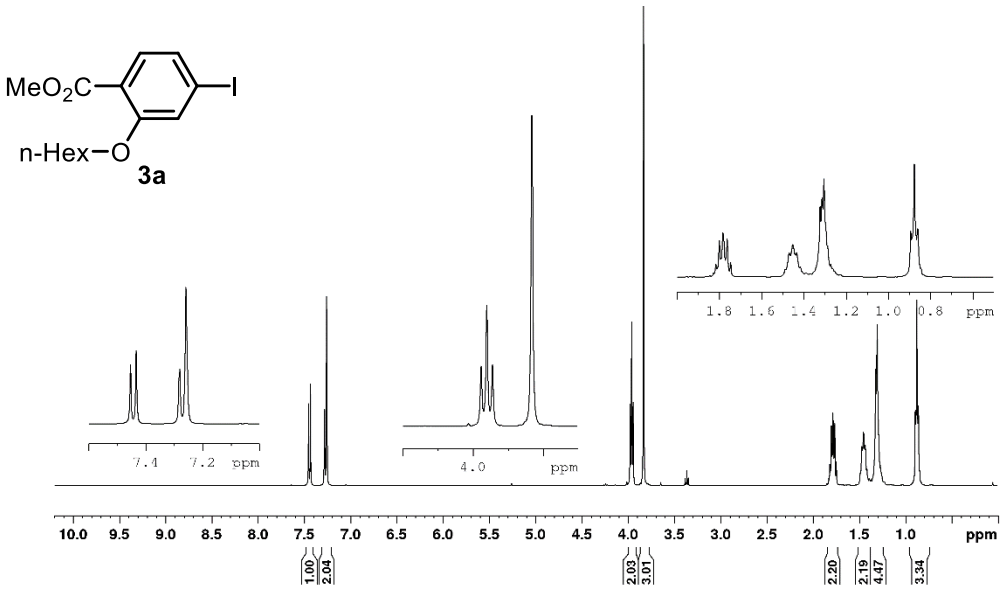

Figure 67 ^{1}H NMR spectrum of **3a** (400 MHz, $CDCl_3$)

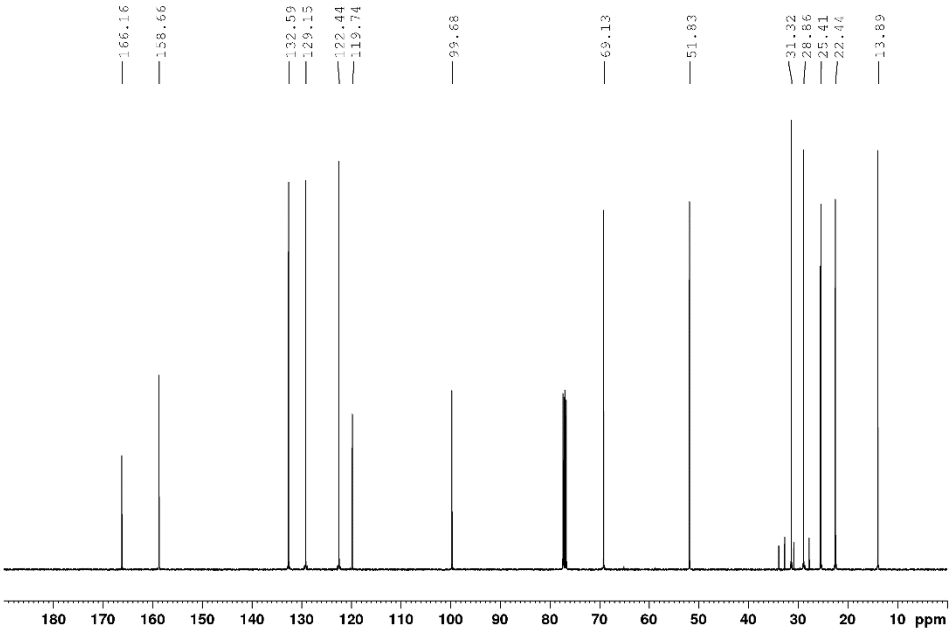

Figure 68 ^{13}C NMR spectrum of **3a** (101 MHz, $CDCl_3$)

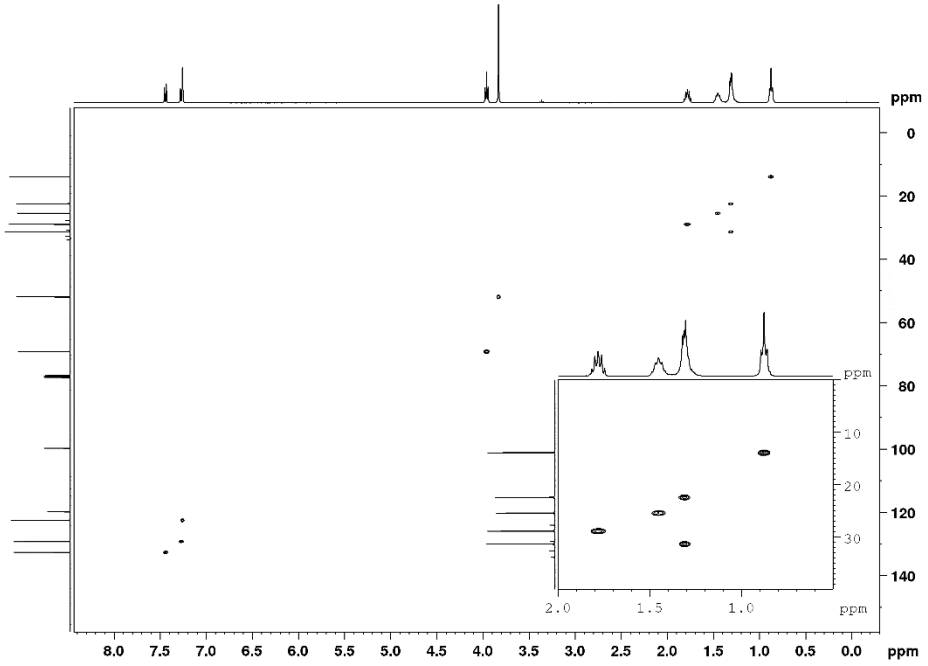

Figure 69 ^{1}H-^{13}C HSQC spectrum of **3a** (400-101 MHz, $CDCl_3$)

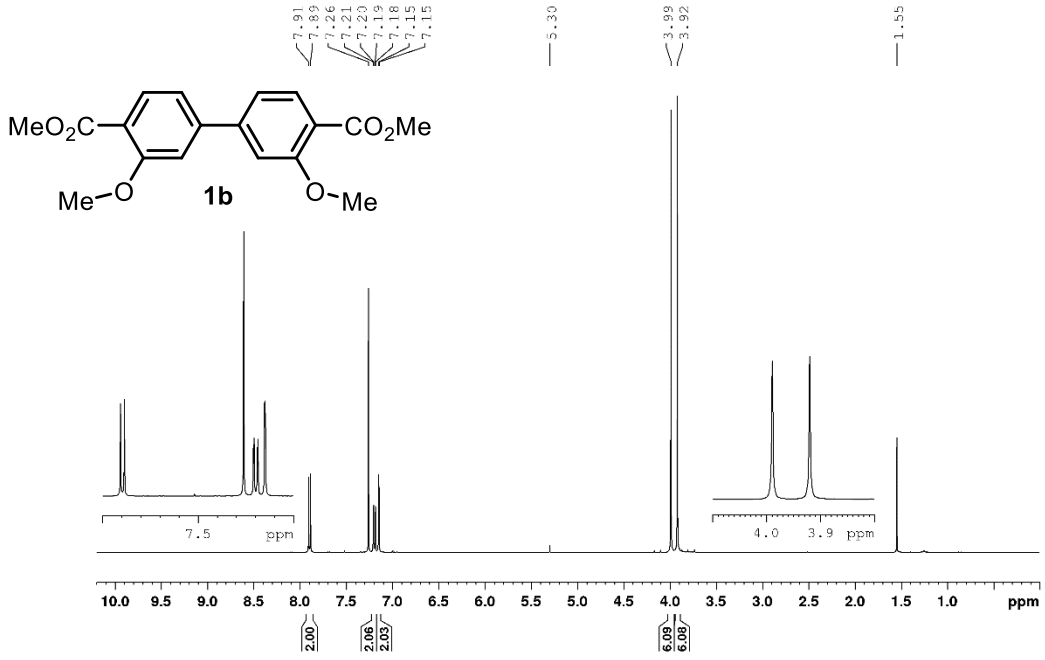

Figure 70 ^{1}H NMR spectrum of **1b** (400 MHz, $CDCl_3$)

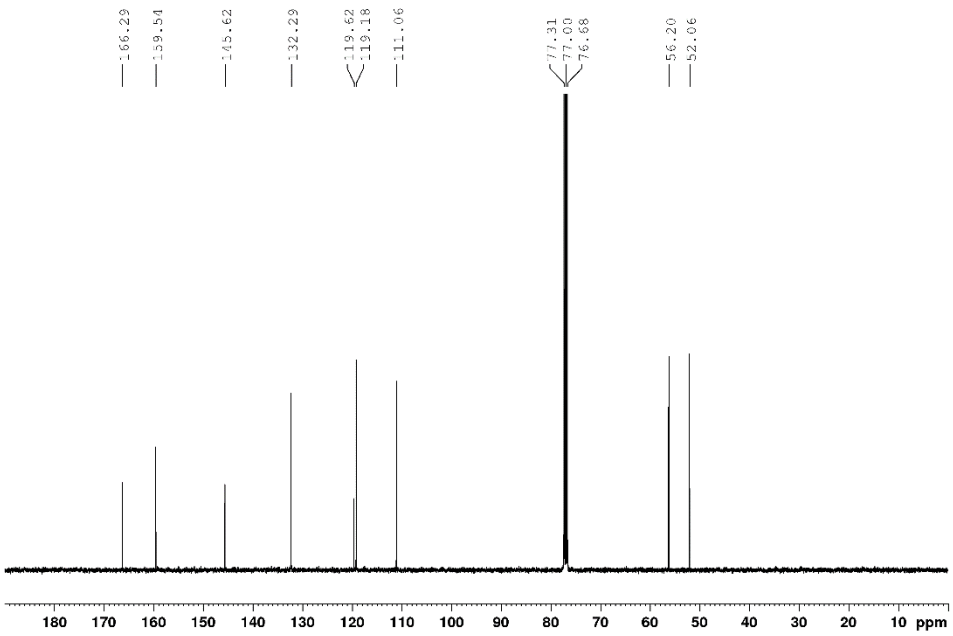

Figure 71 ^{13}C NMR spectrum of **1b** (101 MHz, $CDCl_3$)

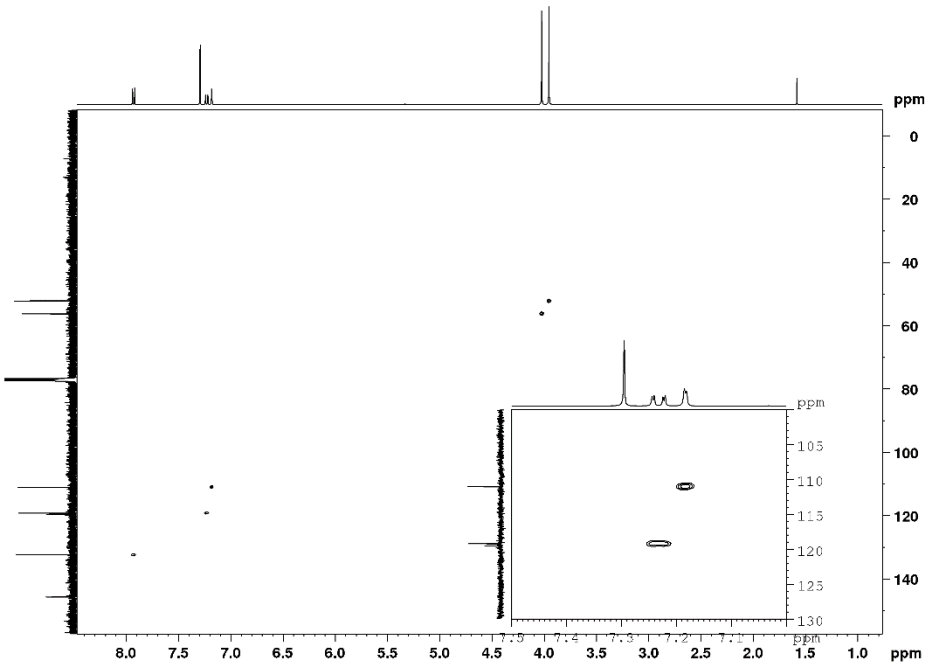

Figure 72 ^{1}H-^{13}C HSQC spectrum of **1b** (400-101 MHz, $CDCl_3$)

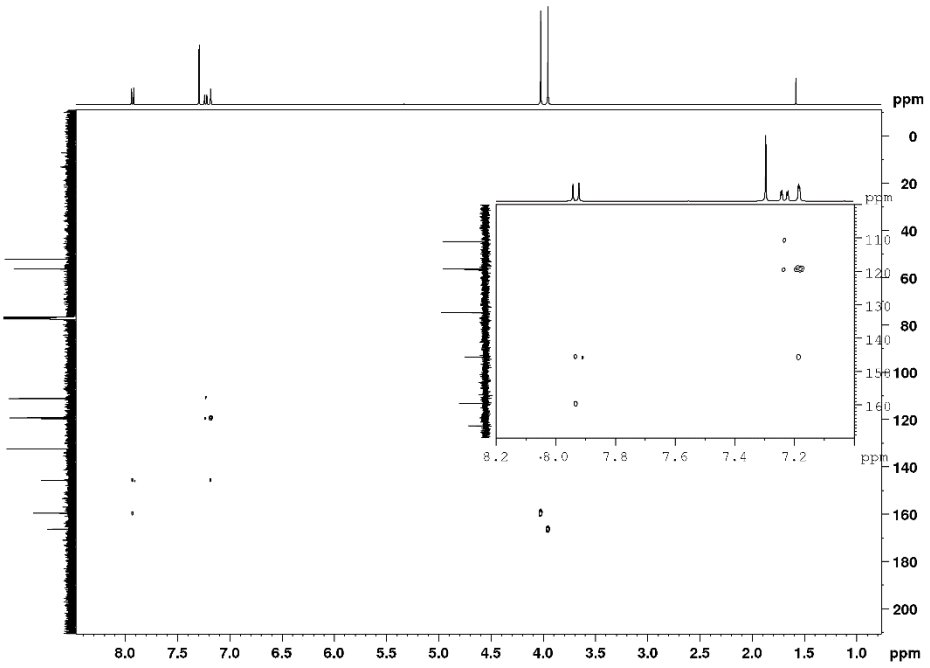

Figure 73 ^{1}H-^{13}C HMBC spectrum of **1b** (400-101 MHz, $CDCl_3$)

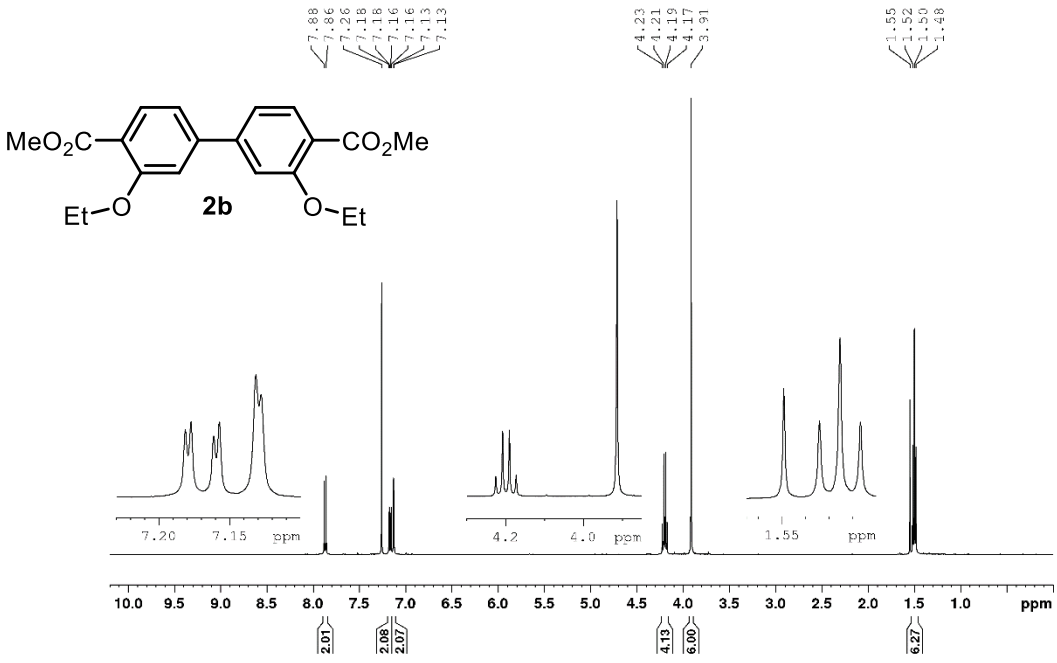

Figure 74 ^{1}H NMR spectrum of **2b** (400 MHz, $CDCl_3$)

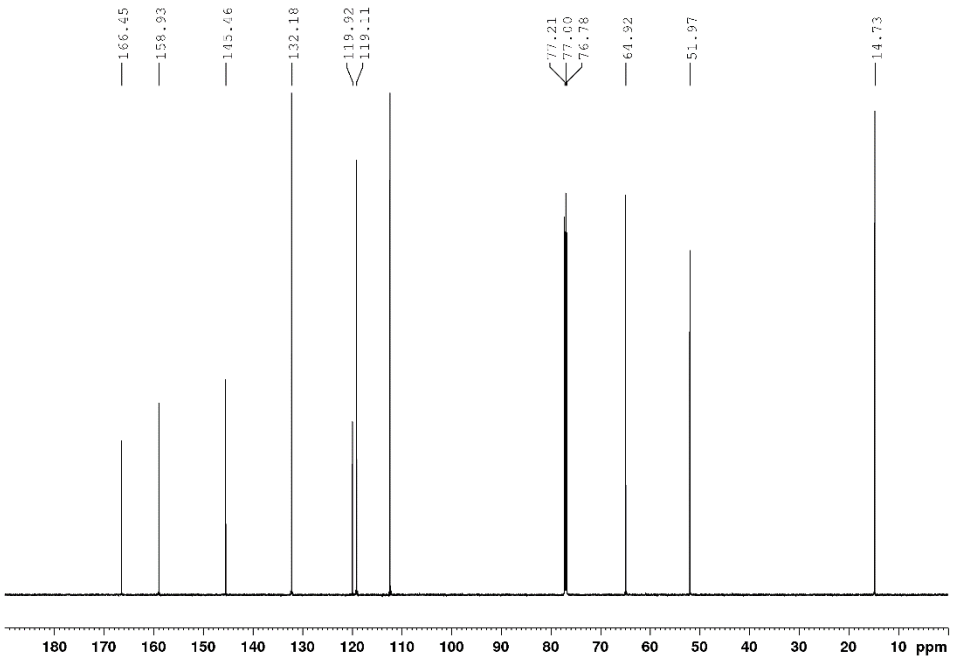

Figure 75 ^{13}C NMR spectrum of **2b** (101 MHz, $CDCl_3$)

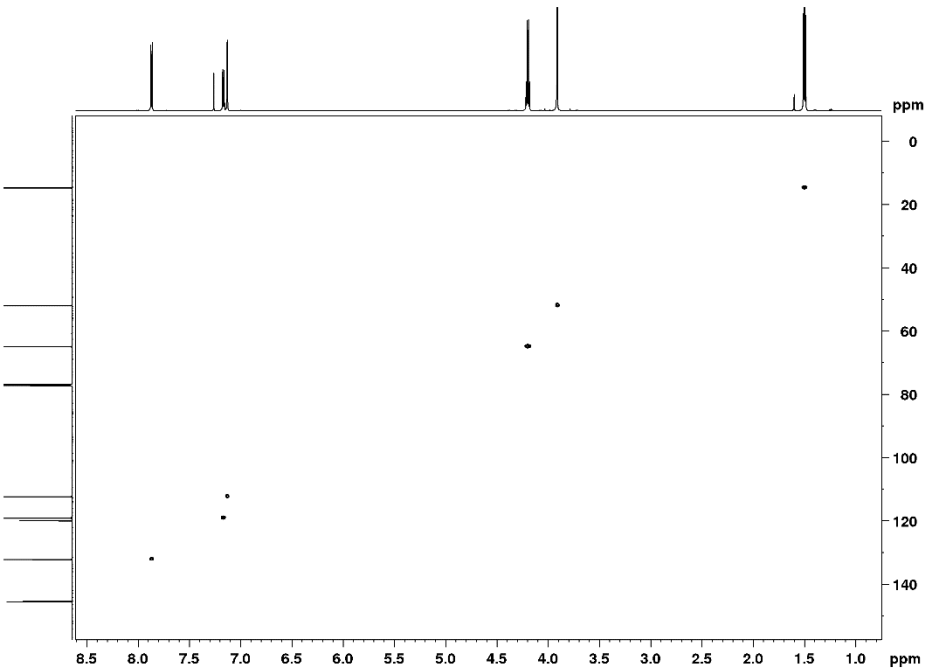

Figure 76 ^{1}H-^{13}C HSQC spectrum of **2b** (400-101 MHz, $CDCl_3$)

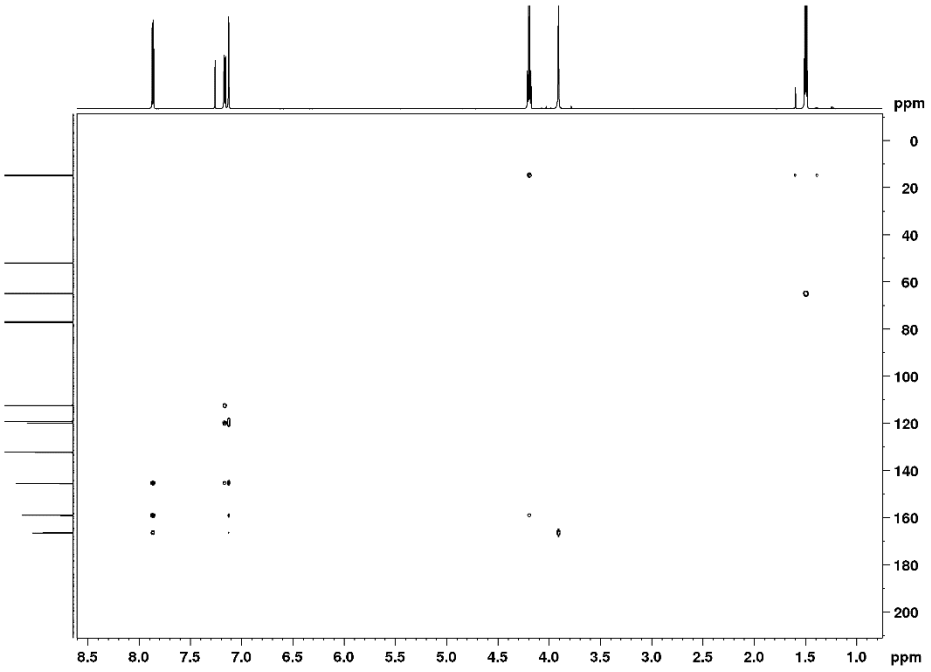

Figure 77 ^{1}H-^{13}C HMBC spectrum of **2b** (400-101 MHz, $CDCl_3$)

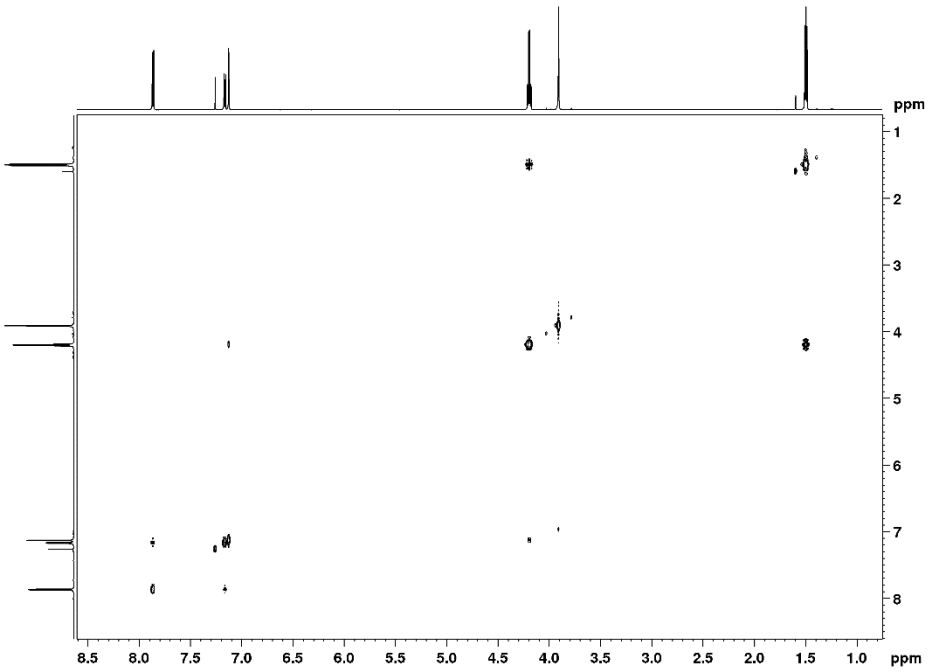

Figure 78 ^{1}H-^{1}H NOESY spectrum of **2b** (400 MHz, $CDCl_3$)

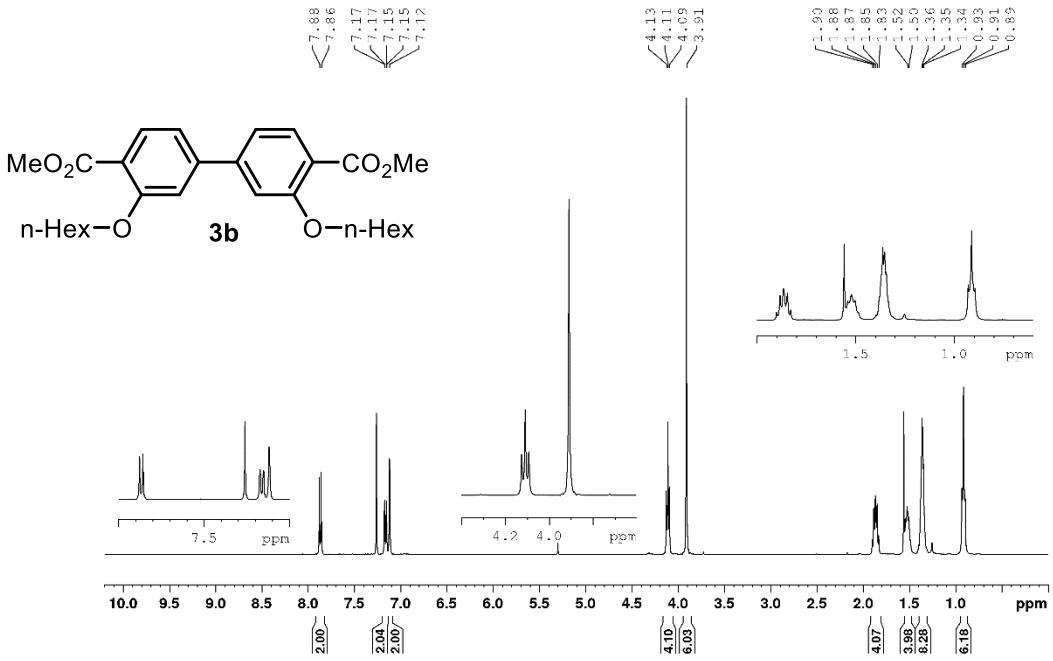

Figure 79 ^{1}H NMR spectrum of **3b** (400 MHz, $CDCl_3$)

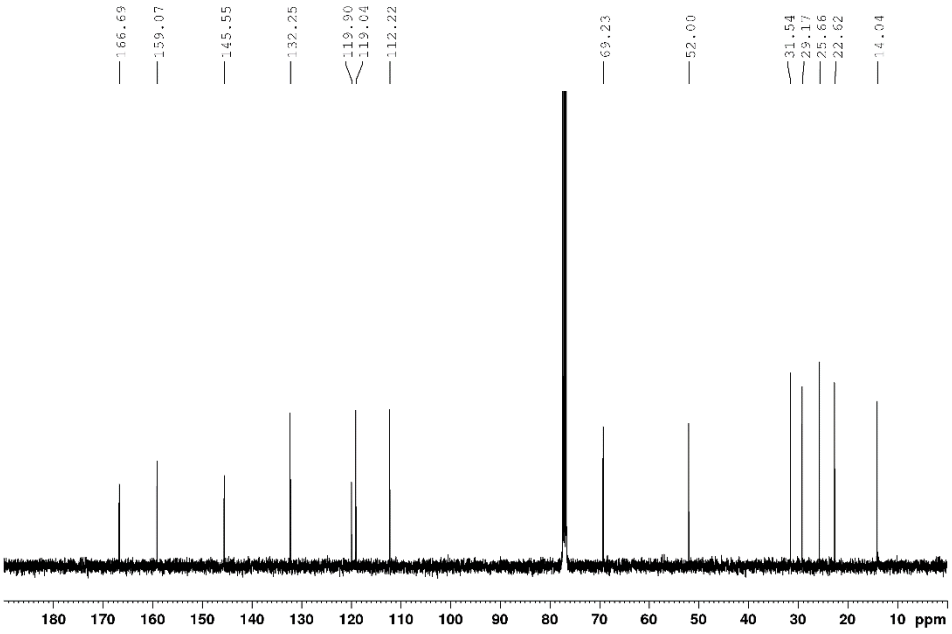

Figure 80 ^{13}C NMR spectrum of **3b** (101 MHz, $CDCl_3$)

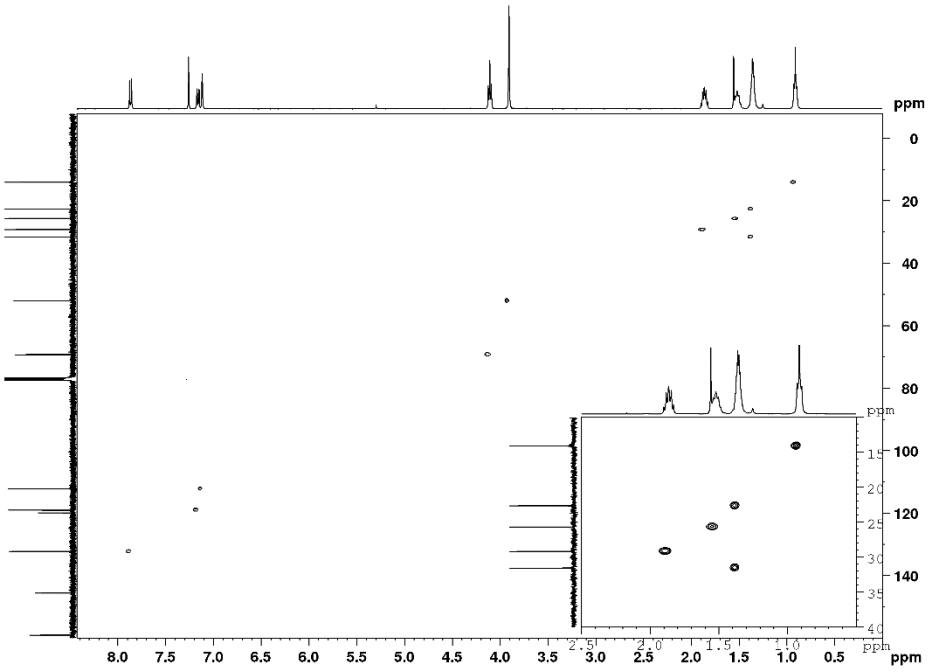

Figure 81 ^{1}H-^{13}C HSQC spectrum of **3b** (400-101 MHz, $CDCl_3$)

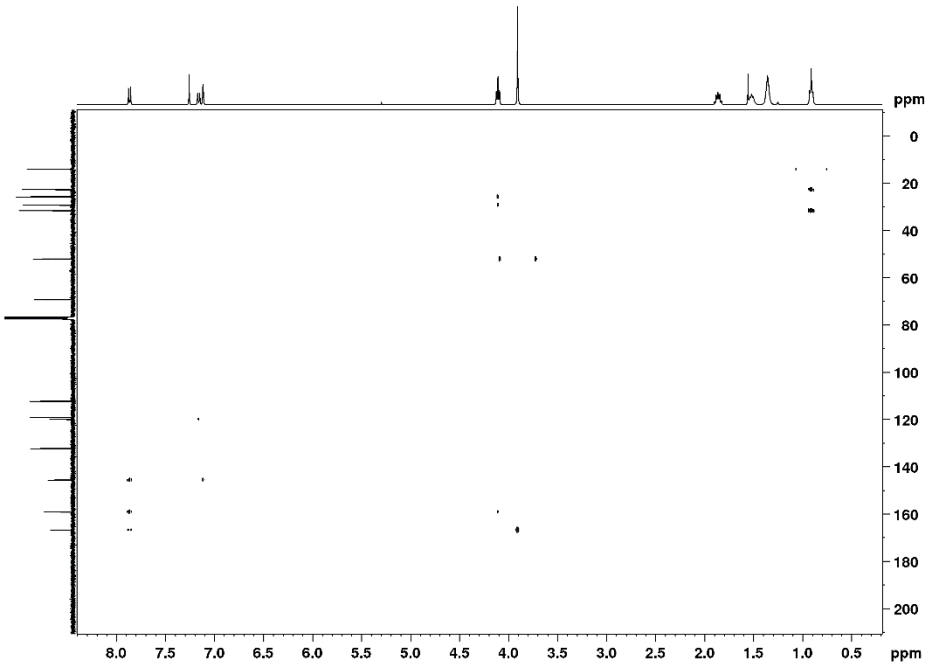

Figure 82 ^{1}H-^{13}C HMBC spectrum of **3b** (400-101 MHz, $CDCl_3$)

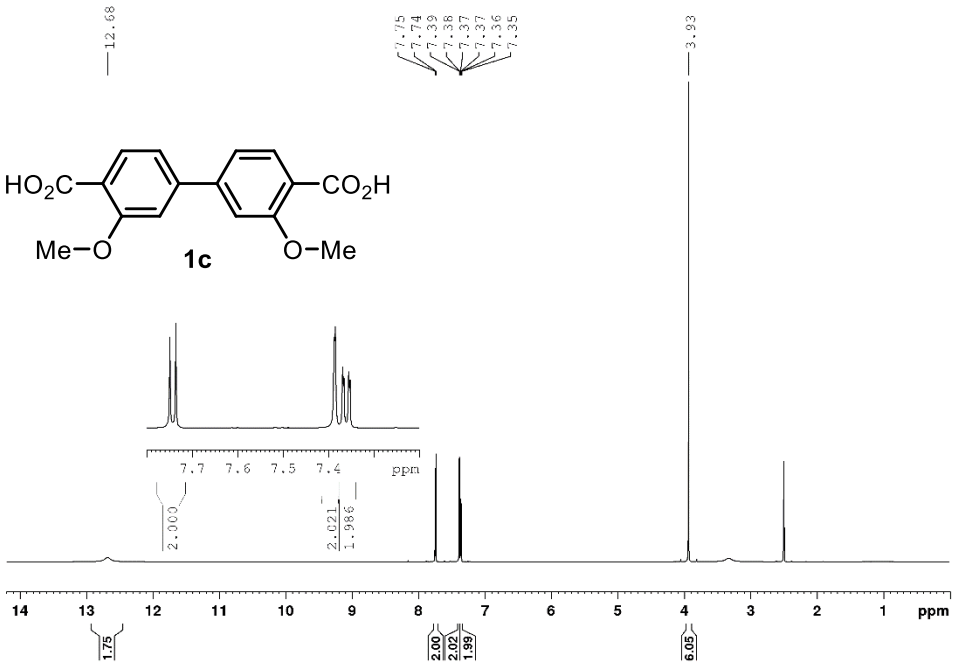

Figure 83 [1]H NMR spectrum of **1c** (600 MHz, DMSO-d_6)

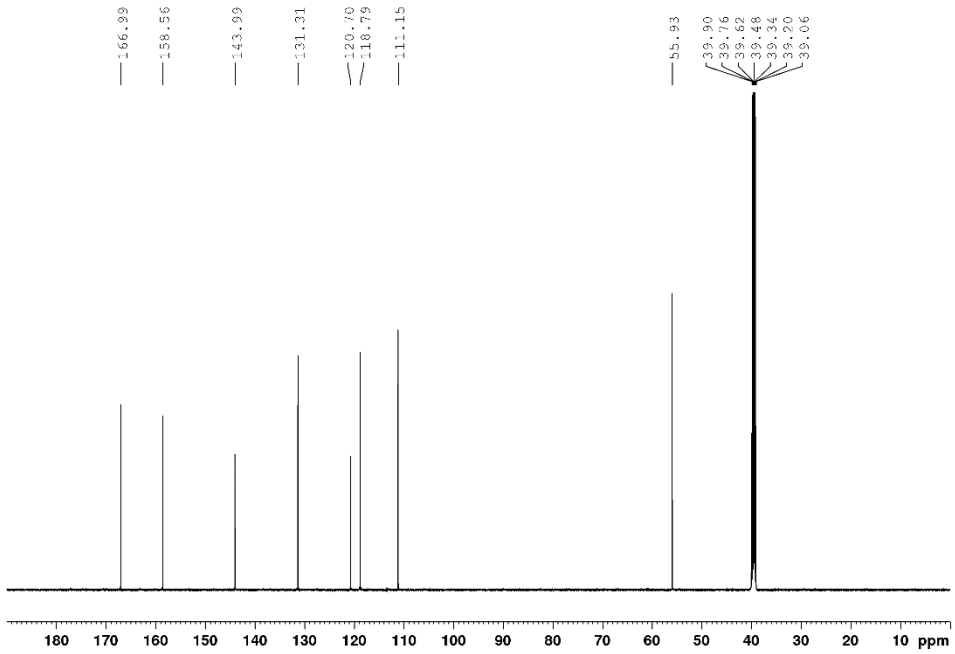

Figure 84 [13]C NMR spectrum of **1c** (151 MHz, DMSO-d_6)

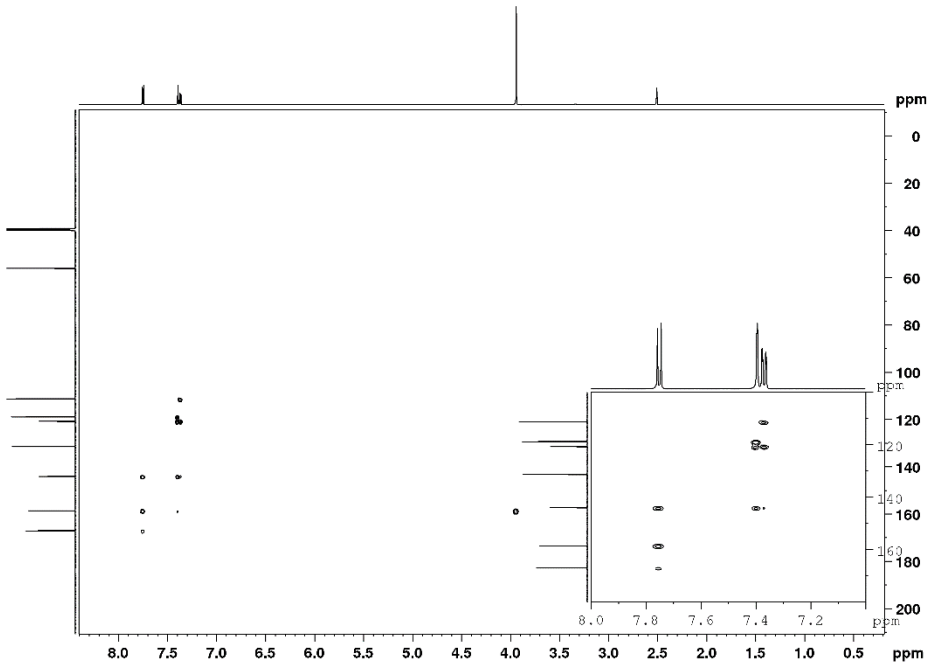

Figure 85 ^{1}H-^{13}C HMBC spectrum of **1c** (600-151 MHz, DMSO-d_6)

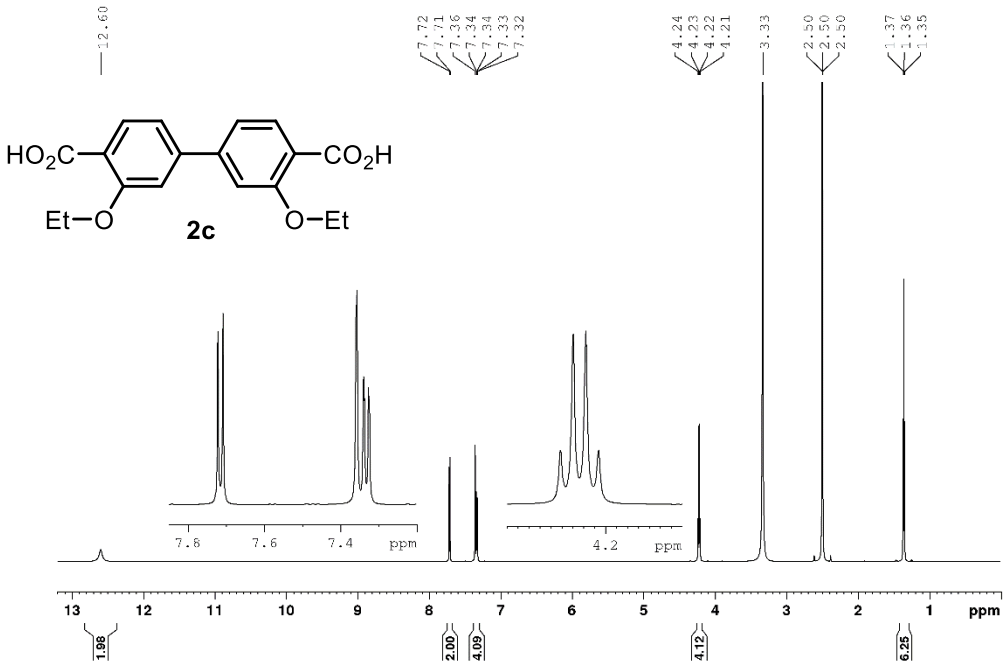

Figure 86 ^{1}H NMR spectrum of **2c** (600 MHz, DMSO-d_6)

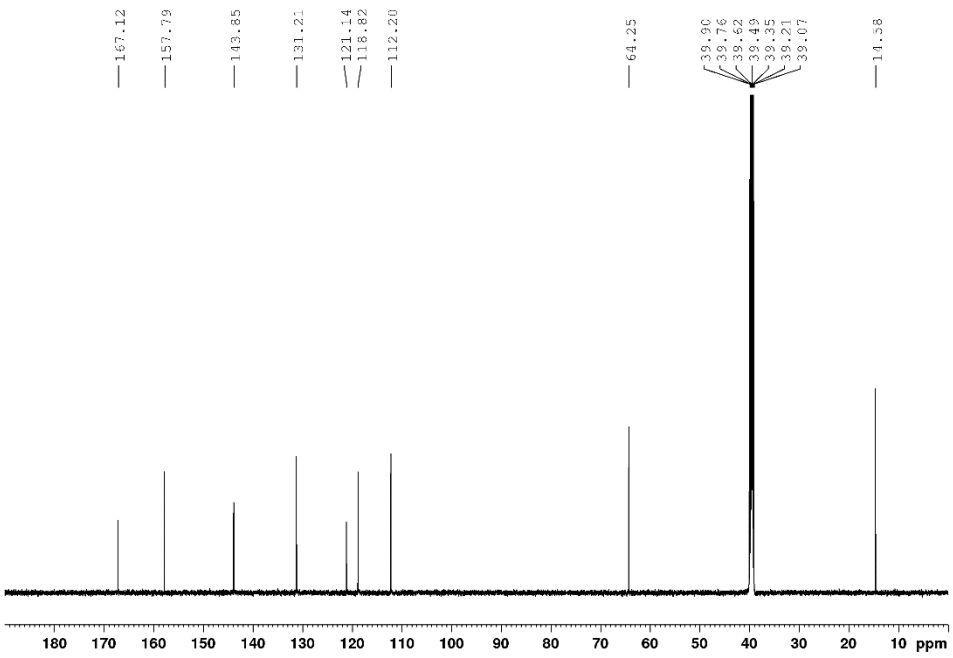

Figure 87 ^{13}C NMR spectrum of **2c** (151 MHz, DMSO-d_6)

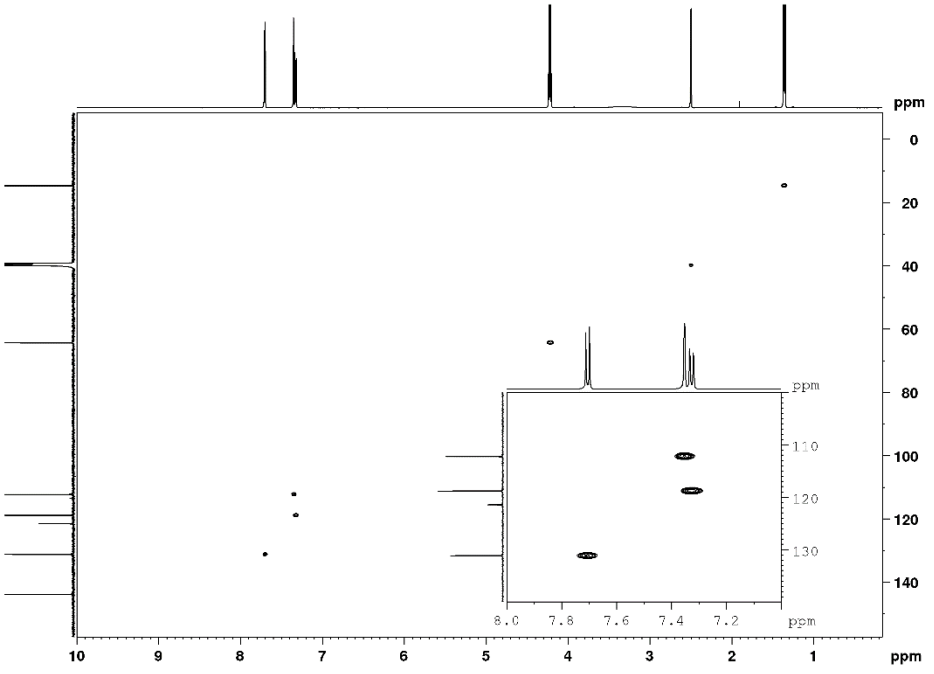

Figure 88 ^{1}H-^{13}C HSQC spectrum of **2c** (600-151 MHz, DMSO-d_6)

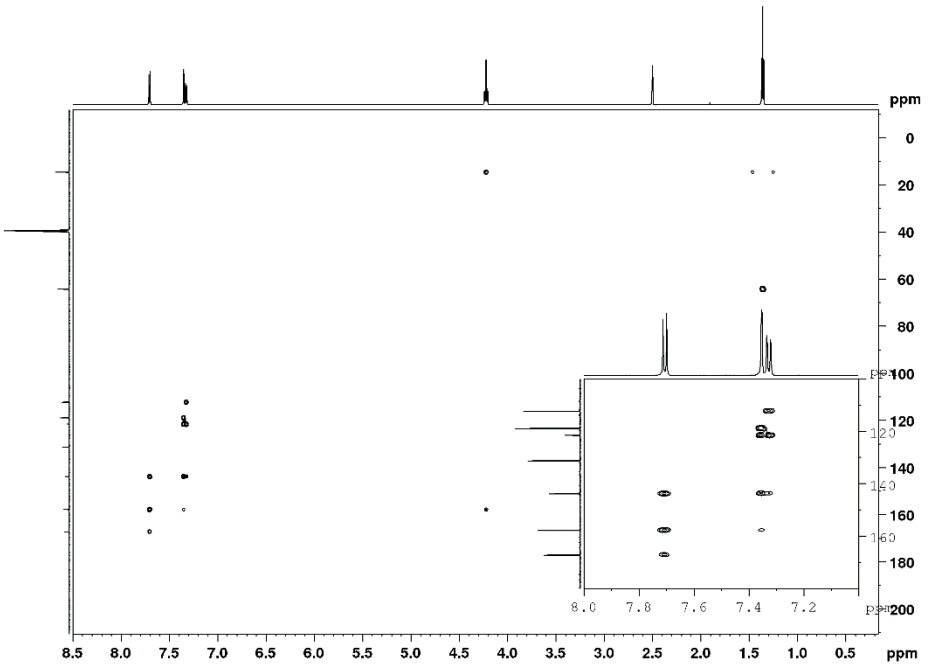

Figure 89 ^{1}H-^{13}C HMBC spectrum of **2c** (600-151 MHz, DMSO-d_6)

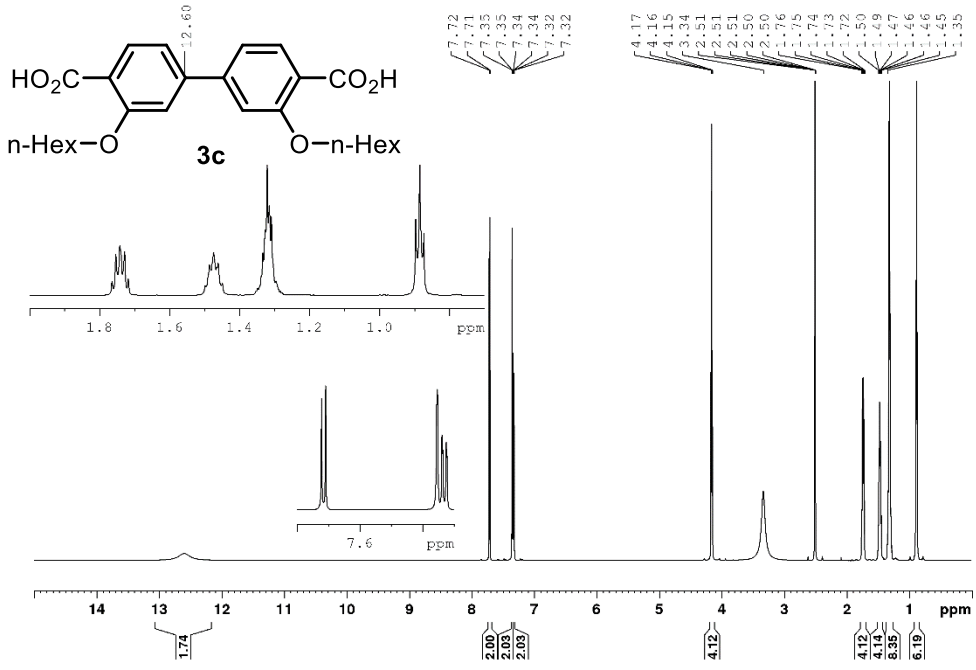

Figure 90 ^{1}H NMR spectrum of **3c** (600 MHz, DMSO-d_6)

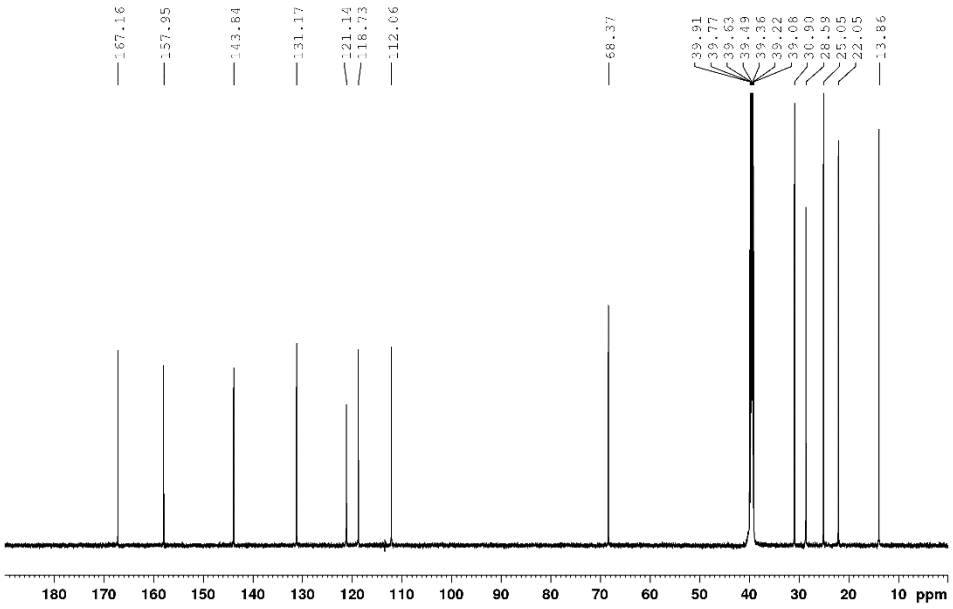

Figure 91 ^{13}C NMR spectrum of **3c** (151 MHz, DMSO-*d*$_6$)

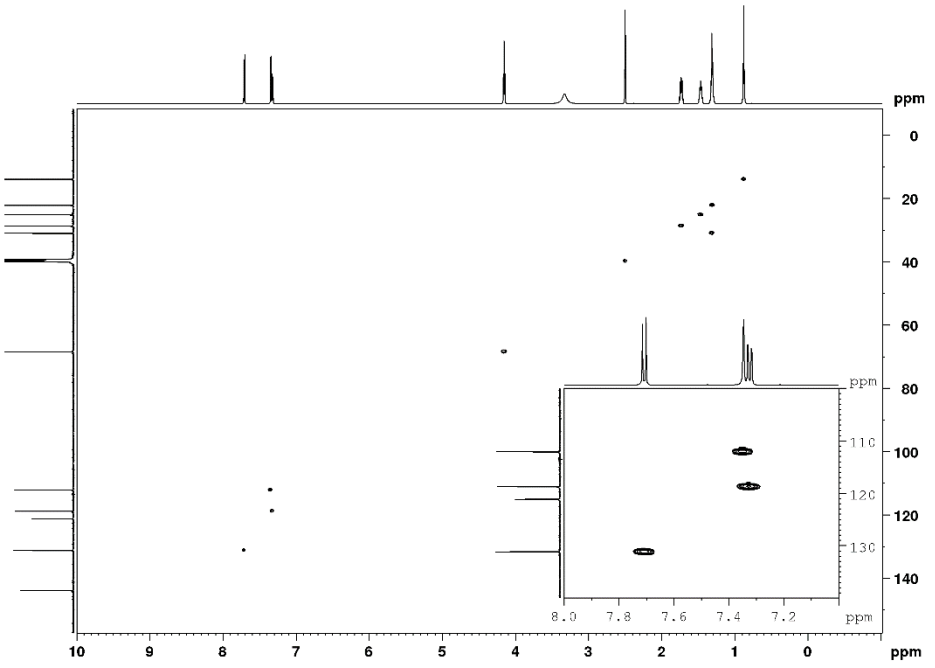

Figure 92 ^{1}H-^{13}C HSQC spectrum of **3c** (600-151 MHz, DMSO-*d*$_6$)

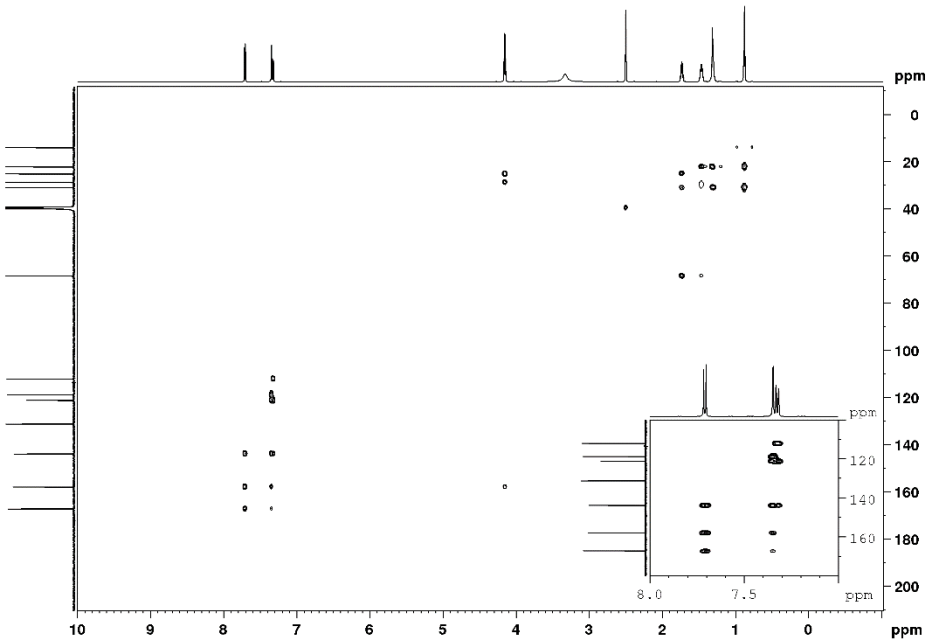

Figure 93 ^{1}H-^{13}C HMBC spectrum of **3c** (600-151 MHz, DMSO-*d*$_6$)

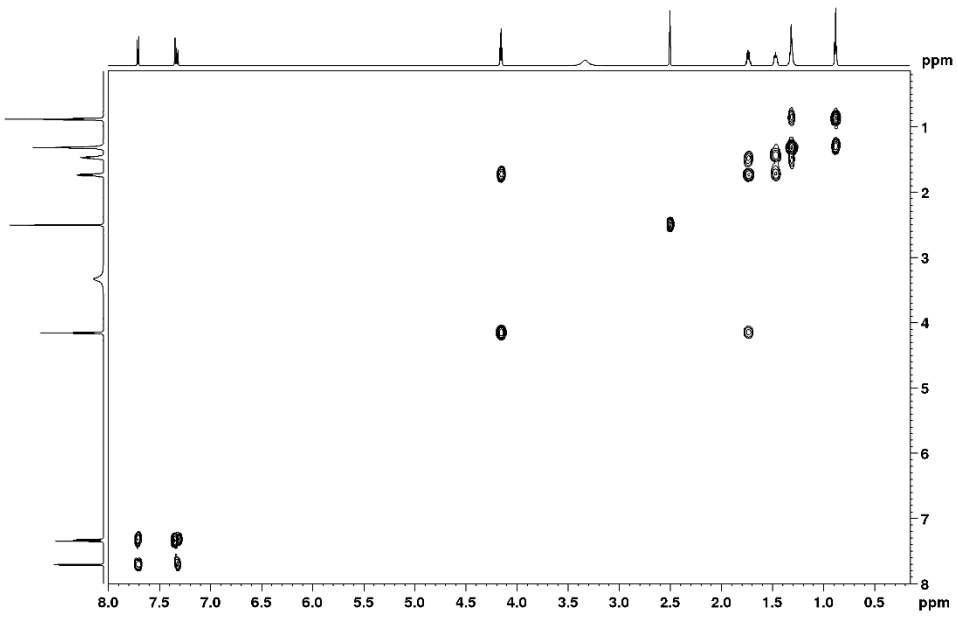

Figure 94 ^{1}H-^{1}H COSY spectrum of **3c** (600 MHz, $CDCl_3$)

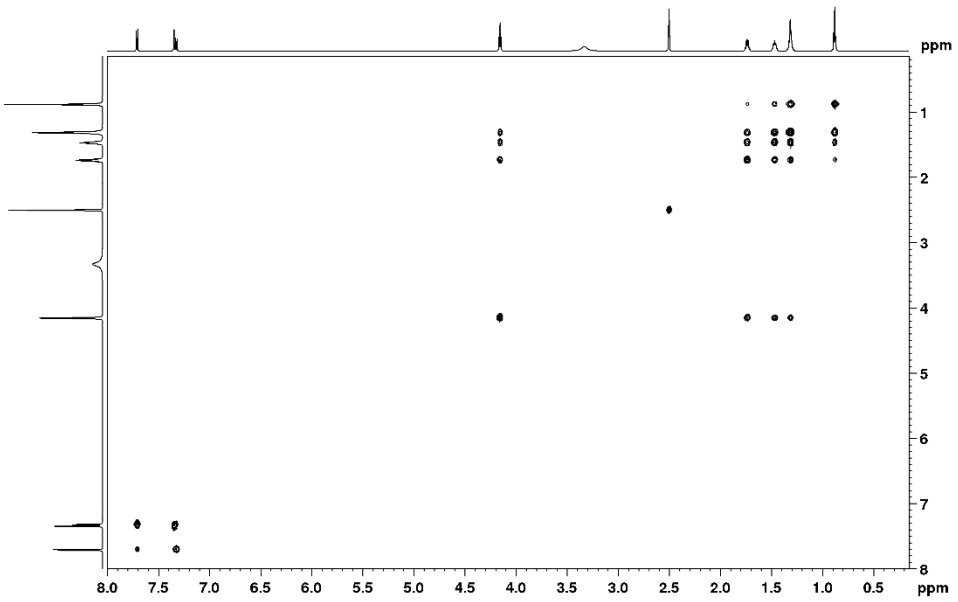

Figure 95 ^{1}H-^{1}H TOCSY spectrum of **3c** (600 MHz, $CDCl_3$)

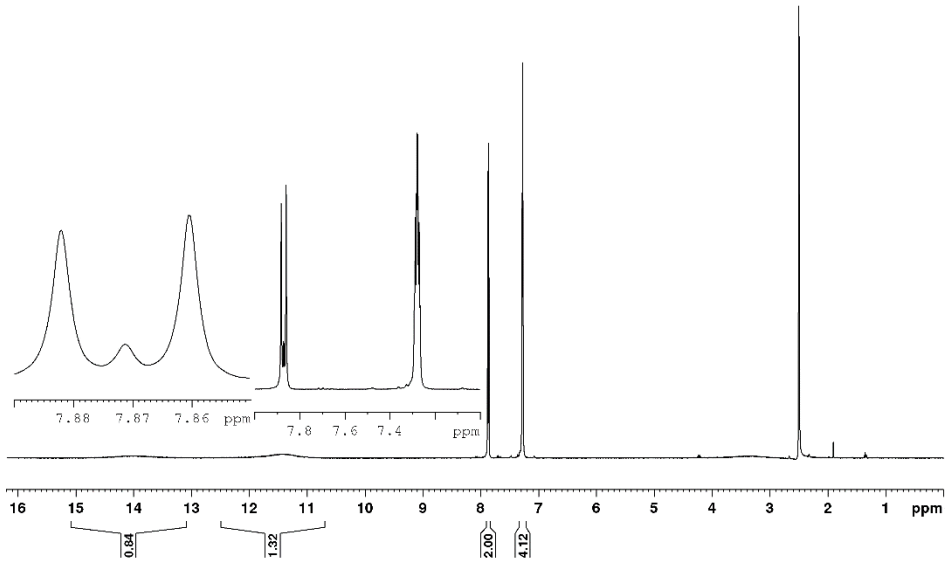

Figure 96 ^{1}H NMR spectrum of **1d** (400 MHz, DMSO-d_6)

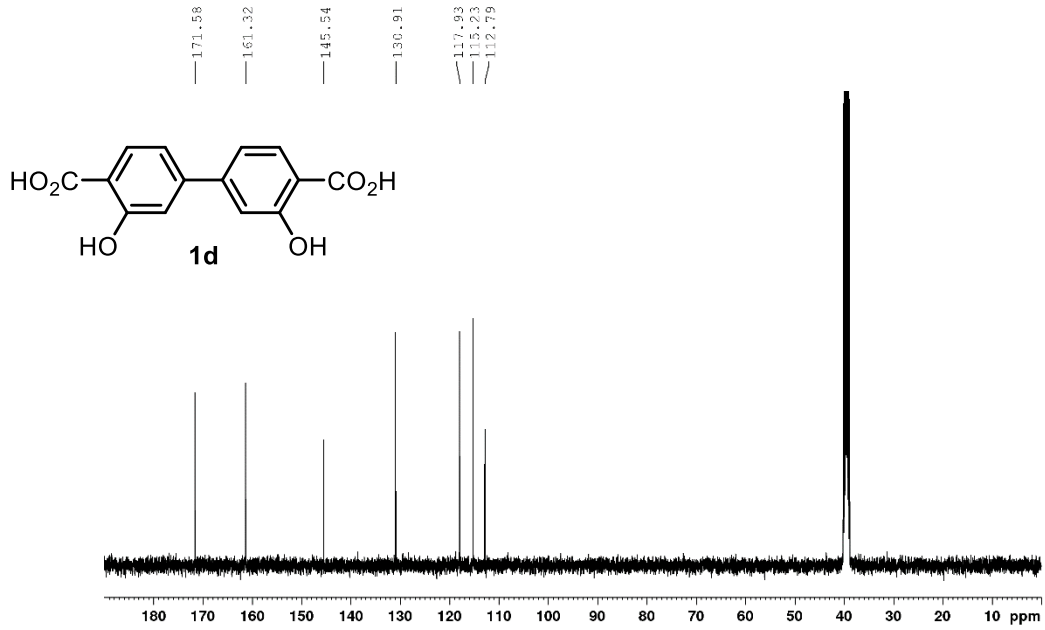

Figure 97 ^{13}C NMR spectrum of **1d** (101 MHz, DMSO-d_6)

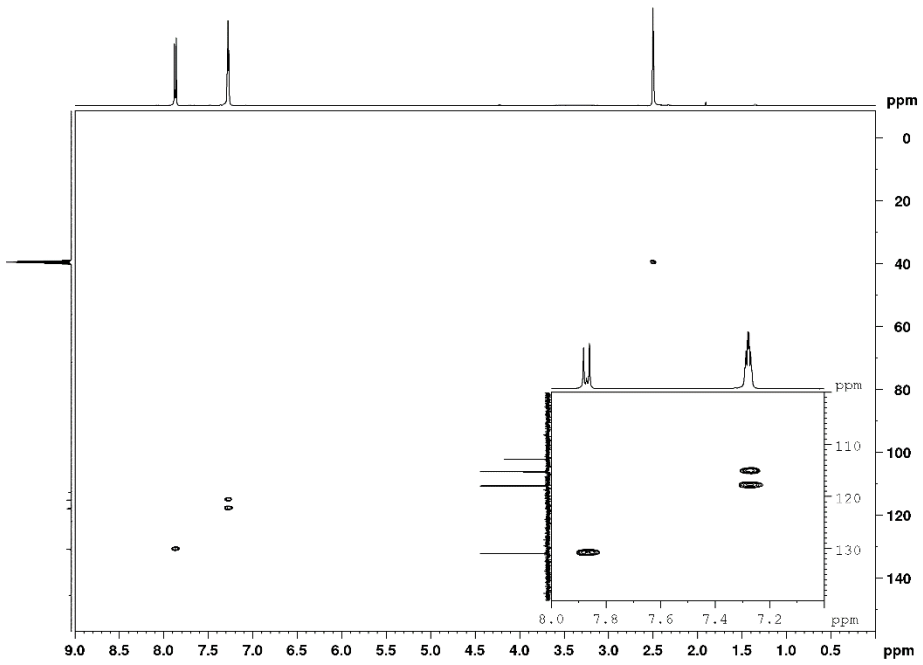

Figure 98 ^{1}H-^{13}C HSQC spectrum of **1**d (400-101 MHz, $CDCl_3$)

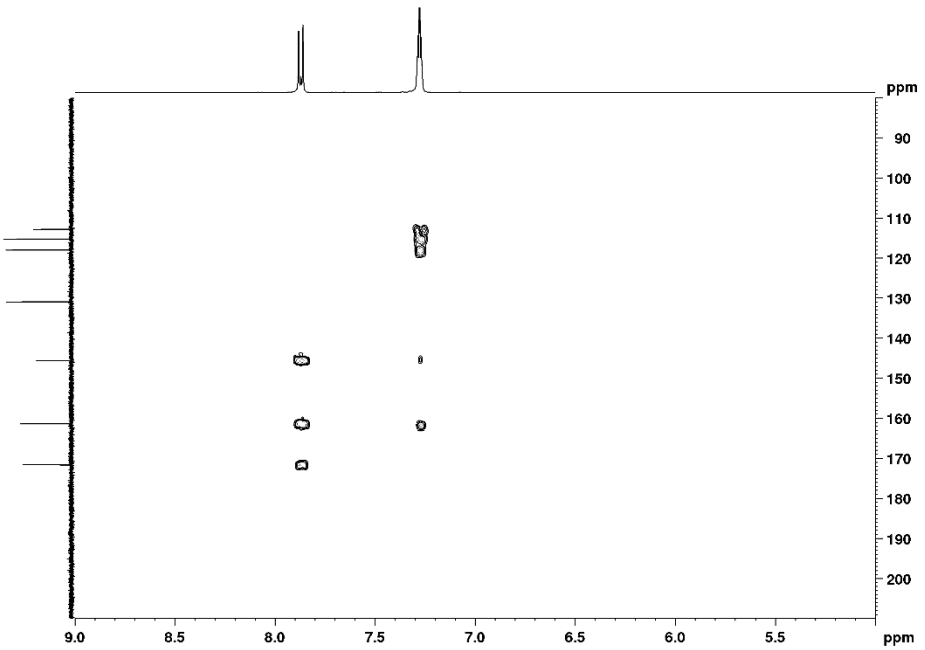

Figure 99 ^{1}H-^{13}C HMBC spectrum of **1d** (400-101 MHz, $CDCl_3$)

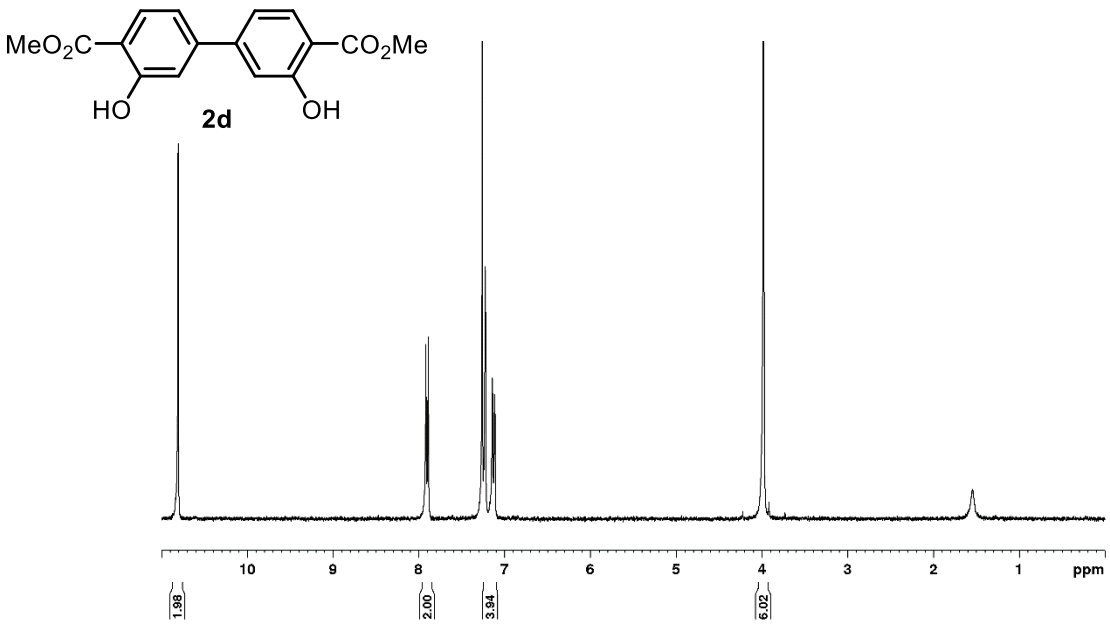

Figure 100 ^{1}H NMR spectrum of **2d** (300 MHz, $CDCl_3$)

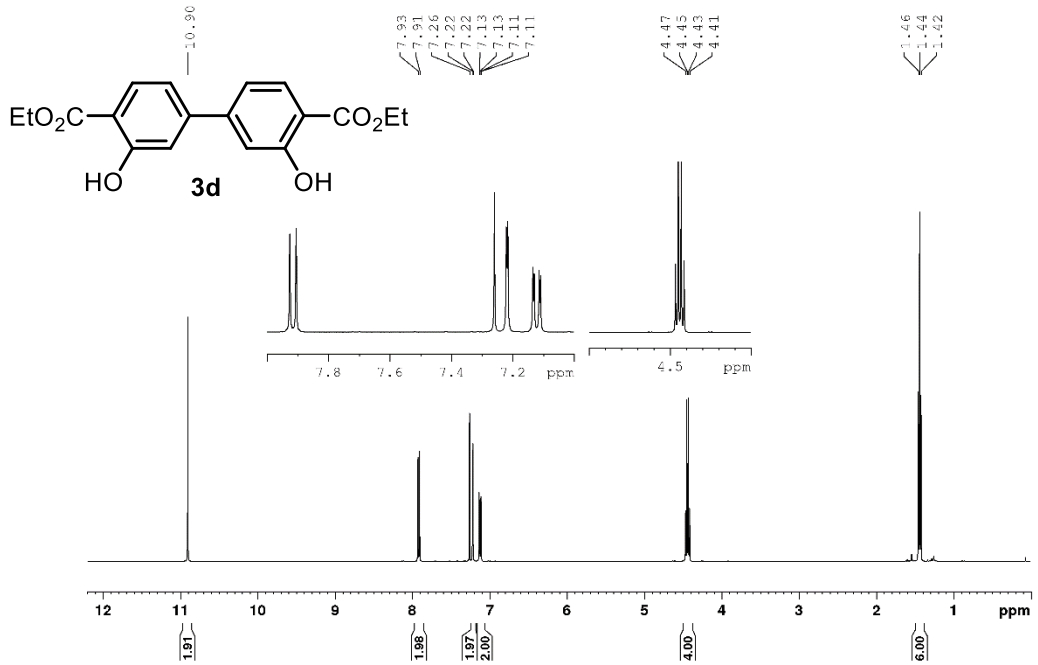

Figure 101 ^{1}H NMR spectrum of **3d** (300 MHz, $CDCl_3$)

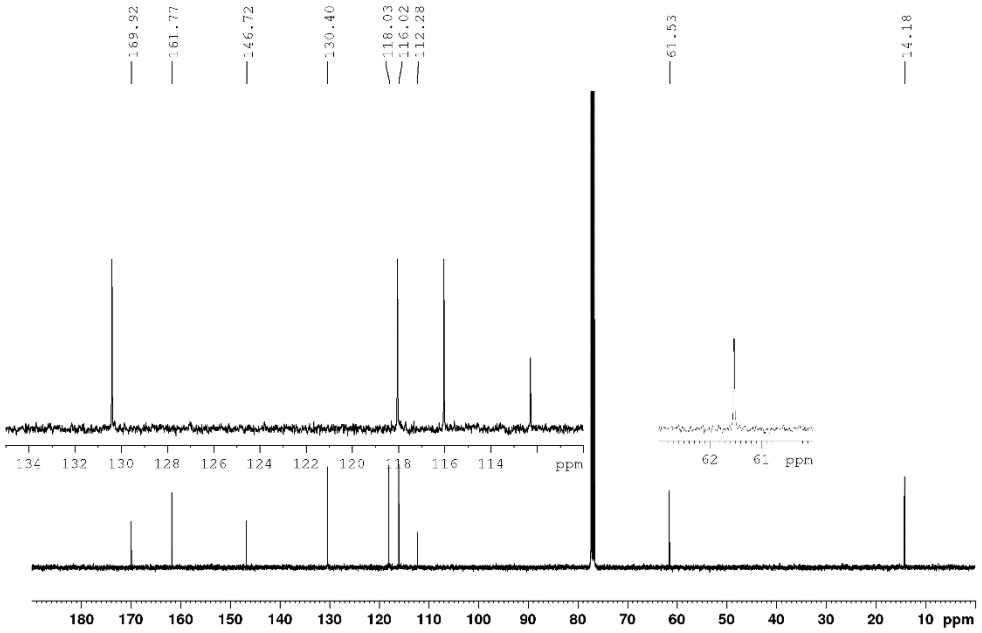

Figure 102 ^{13}C NMR spectrum of **3d** (101 MHz, $CDCl_3$)

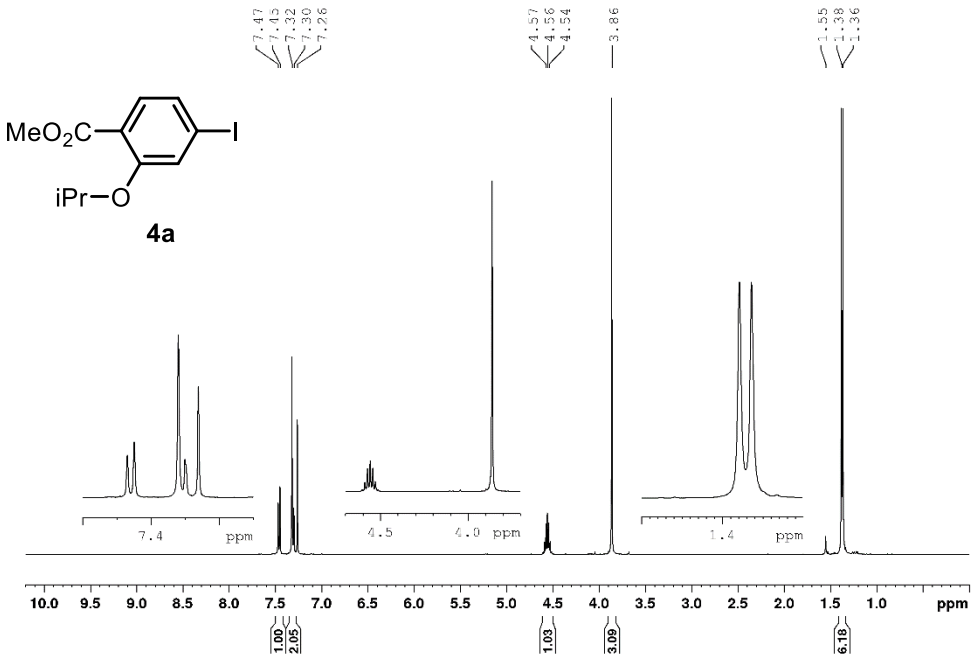

Figure 103 ^{1}H NMR spectrum of **4a** (400 MHz, $CDCl_3$)

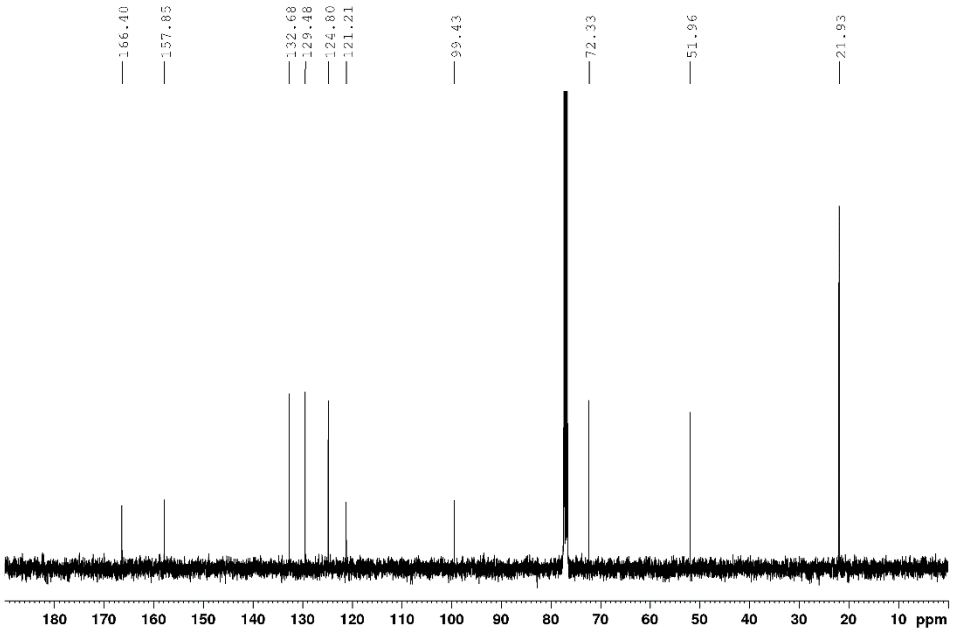

Figure 104 ^{13}C NMR spectrum of **4a** (101 MHz, $CDCl_3$)

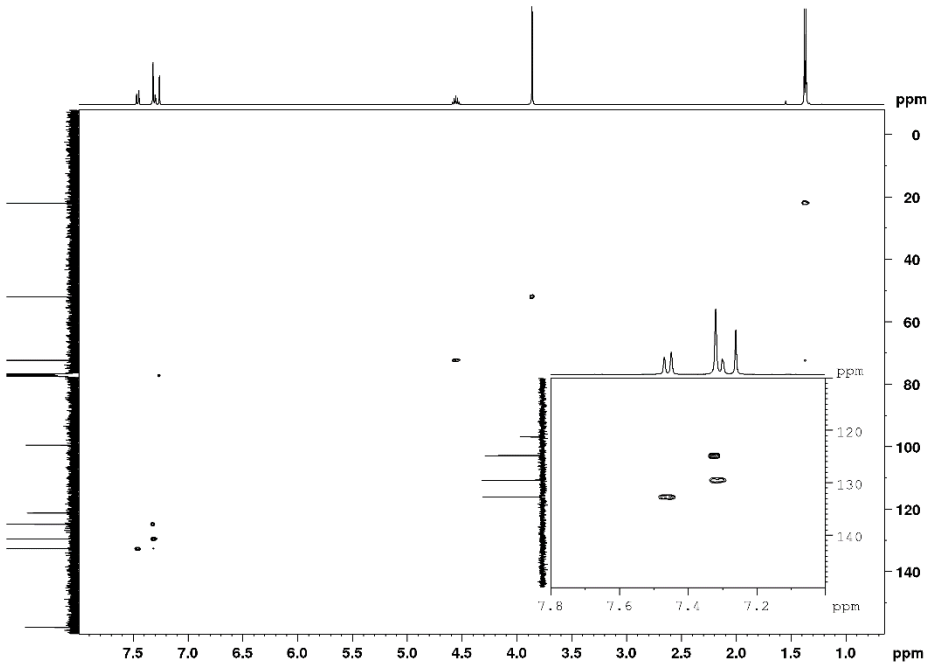

Figure 105 ^{1}H-^{13}C HSQC spectrum of **4a** (400-101 MHz, $CDCl_3$)

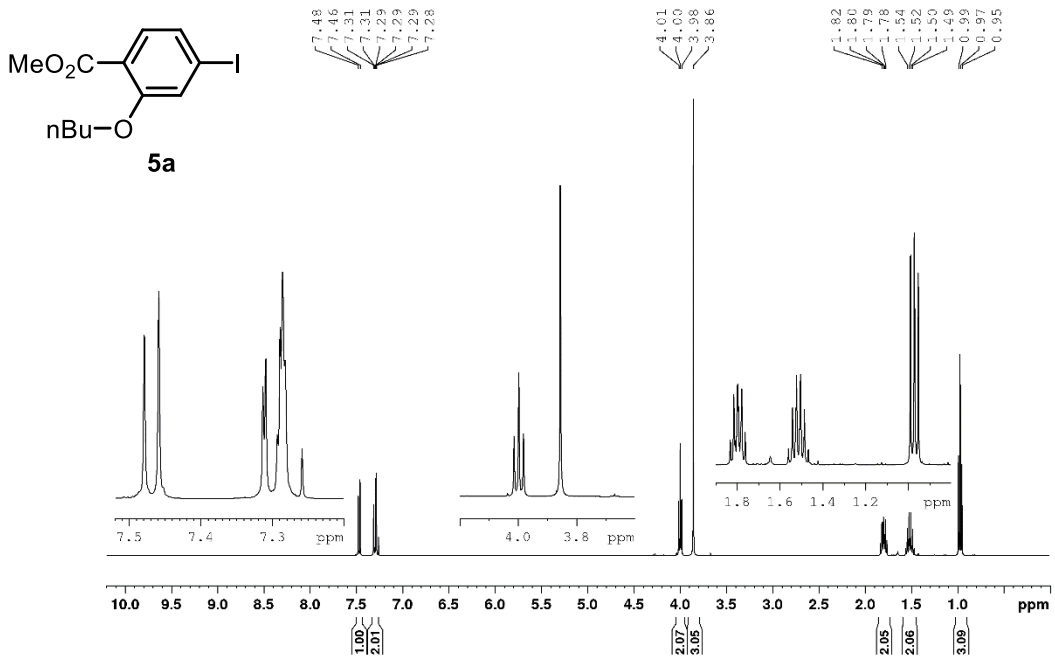

Figure 106 ^{1}H NMR spectrum of **5a** (400 MHz, $CDCl_3$)

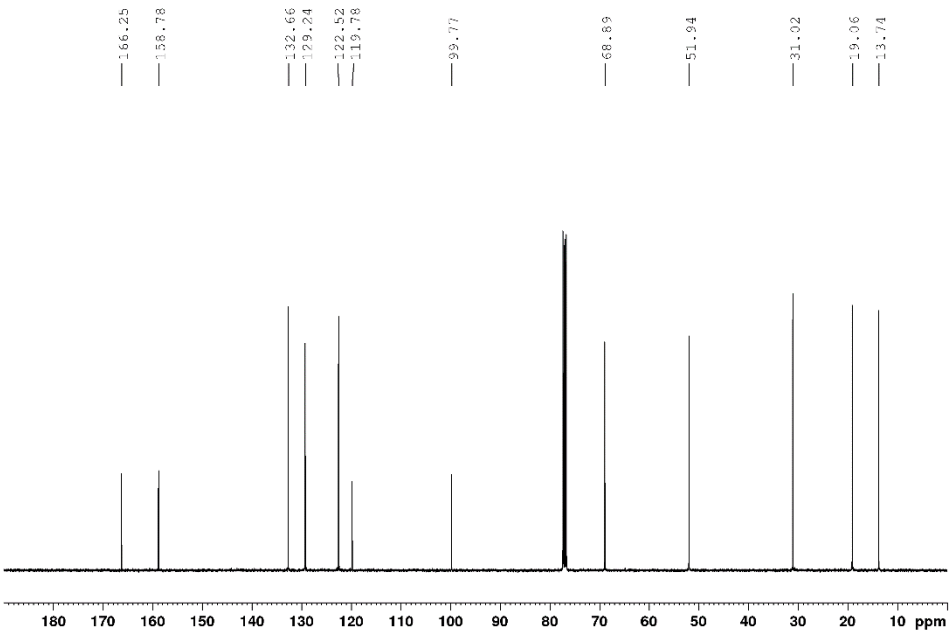

Figure 107 ^{13}C NMR spectrum of **5a** (101 MHz, $CDCl_3$)

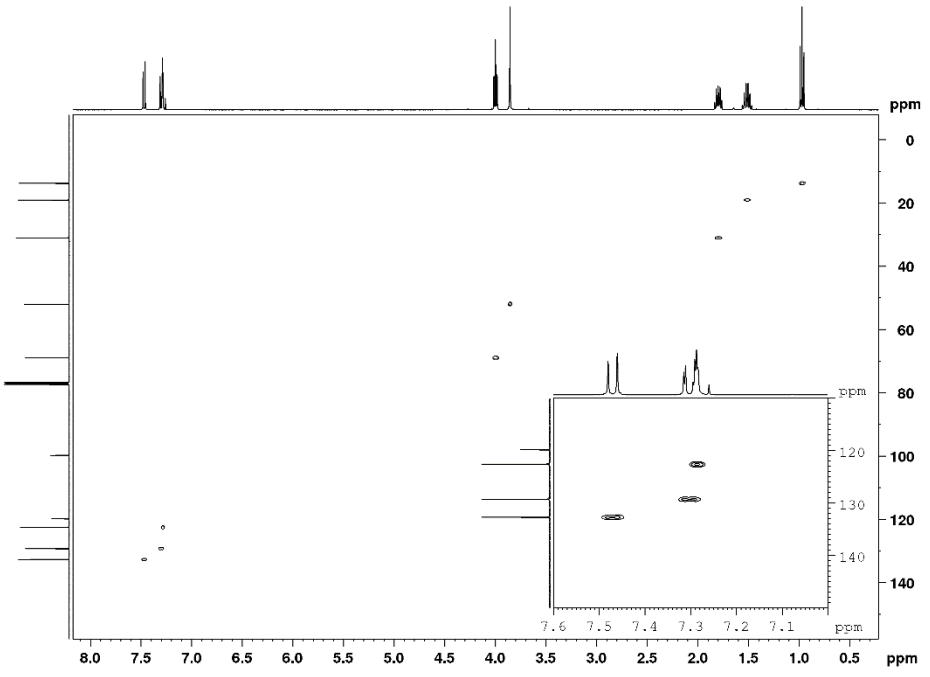

Figure 108 ^{1}H-^{13}C HSQC spectrum of **5a** (400-101 MHz, $CDCl_3$)

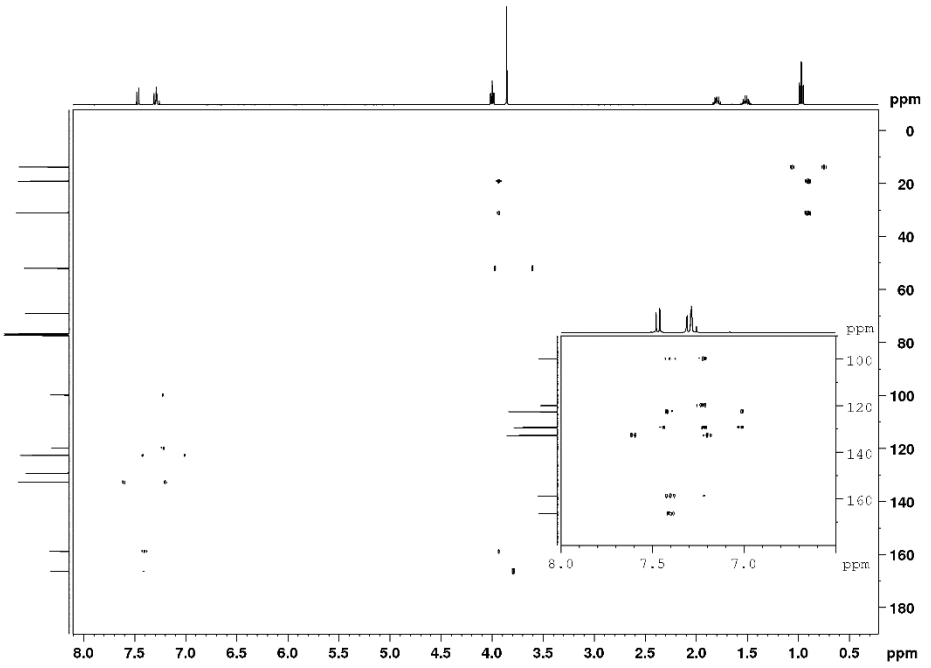

Figure 109 ^{1}H-^{13}C HMBC spectrum of **5a** (400-101 MHz, $CDCl_3$)

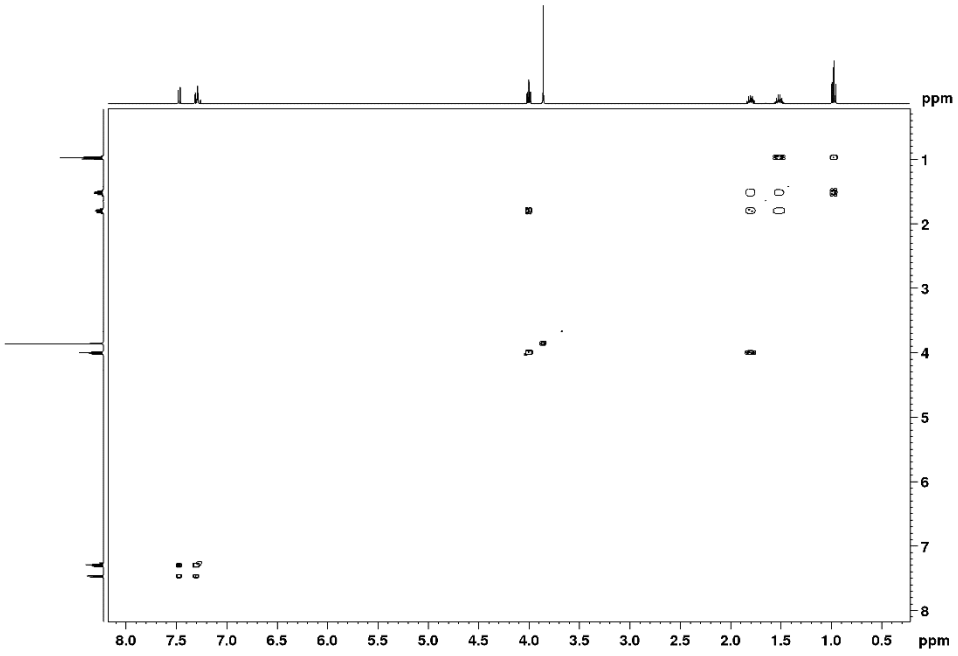

Figure 110 ^{1}H-^{1}H COSY spectrum of **5a** (400 MHz, $CDCl_3$)

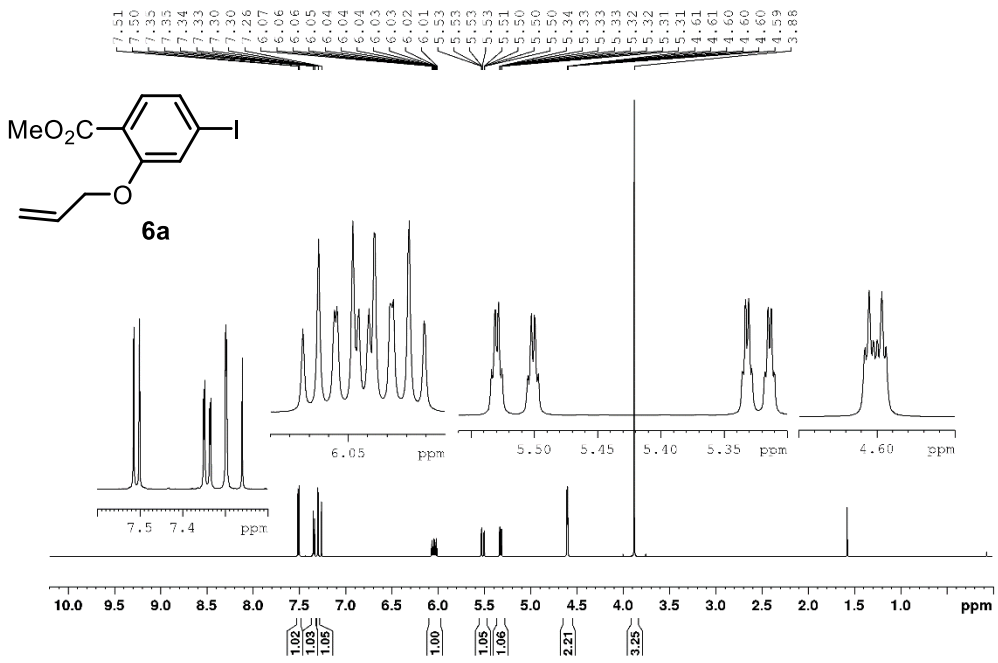

Figure 111 ^{1}H NMR spectrum of **6a** (600 MHz, $CDCl_3$)

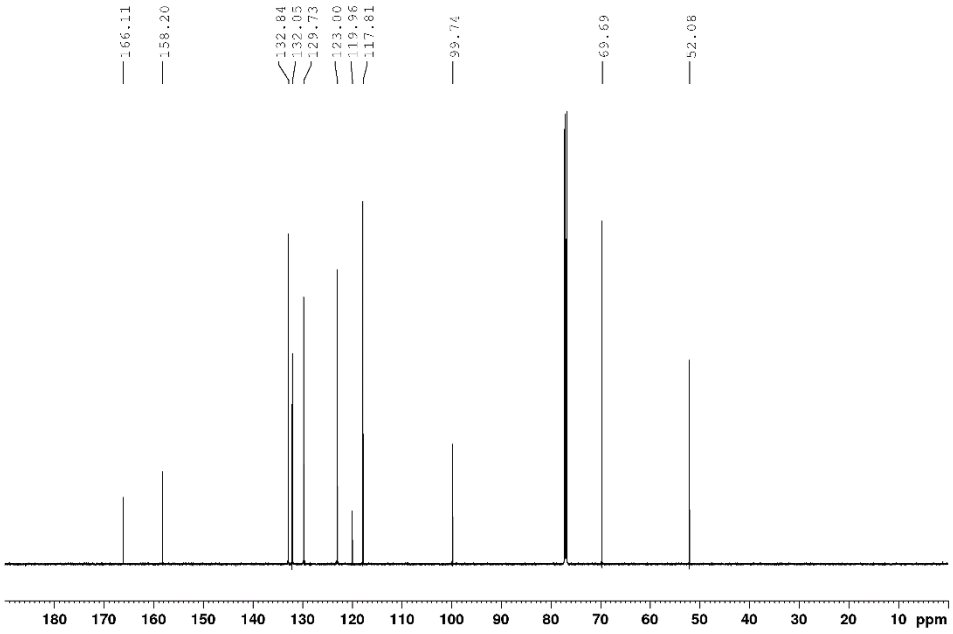

Figure 112 ^{13}C NMR spectrum of **6a** (151 MHz, $CDCl_3$)

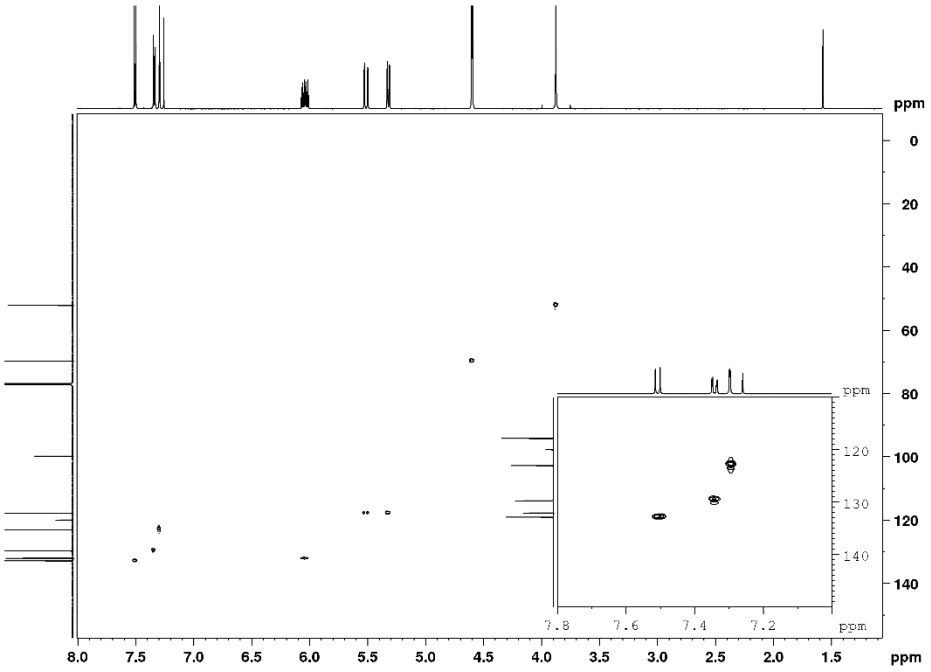

Figure 113 ^{1}H-^{13}C HSQC spectrum of **6a** (600-151 MHz, $CDCl_3$)

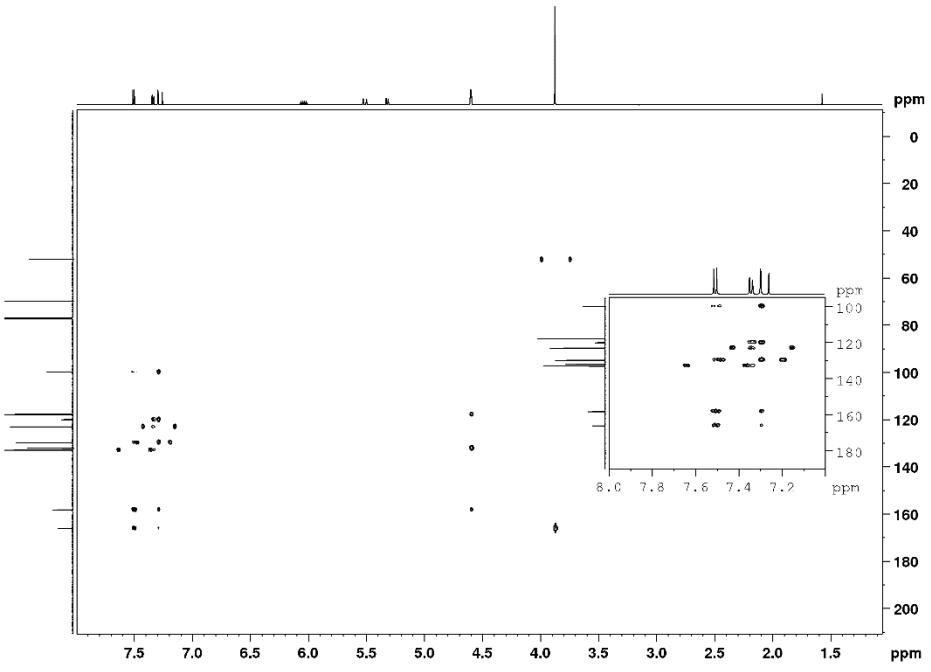

Figure 114 ^{1}H-^{13}C HMBC spectrum of **6a** (600-151 MHz, $CDCl_3$)

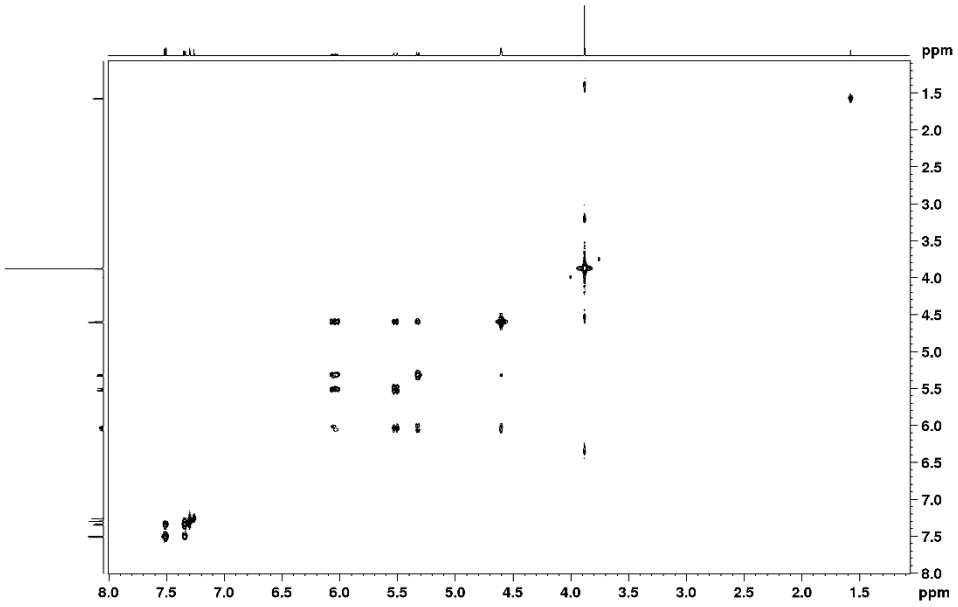

Figure 115 ^{1}H-^{1}H COSY spectrum of **6a** (600 MHz, $CDCl_3$)

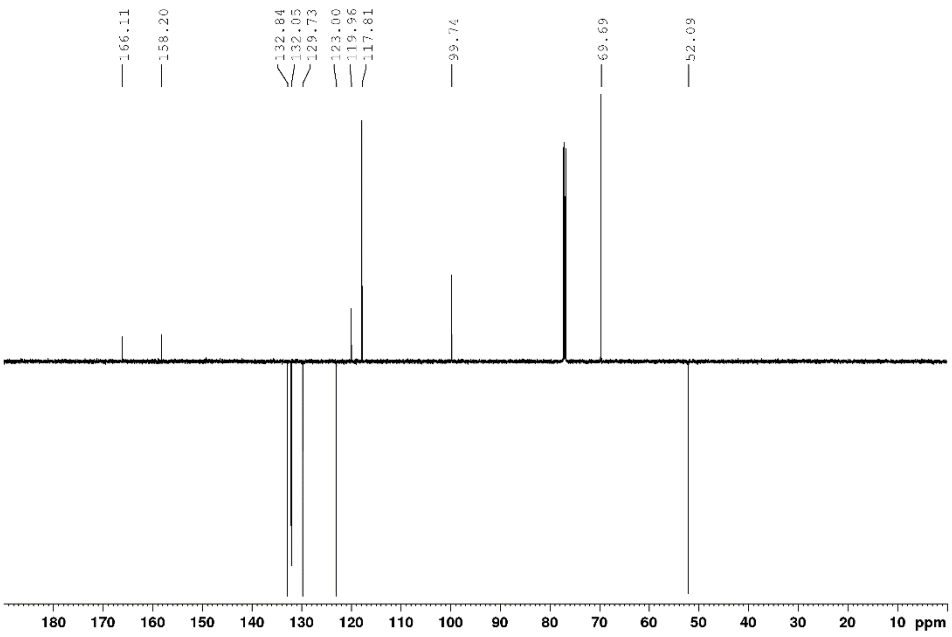

Figure 116 ^{13}C-APT NMR spectrum of **6a** (151 MHz, $CDCl_3$)

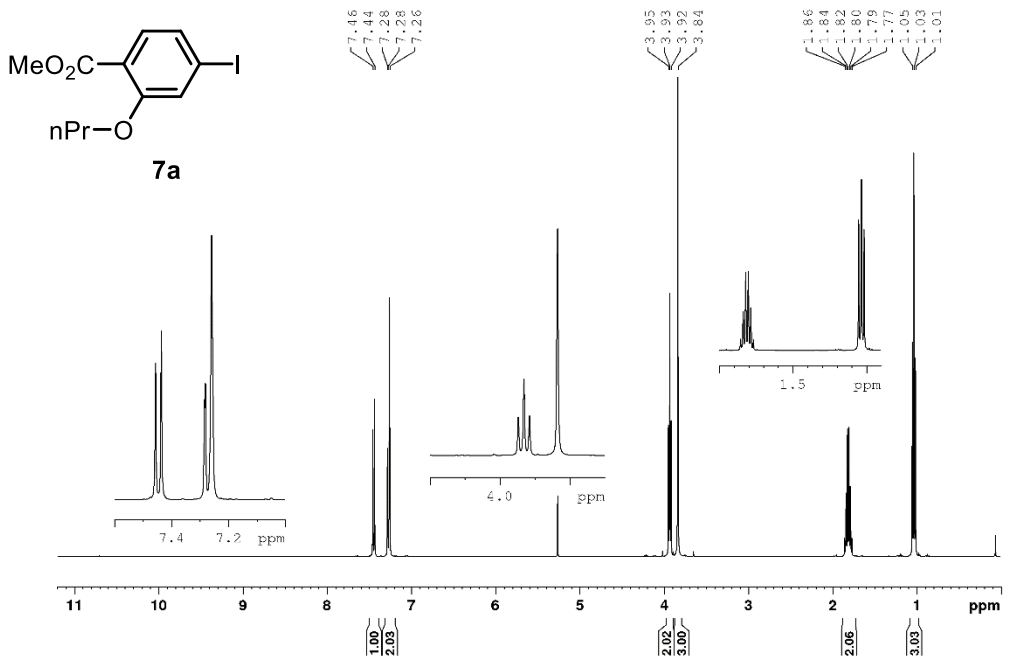

Figure 117 ^{1}H NMR spectrum of **7a** (400 MHz, $CDCl_3$)

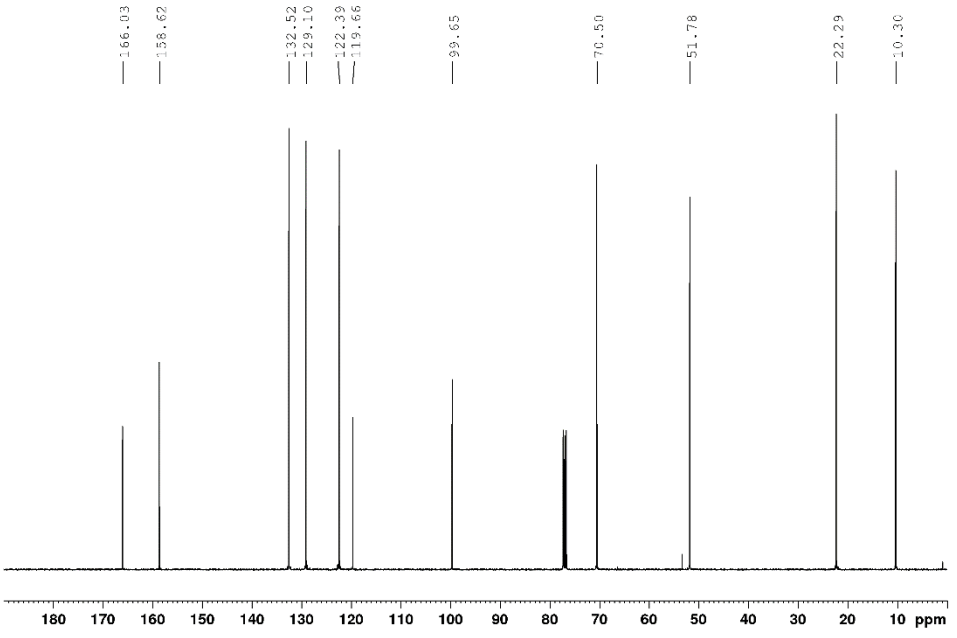

Figure 118 ^{13}C NMR spectrum of **7a** (151 MHz, DMSO-*d*$_6$)

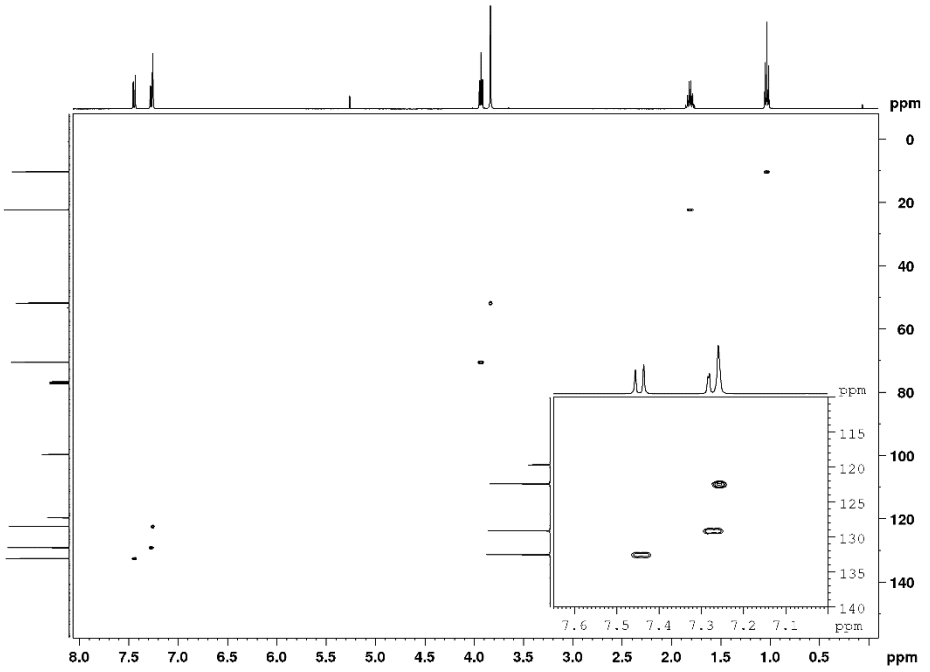

Figure 119 ^{1}H-^{13}C HSQC spectrum of **7a** (400-101 MHz, $CDCl_3$)

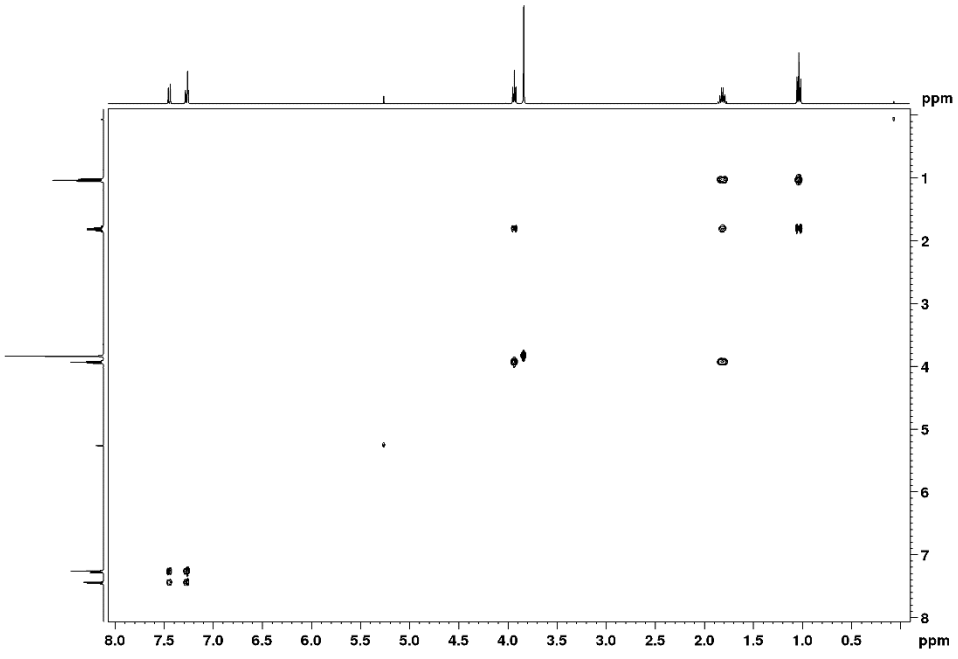

Figure 120 ^{1}H-^{1}H COSY spectrum of **7a** (400 MHz, $CDCl_3$)

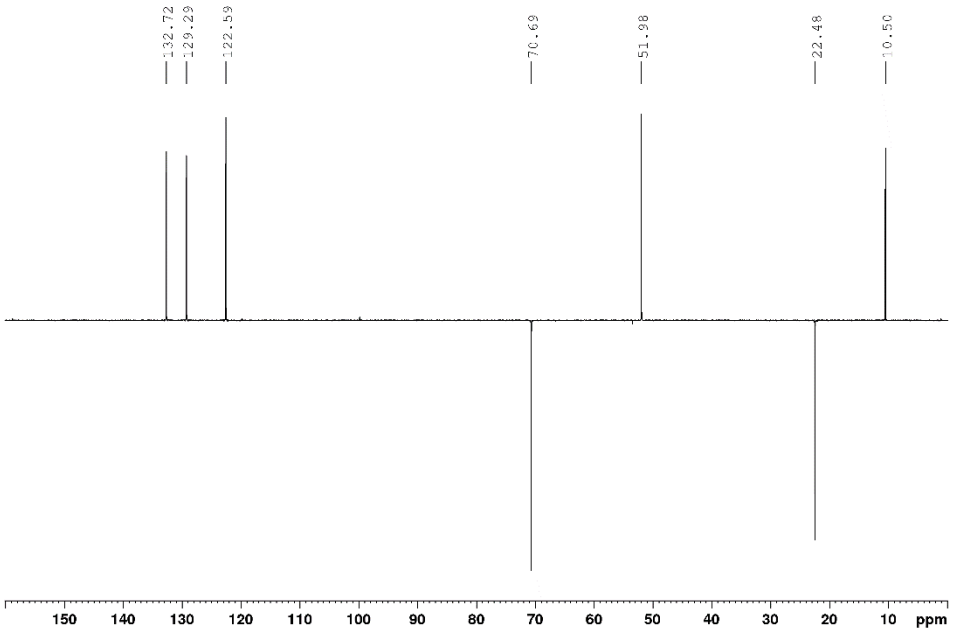

Figure 121 ^{13}C-DEPT NMR spectrum of **7a** (101 MHz, $CDCl_3$)

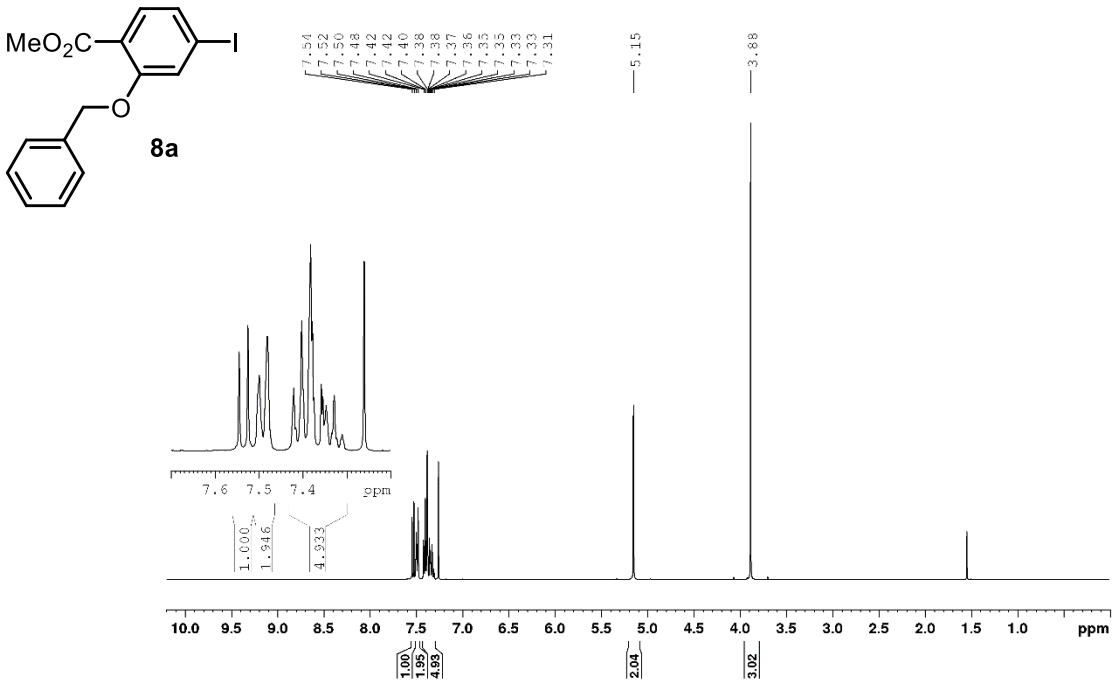

Figure 122 ^{1}H NMR spectrum of **8a** (400 MHz, $CDCl_3$)

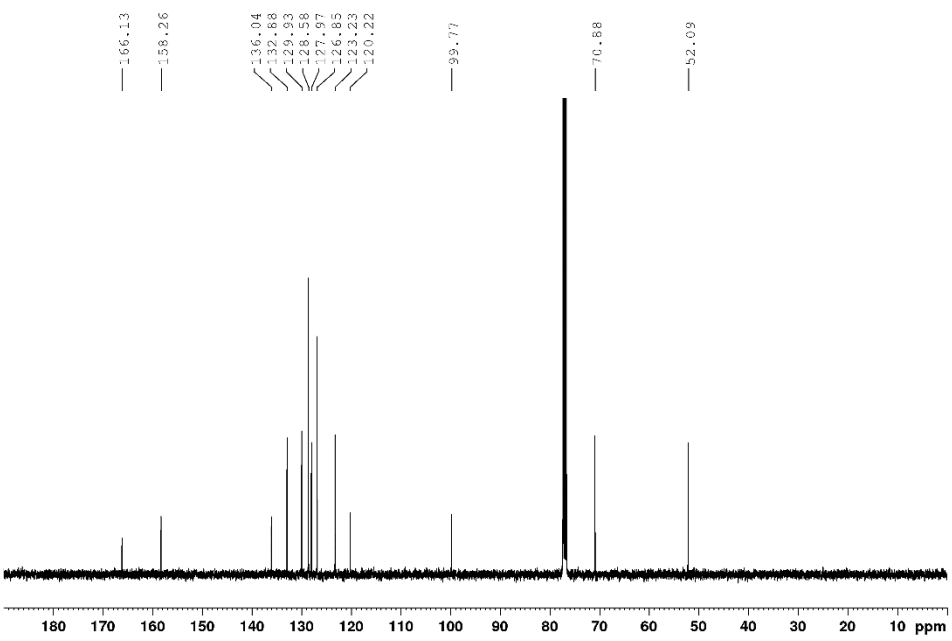

Figure 123 ^{13}C NMR spectrum of **8a** (101 MHz, $CDCl_3$)

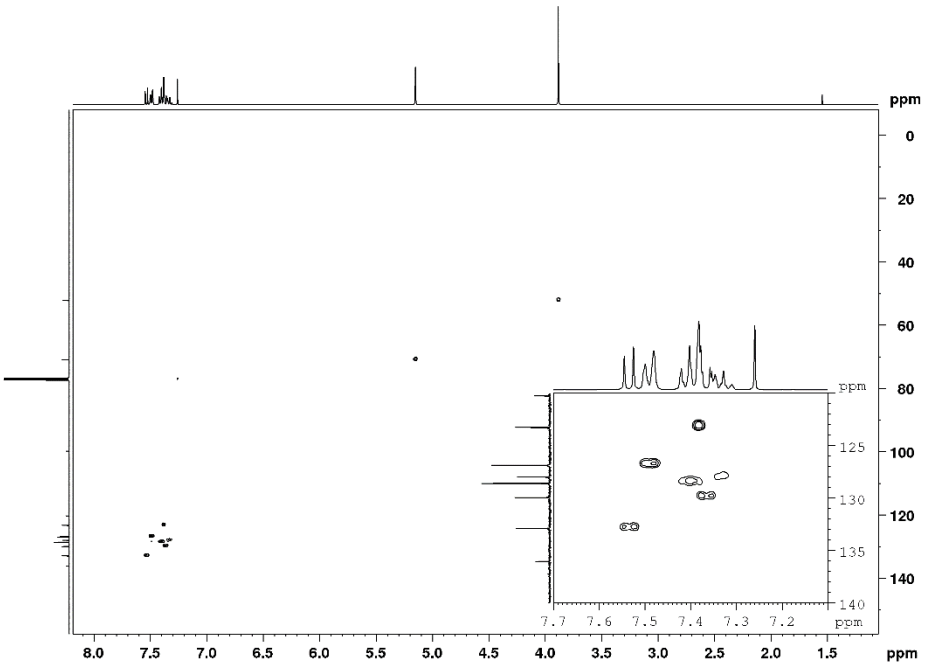

Figure 124 ^{1}H-^{13}C HSQC spectrum of **8a** (400-101 MHz, $CDCl_3$)

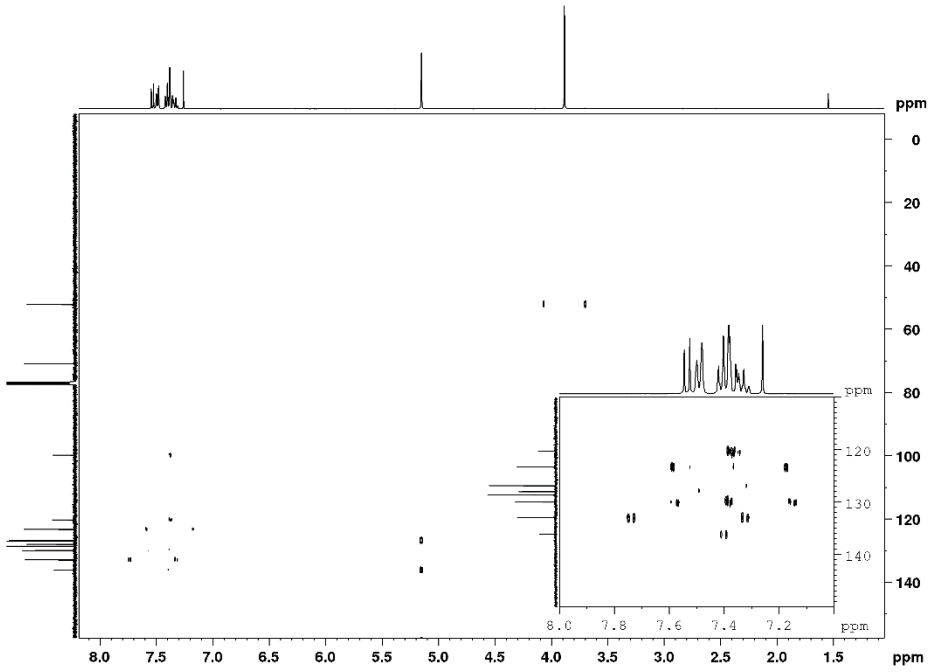

Figure 125 ^{1}H-^{13}C HMBC spectrum of **8a** (400-101 MHz, $CDCl_3$)

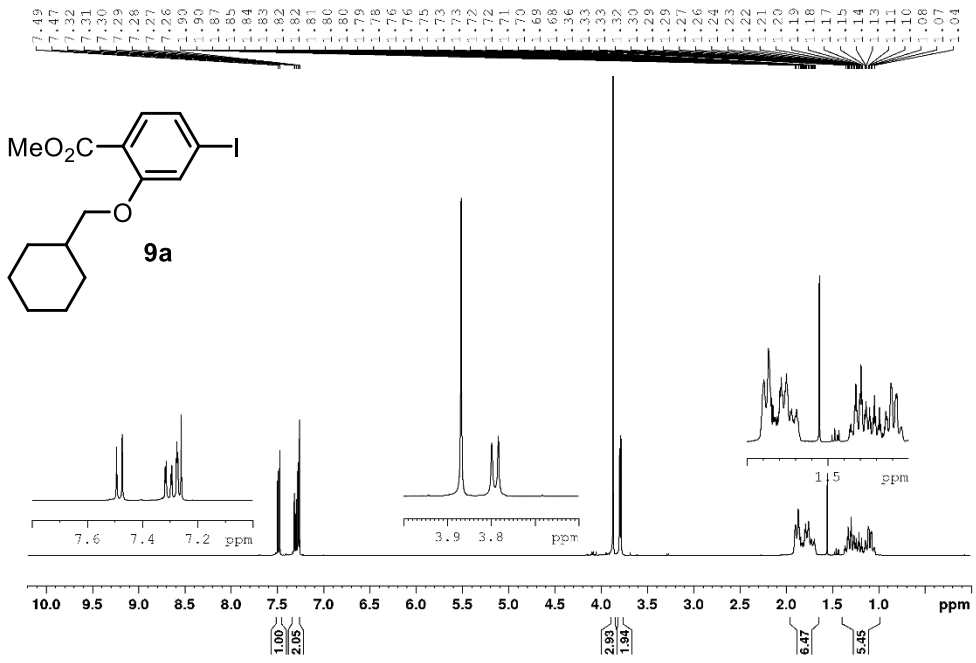

Figure 126 ^{1}H NMR spectrum of **9a** (400 MHz, $CDCl_3$)

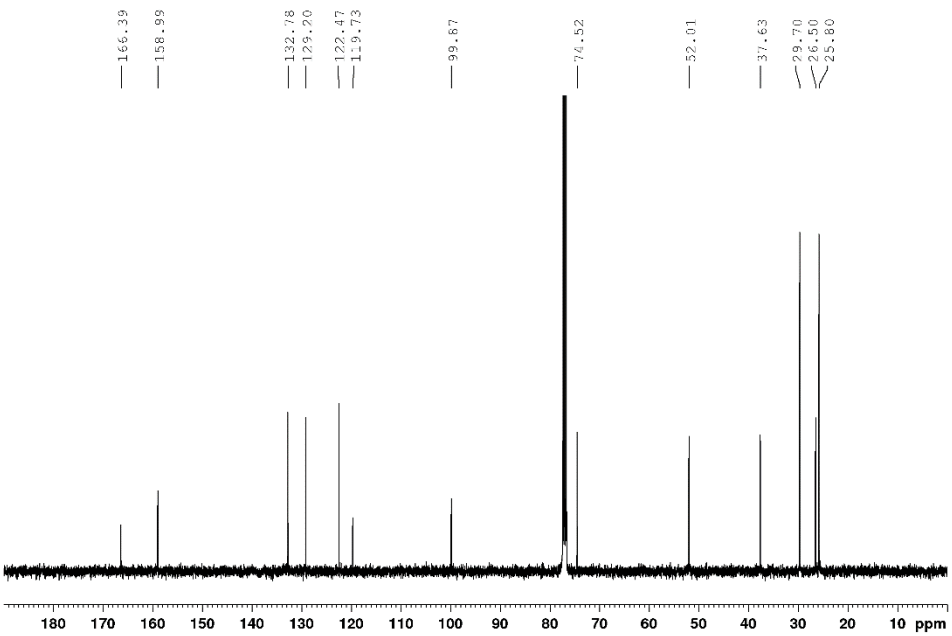

Figure 127 ^{13}C NMR spectrum of **9a** (101 MHz, $CDCl_3$)

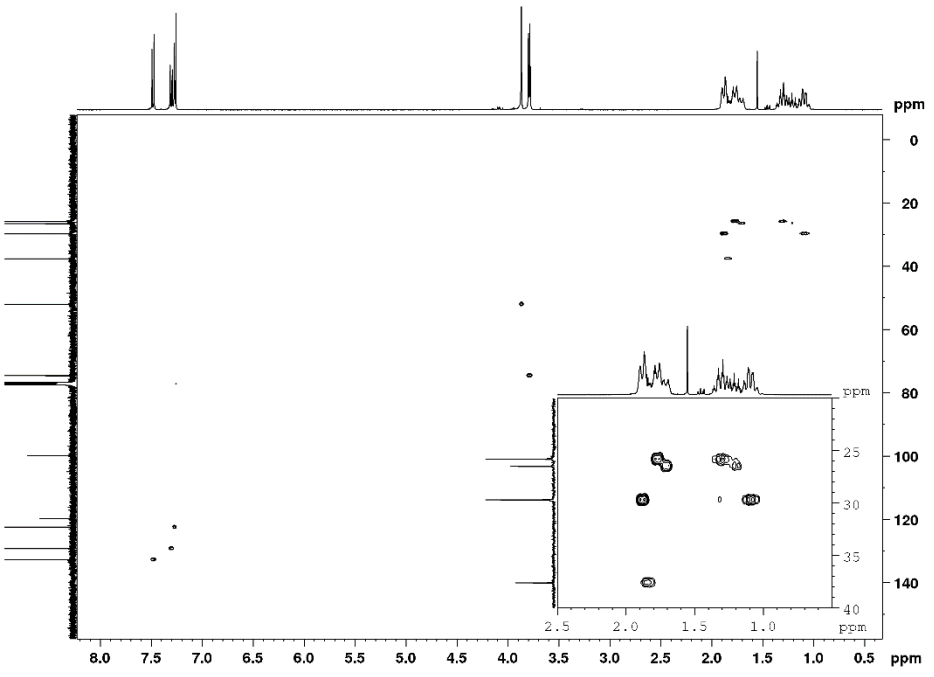

Figure 128 ^{1}H-^{13}C HSQC spectrum of **9a** (400-101 MHz, $CDCl_3$)

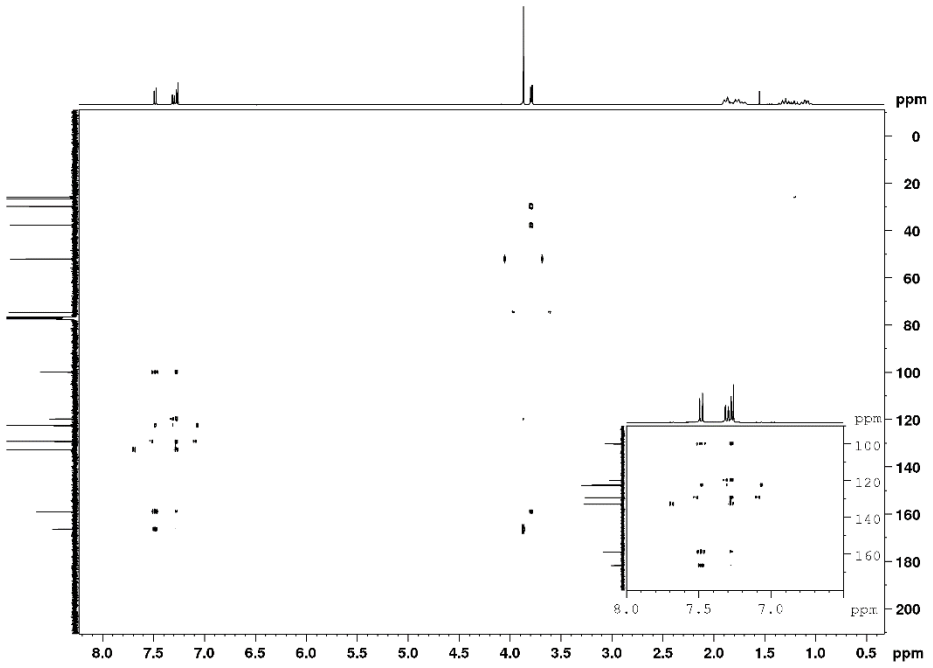

Figure 129 ^{1}H-^{13}C HMBC spectrum of **9a** (400-101 MHz, $CDCl_3$)

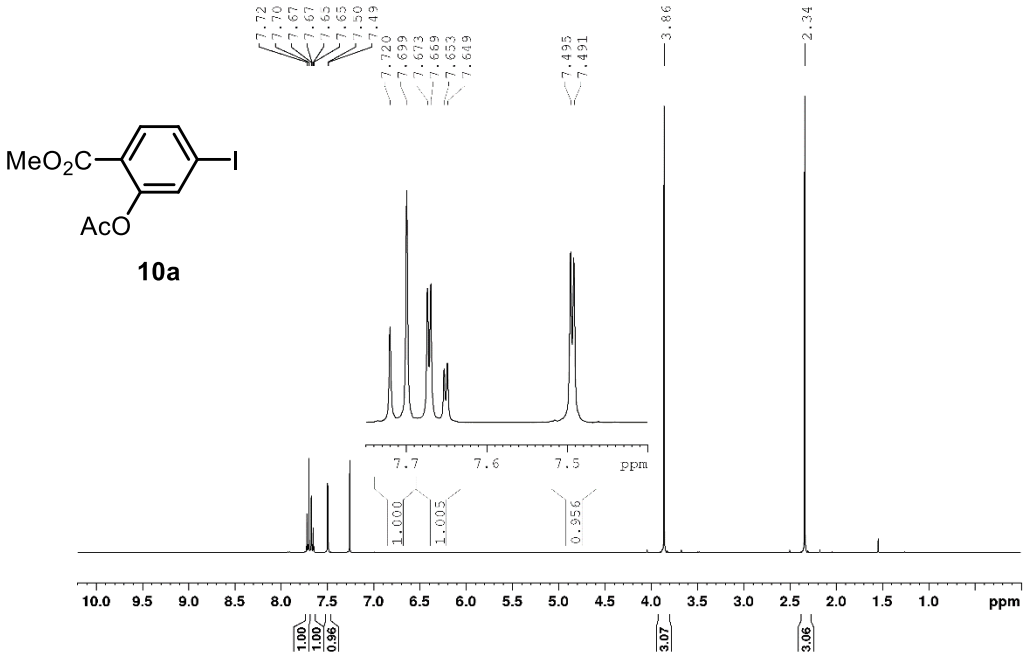

Figure 130 ^{1}H NMR spectrum of **10a** (400 MHz, $CDCl_3$)

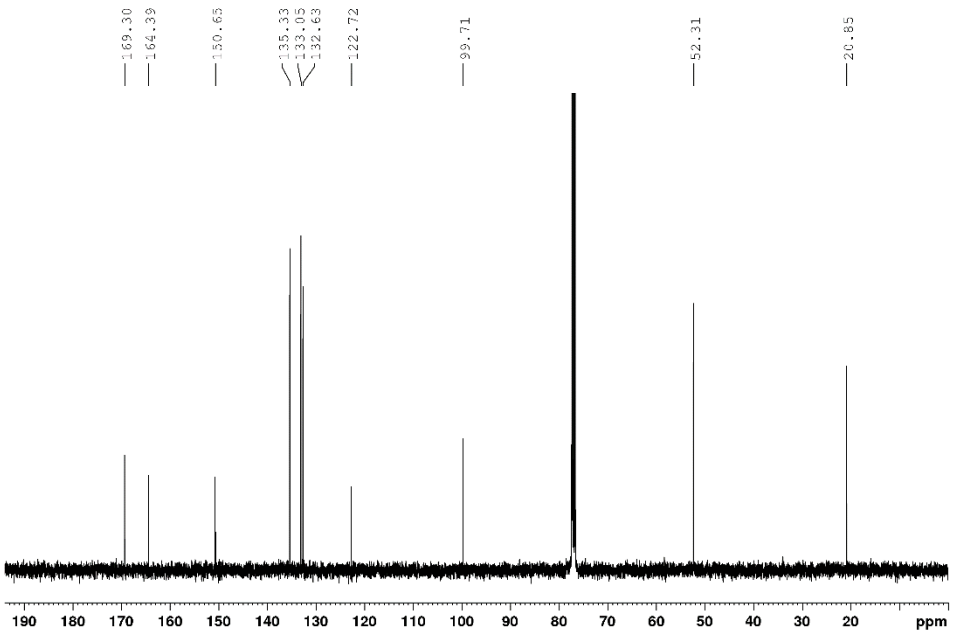

Figure 131 ^{13}C NMR spectrum of **10a** (101 MHz, $CDCl_3$)

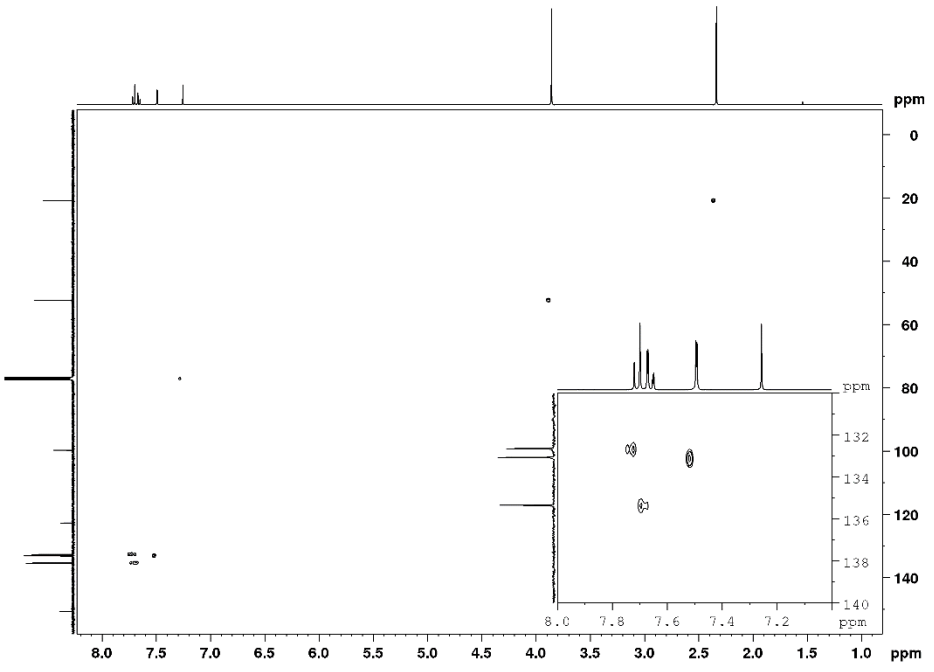

Figure 132 ^{1}H-^{13}C HSQC spectrum of **10a** (400-101 MHz, $CDCl_3$)

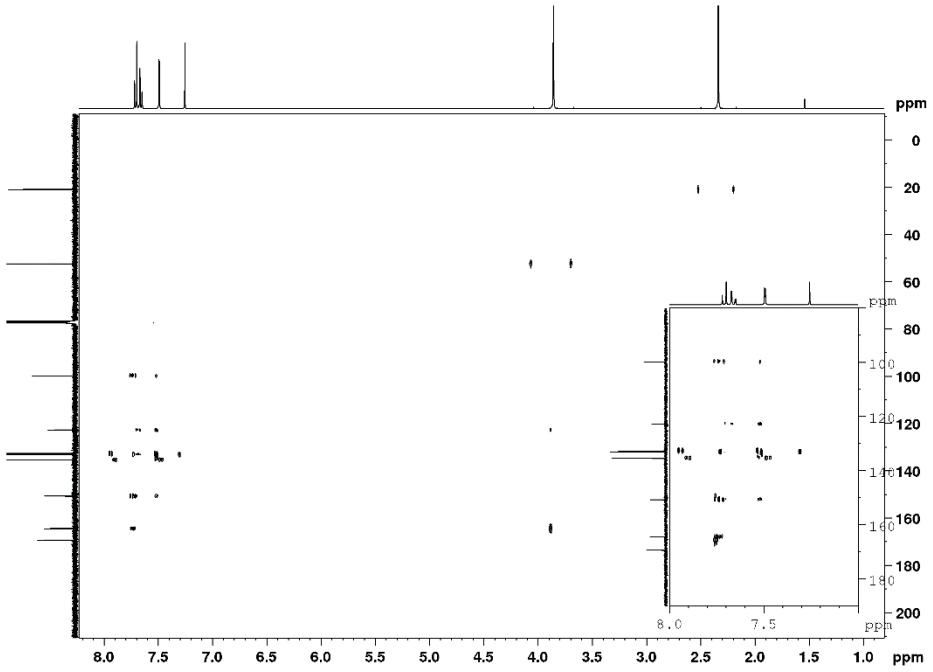

Figure 133 ^{1}H-^{13}C HMBC spectrum of **10a** (400-101 MHz, $CDCl_3$)

Bibliography

[1] J. C. Hafizovic, S. Jakobsen, U. Olsbye, N. Guillou, C. Lamberti, S. Bordiga, K. P. Lillerud, *J. Am. Chem. Soc.* **2008**, *130*, 13850-13851.

[2] S. R. Batten, N. R. Champness, X.-M. Chen, J. Garcia-Martinez, S. Kitagawa, L. Ohrstrom, M. O'Keeffe, M. P. Suh, J. Reedijk, *CrystEngComm* **2012**, *14*, 3001-3004.

[3] O. K. Farha, I. Eryazici, N. C. Jeong, B. G. Hauser, C. E. Wilmer, A. A. Sarjeant, R. Q. Snurr, S. T. Nguyen, A. Ö. Yazaydın, J. T. Hupp, *J. Am. Chem. Soc.* **2012**, *134*, 15016-15021.

[4] J. R. Long, O. M. Yaghi, *Chem. Soc. Rev.* **2009**, *38*, 1213-1214.

[5] P. Horcajada, T. Chalati, C. Serre, B. Gillet, C. Sebrie, T. Baati, J. F. Eubank, D. Heurtaux, P. Clayette, C. Kreuz, J.-S. Chang, Y. K. Hwang, V. Marsaud, P.-N. Bories, L. Cynober, S. Gil, G. Férey, P. Couvreur, R. Gref, *Nature Materials* **2009**, *9*, 172.

[6] Y. Kinoshita, I. Matsubara, T. Higuchi, Y. Saito, *Bull. Chem. Soc. Jpn.* **1959**, *32*, 1221-1226.

[7] O. M. Yaghi, H. Li, *J. Am. Chem. Soc.* **1995**, *117*, 10401-10402.

[8] H. K. Chae, D. Y. Siberio-Pérez, J. Kim, Y. Go, M. Eddaoudi, A. J. Matzger, M. O'Keeffe, O. M. Yaghi, *Nature* **2004**, *427*, 523.

[9] A. Schoedel, M. Yaghi Omar, in *Macrocyclic and Supramolecular Chemistry* (Ed.: R. M. Izatt), **2016**, pp. 200-219.

[10] P. V. Dau, M. Kim, S. J. Garibay, F. H. L. Münch, C. E. Moore, S. M. Cohen, *Inorg. Chem.* **2012**, *51*, 5671-5676.

[11] S. Øien, G. Agostini, S. Svelle, E. Borfecchia, K. A. Lomachenko, L. Mino, E. Gallo, S. Bordiga, U. Olsbye, K. P. Lillerud, C. Lamberti, *Chem. Mater.* **2015**, *27*, 1042-1056.

[12] K. T. Hylland, S. Øien-Ødegaard, K. P. Lillerud, M. Tilset, *Synlett* **2015**, *26*, 1480-1485.

[13] L. Wu, MSc thesis, Department of Chemistry, University of Oslo **2015**.

[14] K. T. Hylland, MSc thesis, Department of Chemistry, University of Oslo **2014**.

[15] X.-Z. Wang, D.-R. Zhu, Y. Xu, J. Yang, X. Shen, J. Zhou, N. Fei, X.-K. Ke, L.-M. Peng, *Crystal Growth & Design* **2010**, *10*, 887-894.

[16] G. L. Kennedy, G. Jay Graepel, *Toxicol. Lett.* **1991**, *56*, 317-326.

[17] A. Vogrig, L. Dorr, N. Bouzidi, B. Boucherle, A.-S. Wattiez, E. Cassier, G. Vallon, I. Ripoche, I. Abrunhosa-Thomas, P. Marin, L. Nauton, V. Thery, C. Courteix, L.-Y. Lian, S. Ducki, *ACS Chemical Biology* **2013**, *8*, 2209-2216.

[18] C. F. Nising, U. K. Schmid, M. Nieger, S. Bräse, *The Journal of Organic Chemistry* **2004**, *69*, 6830-6833.

[19] F. W. McLafferty, F. Tureek, *Interpretation of Mass Spectra*, 4th ed., University Science Books, Sausalito, California, **1993**.

[20] K. T. Hylland, Unpublished results, **2018**

[21] X. Liu, X. Wang, T. Gao, Y. Xu, X. Shen, D. Zhu, *CrystEngComm* **2014**, *16*, 2779-2787.

[22] H. Nishioka, M. Nagasawa, K. Yoshida, *Synthesis* **2000**, *2000*, 243-246.

[23] F. Lundvall, Ph.D thesis, Department of Chemistry, University of Oslo **2014**.

[24] J.-Y. Park, Kim, Seung-Woo, Park, Ho-Joon, Im, Weon-Bin, Lee, Ja-Kyeong, Yoon, Sung-Hwa, *Bull. Korean Chem. Soc.* **2010**, *31*, 3860-3863.

[25] G. E. M. Schukraft, S. Ayala, B. L. Dick, S. M. Cohen, *Chem. Commun.* **2017**, *53*, 10684-10687.
[26] S. Andreas, R. Pascal, G. Adelheid, L. Jann, W. Florian, W. Michael, B. Peter, *Chemistry – A European Journal* **2011**, *17*, 6643-6651.
[27] Z. Hu, Y. Peng, Z. Kang, Y. Qian, D. Zhao, *Inorg. Chem.* **2015**, *54*, 4862-4868.
[28] H. Reinsch, B. Bueken, F. Vermoortele, I. Stassen, A. Lieb, K.-P. Lillerud, D. De Vos, *CrystEngComm* **2015**, *17*, 4070-4074.
[29] Y. Ueno, J. Jose, A. Loudet, C. Pérez-Bolívar, P. Anzenbacher, K. Burgess, *J. Am. Chem. Soc.* **2011**, *133*, 51-55.
[30] M. A. Chowdhury, K. R. A. Abdellatif, Y. Dong, D. Das, G. Yu, C. A. Velázquez, M. R. Suresh, E. E. Knaus, *Biorg. Med. Chem. Lett.* **2009**, *19*, 6855-6861.
[31] P. V. Dau, K. K. Tanabe, S. M. Cohen, *Chem. Commun.* **2012**, *48*, 9370-9372.
[32] J. H. Song, Y. Kim, K. S. Lim, D. W. Kang, W. R. Lee, C. S. Hong, *Inorg. Chem.* **2017**, *56*, 305-312.
[33] J. Zheng, R. S. Vemuri, L. Estevez, P. K. Koech, T. Varga, D. M. Camaioni, T. A. Blake, B. P. McGrail, R. K. Motkuri, *J. Am. Chem. Soc.* **2017**, *139*, 10601-10604.
[34] M. Rodriguez Johanna, L. Nevola, T. Ross Nathan, G. i. Lee, D. Hamilton Andrew, *ChemBioChem* **2009**, *10*, 829-833.